NUREG/CR–5525
SAND89–2398

Hydrogen-Air-Diluent Detonation Study for Nuclear Reactor Safety Analyses

Prepared by
D. W. Stamps, W. B. Benedick, S. R. Tieszen

Sandia National Laboratories
Operated by
Sandia Corporation

Prepared for
U.S. Nuclear Regulatory Commission

AVAILABILITY NOTICE

Availability of Reference Materials Cited in NRC Publications

Most documents cited in NRC publications will be available from one of the following sources:

1. The NRC Public Document Room, 2120 L Street, NW, Lower Level, Washington, DC 20555
2. The Superintendent of Documents, U.S. Government Printing Office, P.O. Box 37082, Washington, DC 20013-7082
3. The National Technical Information Service, Springfield, VA 22161

Although the listing that follows represents the majority of documents cited in NRC publications, it is not intended to be exhaustive.

Referenced documents available for inspection and copying for a fee from the NRC Public Document Room include NRC correspondence and internal NRC memoranda; NRC Office of Inspection and Enforcement bulletins, circulars, information notices, inspection and investigation notices; Licensee Event Reports; vendor reports and correspondence; Commission papers; and applicant and licensee documents and correspondence.

The following documents in the NUREG series are available for purchase from the GPO Sales Program: formal NRC staff and contractor reports, NRC-sponsored conference proceedings, and NRC booklets and brochures. Also available are Regulatory Guides, NRC regulations in the *Code of Federal Regulations*, and *Nuclear Regulatory Commission Issuances*.

Documents available from the National Technical Information Service include NUREG series reports and technical reports prepared by other federal agencies and reports prepared by the Atomic Energy Commission, forerunner agency to the Nuclear Regulatory Commission.

Documents available from public and special technical libraries include all open literature items, such as books, journal and periodical articles, and transactions. *Federal Register* notices, federal and state legislation, and congressional reports can usually be obtained from these libraries.

Documents such as theses, dissertations, foreign reports and translations, and non-NRC conference proceedings are available for purchase from the organization sponsoring the publication cited.

Single copies of NRC draft reports are available free, to the extent of supply, upon written request to the Office of Information Resources Management, Distribution Section, U.S. Nuclear Regulatory Commission, Washington, DC 20555.

Copies of industry codes and standards used in a substantive manner in the NRC regulatory process are maintained at the NRC Library, 7920 Norfolk Avenue, Bethesda, Maryland, and are available there for reference use by the public. Codes and standards are usually copyrighted and may be purchased from the originating organization or, if they are American National Standards, from the American National Standards Institute, 1430 Broadway, New York, NY 10018.

NUREG/CR-5525
SAND89-2398
R3

Hydrogen-Air-Diluent Detonation Study for Nuclear Reactor Safety Analyses

Manuscript Completed: December 1990
Date Published: January 1991

Prepared by
D. W. Stamps, W. B. Benedick, S. R. Tieszen

Sandia National Laboratories
Albuquerque, NM 87185-5800

Prepared for
Division of Systems Research
Office of Nuclear Regulatory Research
U.S. Nuclear Regulatory Commission
Washington, DC 20555
NRC FIN A1246

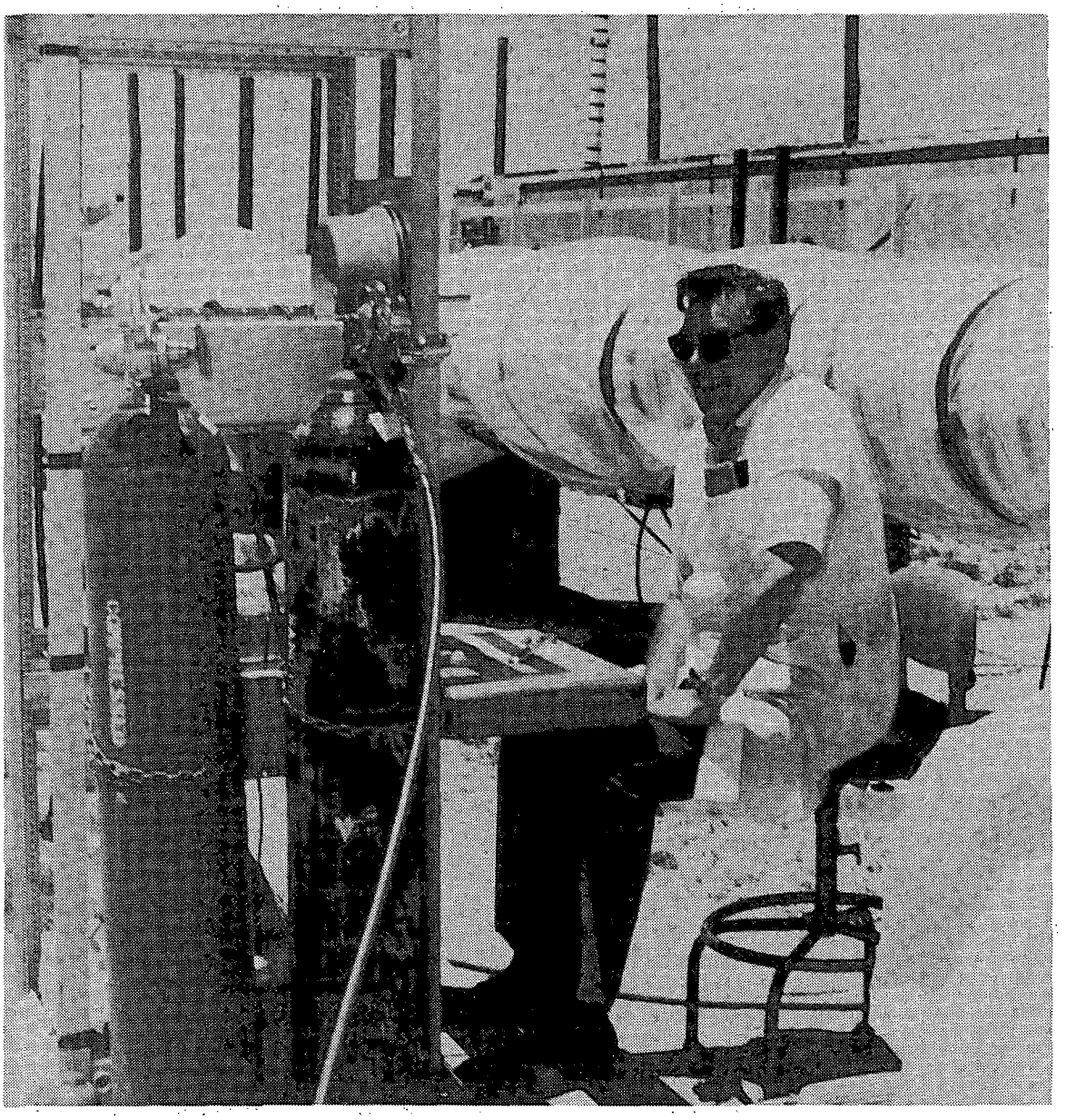

COMMEMORATION

Due to his untimely death, William "Bill" Benedick (1926-1989) was unable to see this report to completion. His unquestionable engineering judgement, clever approach to design simiplification, and enthusiasm for new ideas ensured the success of this project like all other projects he participated in. Bill's enjoyment from conducting experiments, especially those with a "bang," was only superseded by the immense pleasure he derived from working with others.

ABSTRACT

The detonability of hydrogen-air-diluent mixtures was investigated experimentally in the 0.43 m diameter, 13.1 m long Heated Detonation Tube (HDT) for the effects of variations in hydrogen and diluent concentration, initial pressure, and initial temperature. The data were correlated using a ZND chemical kinetics model. The detonation limits in the HDT were obtained experimentally for lean and rich hydrogen-air mixtures and stoichiometric hydrogen-air-steam mixtures.

The addition of a diluent, such as steam or carbon dioxide, increases the detonation cell width for all mixtures. In general, an increase in the initial pressure or temperature produces a decrease in the cell width. In the HDT, the detonable range of hydrogen in a hydrogen-air mixture initially at 1 atm pressure is between 11.6 percent and 74.9 percent for mixtures at 20°C, and 9.4 percent and 76.9 percent for mixtures at 100°C. The detonation limit is between 38.8 percent and 40.5 percent steam for a stoichiometric hydrogen-air-steam mixture initially at 100°C and 1 atm. The detonation limit is between 29.6 percent and 31.9 percent steam for a stoichiometric hydrogen-air-steam mixture for the case where hydrogen and steam are added to air initially at 20°C and 1 atm resulting in a final predetonation mixture temperature and pressure of approximately 100°C and 2.6 atm, respectively.

CONTENTS

LIST OF FIGURES

LIST OF TABLES

ACKNOWLEDGMENTS

The authors appreciate the technical support of C. Daniel, B. Heideman, and M. Naro in obtaining the data. We thank J. Shepherd for his contribution on interpreting the effect of temperature on the detonation cell size. We also thank M. Berman and the NRC contract monitor, P. Worthington, for program support and valuable technical discussions.

EXECUTIVE SUMMARY

The detonability of hydrogen-air-diluent mixtures was investigated experimentally and correlated using a Zeldovich-von Neumann-Doering (ZND) model. The first of our two objectives was to determine the effect of dilution, pressure, and temperature on the detonation cell width of hydrogen-air mixtures. The second objective was to determine the detonability limits for lean and rich hydrogen-air mixtures and stoichiometric hydrogen-air-steam mixtures. The results of this study can be used for safety analyses of nuclear reactor accidents.

The experimental work was conducted in the Heated Detonation Tube (HDT). This facility is 43 cm in internal diameter and 13.1 m long. It can be heated to approximately 390 K and can operate with detonation pressures up to 3.1 MPa. The detonation cell width was recorded on a sooted foil lining the inside of the HDT. The cell width is an intrinsic length scale of a detonation and indicates the "sensitivity" of a mixture. The smaller the cell width, the more likely the mixture is to detonate. Likewise, the larger the cell width, the less likely the mixture is to detonate.

The data were correlated using a model based on a detailed chemical-kinetics reaction set for hydrogen oxidation and the ZND model of a detonation. The model predicts a reaction zone length. The detonation cell width data can be correlated with the reaction zone length by a proportionality factor.

The addition of a diluent, such as steam or carbon dioxide, increases the detonation cell width for all mixtures. For the same conditions, carbon dioxide is not only more effective than steam, but its efficacy increases relative to steam with increasing concentration. In reactor accident scenarios, hydrogen-air mixtures will likely be diluted with steam. In scenarios involving core-concrete interactions, carbon dioxide will also be present.

A large decrease in the detonation cell width is predicted with increasing pressure for hydrogen-air mixtures at low initial pressures with and without steam dilution. With further increase in pressure, the cell width increases slightly to a local maximum and then continues to decrease

slightly. The predicted maximum has not been verified experimentally. The data indicate that the cell size decreases approximately by a factor of two over the range of pressures of interest in reactor safety analysis.

A large decrease in the detonation cell width is predicted initially for hydrogen-air-diluent mixtures with increasing initial temperature. The effect is most pronounced for off-stoichiometric mixtures and highly-diluted mixtures. With further increase in temperature, the cell width reaches a minimum and then increases slightly. While the model has been used to predict the effect of temperature up to 1000 K, it has been assessed only up to 373 K with the data in this report.

Three important points can be made from the model predictions. First, the detonation cell width decreases with increasing initial temperature up to a critical temperature for all mixtures. Second, all mixtures are predicted to have similar cell widths, or likewise similar detonabilities, at elevated temperatures. Third, the mitigative effect of a diluent, such as steam or carbon dioxide, decreases with increasing temperature. If the model is confirmed experimentally at higher temperatures, the model's predictions indicate that detonations may be significantly more probable than previously considered in at least three accident scenarios. These scenarios include direct containment heating, core-concrete interactions, and releases from the reactor coolant system.

The detonable range of hydrogen obtained in the HDT for hydrogen-air mixtures at 20°C and 1 atm is between 11.6 percent and 74.9 percent by volume. Increasing the initial temperature to 100°C expands the range to 9.4 percent and 76.9 percent by volume and illustrates the important effect of increasing temperature. The detonation limit is between 38.8 percent and 40.5 percent steam for stoichiometric hydrogen-air-steam mixtures at 100°C and 1 atm initial pressure. The detonation limit is between 29.6 percent and 31.9 percent steam for a stoichiometric hydrogen-air-steam mixture for the case where hydrogen and steam are added to air initially at 20°C and 1 atm resulting in a final predetonation mixture temperature and pressure of approximately 100°C and 2.6 atm, respectively. The lower value of steam does not represent an intrinsic detonation limit for the HDT, however, and is probably due to insufficient charge strength to initiate the detonation. All

detonation limits are scale and geometry dependent. This means that a wider range of detonable concentrations may be obtained at reactor scale.

A comparison between the various combustion limits yields two important conclusions. First, the detonability limits are similar to the flammability limits for some mixtures. While there is a discrepancy between the limits for the other mixtures, the limits are much closer than previously thought. Second, the detonability limits and flame acceleration limits are similar for most mixtures tested.

1. INTRODUCTION

1.1 Background and Objectives

During a severe accident scenario, hydrogen will be generated if the core is uncovered. The production of hydrogen in the reactor vessel and release through the reactor coolant system can be modeled by a coupled accident analysis code, such as MELPROG/TRAC [1.1]. After the hydrogen is released into the containment, it is mixed and transported by natural and forced convection. These processes can be modeled by lumped-volume (i.e., HECTR [1.2], CONTAIN [1.3], and MELCOR [1.4]) and finite-difference (i.e., HMS [1.5]) accident analysis codes. If sufficient hydrogen accumulates and becomes flammable, these codes also model the combustion process. The codes are restricted, however, to modeling only simple deflagrations. Other modes of combustion, like accelerated flames and detonations, may be possible if larger quantities of hydrogen accumulate before ignition occurs such as during a station blackout scenario. Presently, empirical correlations and qualitative methodologies are the only means available to estimate the possibility or likelihood of one of these modes of combustion. This report provides the detonation length scales necessary for these correlations and methodologies.

Correlations exist to estimate (1) the energy required to initiate a detonation directly, (2) the possibility a detonation will be initiated indirectly through an accelerated flame if direct initiation is unlikely, (3) the propagation of a detonation through different geometries, and (4) the transmission of a detonation from a confined region to an unconfined one. All of these correlations require an experimentally measured length scale called the detonation cell width. The correlations have been discussed in detail [1.6-1.14] and only a brief review is given here.

Several models are available to estimate the energy required to initiate a detonation directly [1.6-1.8]. A common feature of all models is to relate the critical energy for direct initiation, E_{CR}, to the detonation cell width, λ, or $E_{CR} \propto \lambda^n$. The values of the exponent, n, are 1, 2, or, 3 corresponding to planar, cylindrical, or spherical detonations. Since direct initiation of a detonation may be unlikely in a severe accident due to the large energy requirements, a more likely mode of initiation may be through

flame acceleration and deflagration to detonation transition (DDT). A method has been developed [1.9] to estimate the likelihood of a DDT during degraded-core accidents. This method ranks geometries by scale, obstacles, and confinement, and mixtures by their chemical sensitivity based on λ. While this method is qualitative, a quantitative criterion has been proposed recently to estimate the transition of a deflagration to a detonation, but the criterion may only be applicable to obstacle-filled tubes [1.10]. This criterion states that if a mixture flame speed is on the order of the sound speed of the combustion products, a DDT is possible if λ is on the order of, or smaller than, the minimum transverse dimension of the tube. Once a detonation is initiated, either directly or indirectly by a DDT, the possibility that the detonation will propagate in a compartment has been empirically correlated using the geometric scale relative to λ. Propagation criteria have been determined for different geometries [1.11-1.13] as shown in Figure 1.1. For safety analyses, we recommend $D_{min} = \lambda/2$ for propagation down a wide channel (Figure 1.1) since the boundaries may support a half cell. Recent research [1.14] indicates there is still some uncertainty in the values of the proportionality constants in the correlations. The transmission of the detonation between compartments also depends on λ [1.11-1.13]. Figures 1.2 and 1.3 show criteria for the transmission of a detonation from a confined region to an unconfined one for different geometries. These criteria are also valid for tranmission through an orifice if the effective diameter is used [1.12].

The purpose of the previous discussion is to emphasize that λ is a fundamental length scale for all aspects of detonations including initiation, propagation, and transmission. The application of these criteria to safety analyses requires a knowledge of λ for different thermodynamic conditions: fuel and diluent concentrations, temperature, and pressure.

A wide range of conditions may occur depending on the time after the accident. Early in the accident during the release of hydrogen, mixtures in the source compartment will be at elevated temperatures, pressures close to atmospheric, and diluted with large quantities of steam. At later times, the mixtures may be at temperatures near saturation, elevated pressures, fuel lean, and diluted with moderate quantities of steam depending on factors such as the amount of mixing, steam condensation, and engineering safety features employed.

•Propagation Down a Cylinder (One-Dimensional):

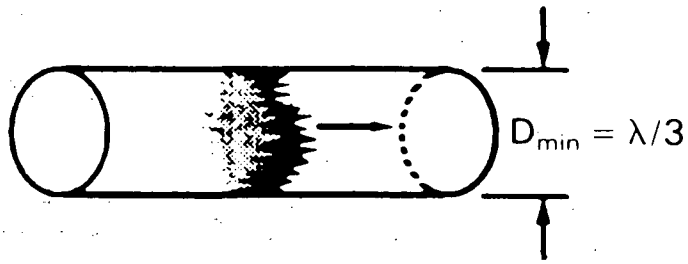

•Propagation Down a Wide Channel (Two-Dimensional):

Figure 1.1 **Schematic illustrations for the empirically determined propagation criteria for different geometries (from Reference 1.11)**

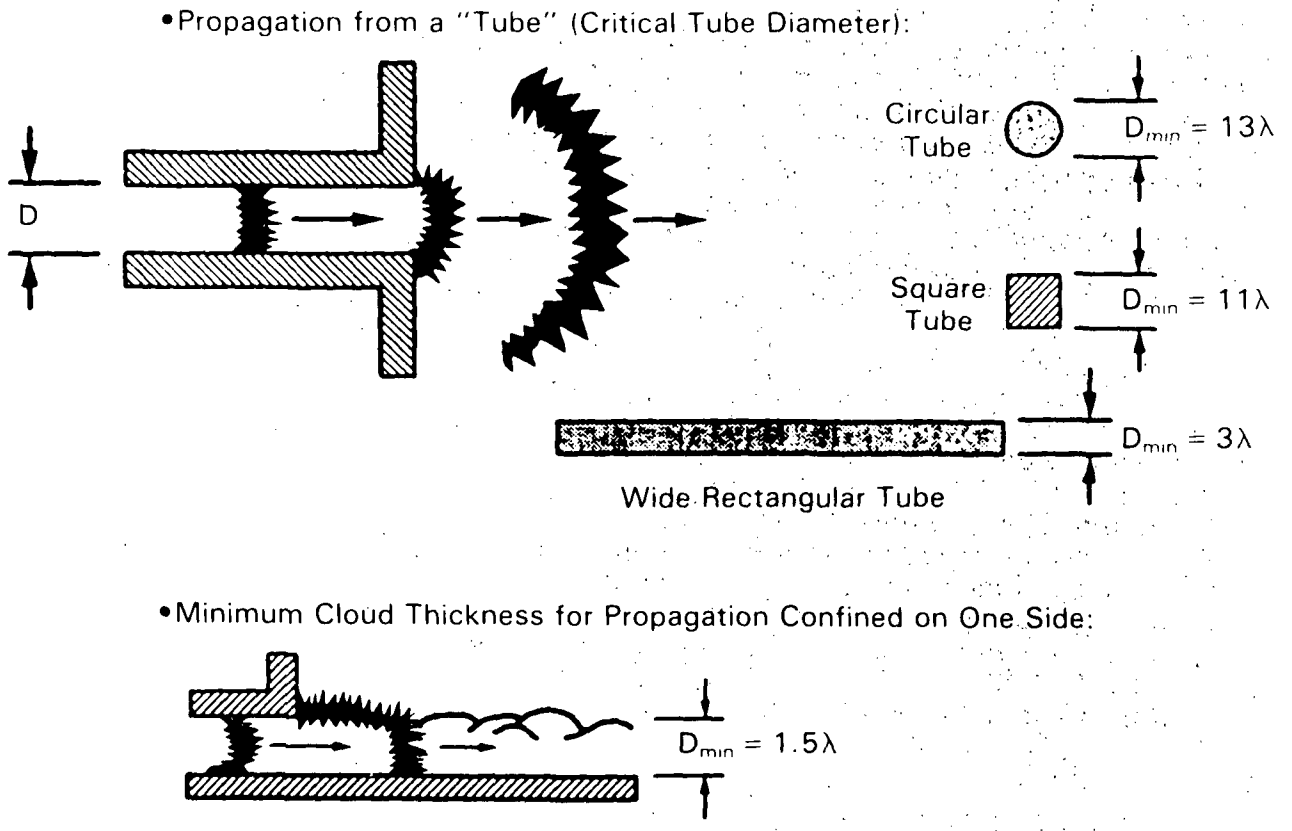

Figure 1.2 **Schematic illustrations of the empirically determined transmission criteria for different geometries (from Reference 1.11)**

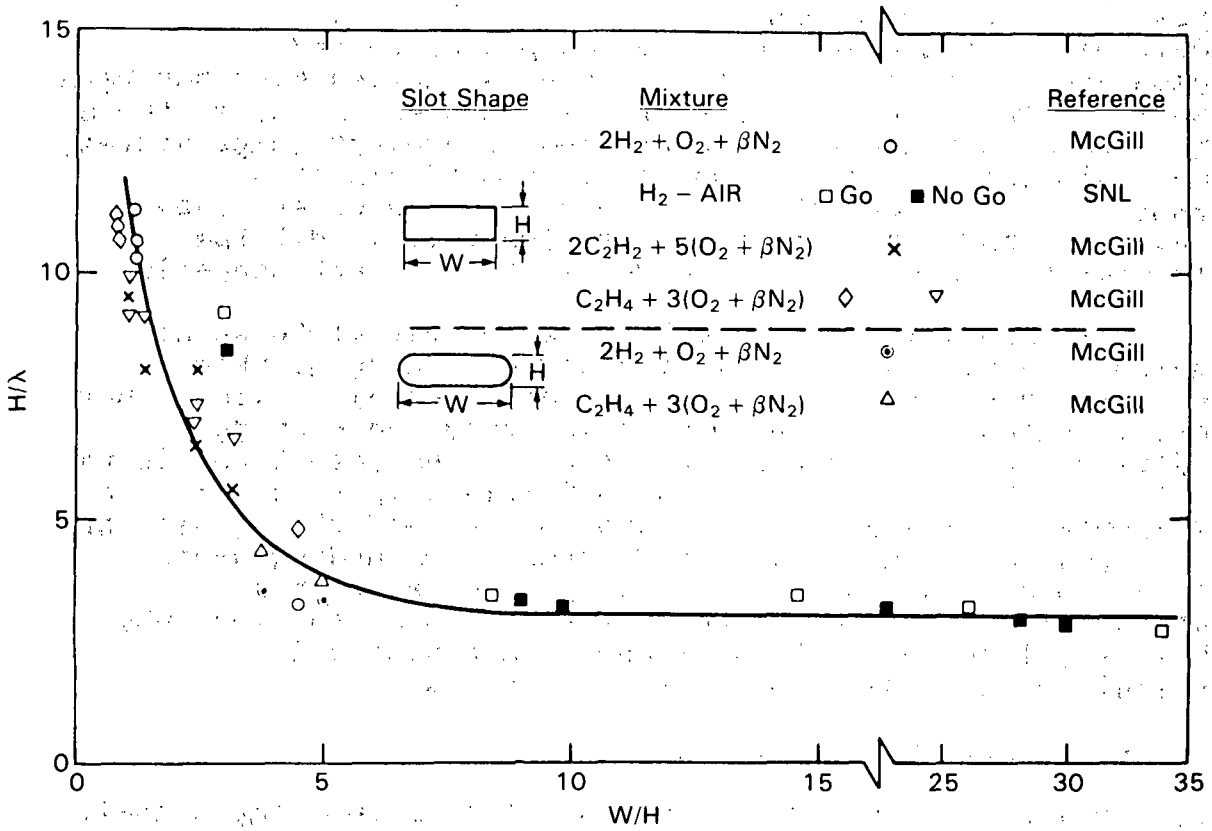

Figure 1.3 Transmission criteria for a rectangular channel as a function of aspect ratio (from Reference 1.11)

While a large data base exists for hydrogen-air detonations [1.8, 1.12, 1.15], little information exists for conditions associated with reactor accidents. Most of the data show the effect of variations in fuel concentration for non-diluted hydrogen-air mixtures. If the mixtures are diluted, it is usually with a gas such as argon, helium, or nitrogen. Typically the diluents found in reactor accident scenarios are steam and/or carbon dioxide and the effect of these diluents are shown by Tieszen et al. [1.16]. Additionally the effect of elevated pressures and temperatures associated with accident scenarios have not been studied. The effect of pressure has been shown for mixtures at or below atmospheric pressure and at ambient temperatures. Some calculations have shown the effect of elevated temperatures for stoichiometric mixtures. However, these studies do not consider the off-stoichiometric diluted mixtures that are likely to occur in an accident scenario.

The detonation cell width is needed for mixtures at accident conditions for safety analyses. Some of this information has been obtained by Tieszen et al. [1.16]. Our work is intended to supplement this study and provide additional data for conditions at early and late times in the accident. The first of our two objectives is to report the experimental data and predictions for the effects of diluent concentration, temperature, and pressure on hydrogen-air detonations. The second objective is to report the detonability limits obtained in the Heated Detonation Tube (HDT) for lean and rich hydrogen-air mixtures and stoichiometric hydrogen-air-steam mixtures.

1.2 References for Chapter 1

1.1 Dosanjh, S. S., "MELPROG-PWR/MOD1: A Two-Dimensional, Mechanistic Code for Analysis of Reactor Core Melt Progression and Vessel Attack Under Severe Accident Conditions," NUREG/CR-5193, SAND88-1824, Sandia National Laboratories, Albuquerque, NM, May 1989.

1.2 Dingman, S. E., Camp, A. L., Wong, C. C., King, D. B., and Gasser, R. D., "HECTR Version 1.5 User's Manual," NUREG/CR-4507, SAND86-0101, Sandia National Laboratories, Albuquerque, NM, April 1986.

1.3 Bergeron, K. D., et al, "User's Manual for CONTAIN 1.0, A Computer Code for Severe Nuclear Reactor Accident Containment Analysis," NUREG/CR-4085, SAND84-1204, Sandia National Laboratories, Albuquerque, NM, May 1985.

1.4 Haskin, F. E., Webb, S. W., and Summers, R. M., "Development and Status of MELCOR," SAND86-2115, Proceedings of the Fourteenth Light Water Reactor Meeting, October 1986.

1.5 Travis, J. R., "HMS: A Computer Program for Transient Three-Dimensional Mixing Gases," Los Alamos National Laboratory Report, LA10-267-MS (NUREG/CR-4020), November 1984.

1.6 Lee, J. H. S., "Initiation of Gaseous Detonation," Annual Review of Physical Chemistry, V28, pp. 75-104, 1977.

1.7 Benedick, W. B., Guirao, C. M., Knystautas, R., and Lee, J. H., "Critical Charge for the Direct Initiation of Detonation in Gaseous Fuel-Air Mixtures," Dynamics of Explosions: Progress in Astronautics and Aeronautics, (edited by Bowen, Leyer, and Soloukhin) AIAA, New York, V106, pp. 181-202, 1986.

1.8 Vasil'ev, A. A., Mitrofanov, V. V., and Topchiyan, M. E., "Detonation Waves in Gases," Fizika Goreniya i Vzryva, V23, No. 5, pp. 109-131, 1987.

1.9 Sherman, M. P., and Berman, M., "The Possibility of Local Detonations During Degraded-Core Accidents in the Bellefonte Nuclear Power Plant," Nuclear Technology, V81, pp. 63-77, 1988.

1.10 Peraldi, O., Knystautas, R., and Lee, J. H., "Criteria for Transition to Detonation in Tubes," Twenty-First Symposium (International) on Combustion, The Combustion Institute, pp. 1629-1637, 1986.

1.11 Berman, M., "A Critical Review of Recent Large-Scale Experiments on Hydrogen-Air Detonations," Nuclear Science and Engineering, V93, pp. 321-347, 1986.

1.12 Lee, J. H. S., "Dynamic Parameters of Gaseous Detonations," Annual Review of Fluid Mechanics, V16, pp. 311-336, 1984.

1.13 Guirao, C. M., Knystautas, R., and Lee, J. H., "A Summary of Hydrogen-Air Detonations for Nuclear Reactor Safety," NUREG/CR-4961, SAND87-7128, May 1989.

1.14 Dupre, G., Peraldi, O., Joannon, J., Lee, J., and Knystautas, R., "On the Limit Criterion of Detonation in Circular Tubes," presented at the 12th ICDERS meeting, July 23-28, 1989, Ann Arbor, MI.

1.15 Oppenheim, A. K., Soloukhin, R. I., "Experiments in Gasdynamics of Explosions," Annual Review of Fluid Mechanics, V5, pp. 31-58, 1973.

1.16 Tieszen, S. R., Sherman, M. P., Benedick, W. B., Shepherd, J. E., Knystautas, R., and Lee, J. H. S., "Detonation Cell Size Measurements in Hydrogen-Air-Steam Mixtures," Dynamics of Explosions: Progress in Astronautics and Aeronautics, (edited by Bowen, Leyer, and Soloukhin) AIAA, New York, V106, pp. 205-219, 1986.

2. EXPERIMENTAL METHOD

2.1 HDT Description and Procedure

The experimental detonation cell width data are obtained in the HDT shown in Figure 2.1, which is a heated detonation tube 0.43 m in diameter and 13.1 m long. The temperature of the tube has been raised to 388 K by resistive heaters on the surface of the tube. The tube has been approved to operate with detonation pressures up to 3.1 MPa.

The following discussion gives the general procedures for the experiments conducted in the HDT. Details of the facility and experimental procedure were given by Tieszen et al. [2.1].

Prior to an experiment, an aluminum sheet 3.66 m long by 1.22 m wide that is used to record the detonation cell width has a thin layer of soot applied uniformly on the surface. This sheet is formed into a cylinder to line the terminal end of the tube. A planar charge of DuPont Detasheet with up to 110 gm of high explosive is used to initiate the detonation directly and is placed in the tube at the opposite end of the aluminum sheet.

Initially the tube is evacuated to approximately 3 mm Hg before gases are introduced. Dry air is added first followed by hydrogen and either steam or carbon dioxide if the mixtures are diluted. Gases are introduced slowly for uniform mixing. The mixture in the tube is continuously circulated during the introduction of new gases. The final mixture is recirculated for a change of two to three tube volumes to provide additional mixing. After each gas is added, the gas temperature is recorded with a K-type thermocouple. Additionally, the pressure is recorded by one of three types of pressure gauges. These measurements are used to calculate hydrogen and diluent concentrations based on the method of partial pressures.

After the detonation is initiated with the high explosive, the detonation propagates down the tube and the detonation cellular tracks are recorded on the sooted sheet. Detonation time-of-arrival measurements are recorded by up to 12 fast response quartz piezoelectric pressure transducers (either PCB Model 113A20 or Kistler Model 211B3) spaced approximately uniformly along the length of the tube. The

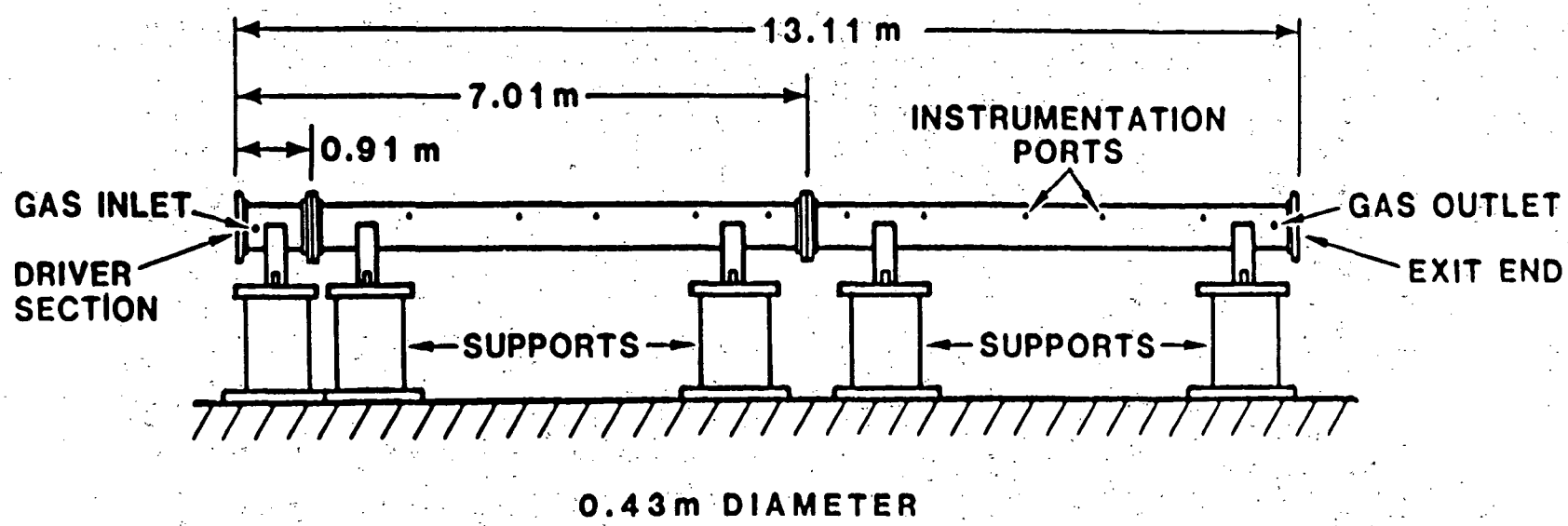

Figure 2.1 Schematic of the Heated Detonation Tube

detonation velocity is obtained from these measurements. A self-sustained wave is checked by verifying a constant detonation velocity along the latter section of the HDT. In some cases, this is verified by showing the cell width is independent of the initiating charge strength. Pressure transducer output is recorded by six Tektronix 7612D transient digitizers, each with two data channels recording at typically 1 μs/sample at the leading edge of the detonation.

2.2 Uncertainty

The uncertainty is estimated for the measured and calculated thermodynamic variables, such as temperature, pressure, equivalence ratio, and diluent concentrations, the detonation velocity, and the detonation cell width. A detailed discussion of the methods to estimate uncertainty is given in Appendix A.

A quantitative estimate of the uncertainty in the thermodynamic variables is obtained using a technique termed single-sample uncertainty analysis [2.2]. The detonation velocity is determined from the slope of the time-of-arrival measurements and a standard statistical package is used to obtain a linear regression fit of the data. The uncertainty bounds for the velocity are determined from the standard error estimates in the slope. Attempts have been made to make quantitative estimates of the detonation cell width. A recent study [2.3] uses digital image processing and a two-dimensional spectral analysis to estimate the dominate cell width and the degree of regularity. Only a limited set of data have been analyzed which yield a set of probable detonation cell widths for each experiment. However, within this set of probable cell widths, the dominant cell width cannot be determined with any level of confidence that can be quantified. Until a statistical model is developed to quantify the confidence level of the spectral analysis, visual observation appears to be the most appropriate means to estimate the cell width.

The detonation cell width is determined using the method of selecting high-contrast long-running parallel lines termed the dominant-mode method [2.4]. Hydrogen-air detonations may produce irregularly spaced lines or cells that make the dominant-mode method difficult to use because of substructure. The uncertainty in cell width is estimated by independent measurements of the authors. Occasionally, these

estimates vary by roughly a factor of two due to our inability to distinguish the dominant mode from the substructure. Independent measurements were taken for about half of the data. For this reason, the standard deviation of 0.13 λ for this set of data is assumed to be representative of the entire set. Because the cell width measurements are subjective and are influenced by human bias, we recommend the most probable cell width measurements listed in Appendix B be divided by 2 for safety analysis.

Uncertainty estimates that are typical, but not necessarily conservative, are given for the thermodynamic variables in Appendices A and B. The gas temperature was measured with a Chromel-Alumel thermocouple with an uncertainty of ±1°C. The gas mixture was measured with either one of three gauges: Wallace and Tiernan 0-100 mm Hg or 0-800 mm Hg absolute gauges each with an uncertainty of ±0.5 mm Hg or a Wallace and Tiernan 0-50 psia gauge with an uncertainty of ±0.04 psia. Typical bounds for the equivalence ratio are less than ±4 percent.

2.3 References for Chapter 2

2.1 Tieszen, S. R., Sherman, M. P., Benedick, W. B., and Berman, M., "Detonability of H_2-Air-Diluent Mixtures," NUREG/CR-4905, SAND85-1263, Sandia National Laboratories, Albuquerque, NM, June 1987.

2.2 Moffat, R.J., "Describing the Uncertainties in Experimental Results," Experimental Thermal and Fluid Science, V1, pp. 3-17, 1988.

2.3 Shepherd, J. E. and Tieszen, S. R., "Detonation Cellular Structure and Image Processing," Sandia National Laboratories, Albuquerque, NM, SAND86-0033, June 1986.

2.4 Moen, I. O., Murry, S. B., Bjerketvedt, O., Rinnan, A., Knystautas, R., and Lee, J. H. S., "Diffraction of Detonation From Tubes Into A Large Fuel-Air Explosive Cloud," Nineteenth Symposium (International) on Combustion, The Combustion Institute, Pittsburgh, PA, pp. 635-645, 1982.

3. MODEL

3.1 ZND Model Description

The data obtained in the HDT are correlated with predictions obtained using a model [3.1] based on a detailed chemical-kinetics reaction set for hydrogen oxidation [3.2] and the ZND model of a detonation. A detailed discussion of the model is given by Shepherd [3.1]. According to the ZND model, a one-dimensional shock wave traveling at the Chapman-Jouguet (CJ) velocity elevates the gas temperature and pressure to the von Neumann state. The reaction zone behind the shock consists of an induction zone during which the temperature and pressure are nearly constant followed by a rapid release of chemical energy leading eventually to the final CJ state. The release of chemical energy is governed by a set of 23 reactions and 11 species that constitute the chemical kinetic model for hydrogen oxidation as shown in Table 3.1. The reaction zone structure is obtained by simultaneously solving the conservation equations behind the shock as a function of distance. Although the ZND model does not represent the three-dimensional physical structure of a detonation, it does give a characteristic length, or time, of heat release that can be correlated with the experimental detonation cell width.

The experimentally measured detonation cell width, λ, can be linearly correlated to a first approximation, to the reaction zone length, Δ, or $\lambda=A\Delta$. While the empirically determined factor, A, has been shown to vary with fuel concentration, as shown in Figure 3.1, sufficient accuracy is obtained by assuming A is a constant. The value of A also depends on how the reaction zone length is defined. The location where the reaction zone is considered complete must be chosen since the chemical reactions proceed to their equilibrium CJ state asymptotically according to the ZND model. Figure 3.2 shows different reaction zone lengths on a reaction zone temperature profile. Table 3.2 shows the corresponding values of A for the different lengths. The ZND reaction zone length based on where the Mach number reaches 0.75 and A is equal to 22 has proven most successful in correlating the experimentally measured cell width [3.1]. This length includes more than the induction zone and extends into the final phase of the heat release zone where the three-body reactions are important. In general, our calculations will use this length. Any exceptions will be specifically noted.

Reaction	a	β	E
1. $H_2 + O_2 = OH + OH$	1.70×10^{13}	0.00	47780
2. $OH + H_2 = H_2O + H$	1.17×10^{9}	1.30	3626
3. $H + O_2 = OH + O$	5.13×10^{16}	-0.82	16507
4. $O + H_2 = OH + H$	1.80×10^{10}	1.00	8826
5. $H + O_2 + M = HO_2 + M$	2.10×10^{18}	-1.00	0
6. $H + O_2 + O_2 = HO_2 + O_2$	6.70×10^{19}	-1.42	0
7. $H + O_2 + N_2 = HO_2 + N_2$	6.70×10^{19}	-1.42	0
8. $OH + HO_2 = H_2O + O_2$	5.00×10^{13}	0.00	1000
9. $H + HO_2 = OH + OH$	2.50×10^{14}	0.00	1900
10. $O + HO_2 = O_2 + OH$	4.80×10^{13}	0.00	1000
11. $OH + OH = O + H_2O$	6.00×10^{8}	1.30	0
12. $H_2 + M = H + H + M$	2.23×10^{12}	0.50	92600
13. $O_2 + M = O + O + M$	1.85×10^{11}	0.50	95560
14. $H + OH + M = H_2O + M$	7.50×10^{23}	-2.60	0
15. $H + HO_2 = H_2 + O_2$	2.50×10^{13}	0.00	700
16. $HO_2 + HO_2 = H_2O_2 + O_2$	2.00×10^{12}	0.00	0
17. $H_2O_2 + M = OH + OH + M$	1.30×10^{17}	0.00	45500
18. $H_2O_2 + H = HO_2 + H_2$	1.60×10^{12}	0.00	3800
19. $H_2O_2 + OH = H_2O + HO_2$	1.00×10^{13}	0.00	1800
20. $HO_2 + CO = CO_2 + OH$	1.51×10^{13}	0.00	22934
21. $CO + O + M = CO_2 + M$	3.20×10^{13}	0.00	-4200
22. $CO + OH = CO_2 + H$	1.51×10^{7}	1.30	-758
23. $CO + O_2 = CO_2 + O$	1.60×10^{13}	0.00	41000

+Reaction rate coefficients are in the form $k_f = aT^{\beta} \exp -E/RT$. Units are moles, cubic centimeters, seconds, Kelvins, and calories/mole. Third body efficiencies: $k_5(H_2O) = 21k_5(Ar)$; $k_5(H_2) = 3.3k_5(Ar)$; $k_5(CO_2) = 5k_5(Ar)$; $k_5(CO) = 2k_5(Ar)$; $k_{12}(H_2O) = 6k_{12}(Ar)$; $k_{12}(H) = 2k_{12}(Ar)$; $k_{12}(H_2) = 3k_{12}(Ar)$; $k_{14}(H_2O) = 20k_{14}(Ar)$.

Table 3.1 Hydrogen oxidation mechanism and rate constants+ (from Reference 3.2)

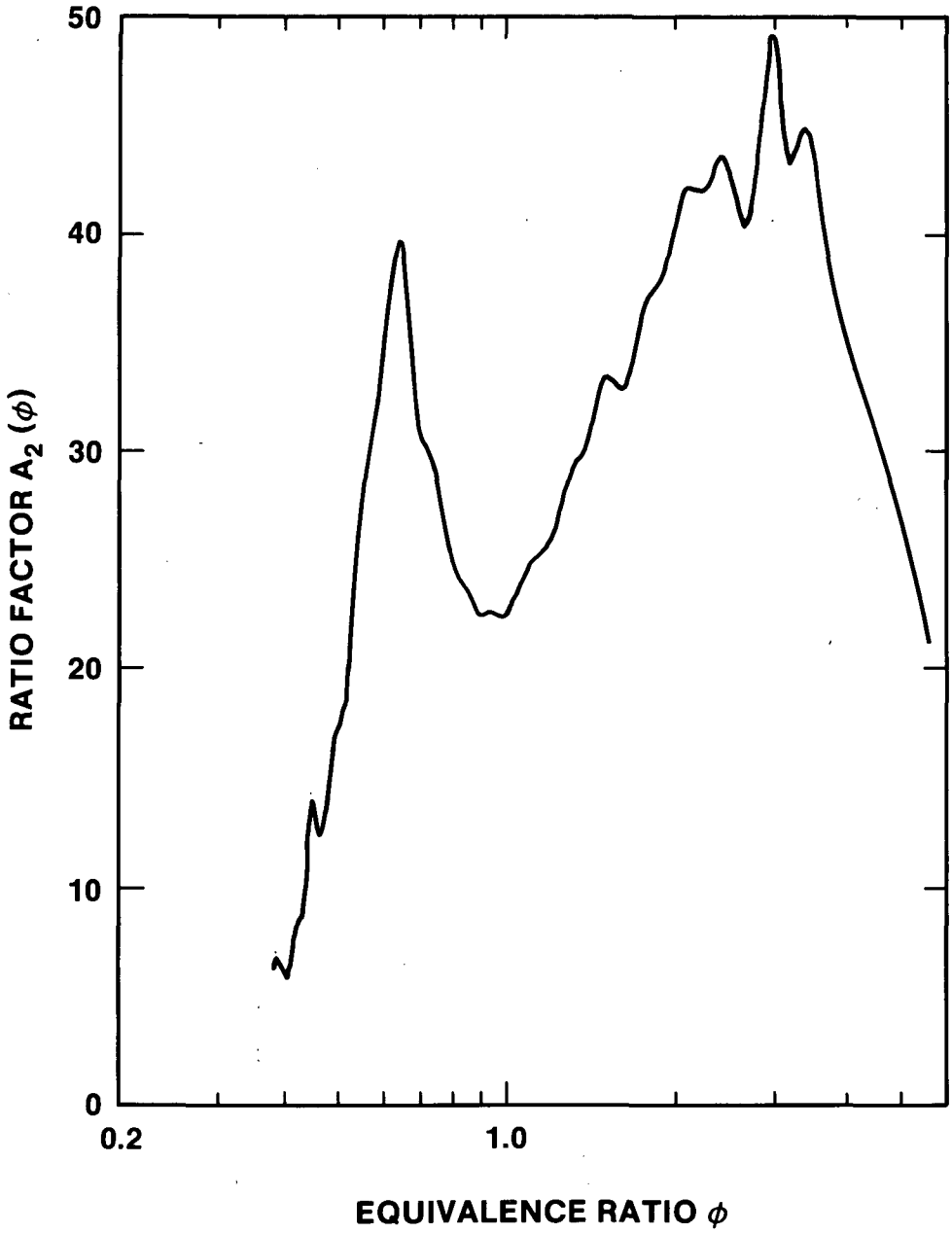

Figure 3.1 Ratio $A_2(\phi)$ of cell width λ to reaction zone length Δ_2 for hydrogen-air detonations at standard initial conditions (from Reference 3.1). The reaction zone length Δ_2 is described in Table 3.2 and illustrated in Figure 3.2.

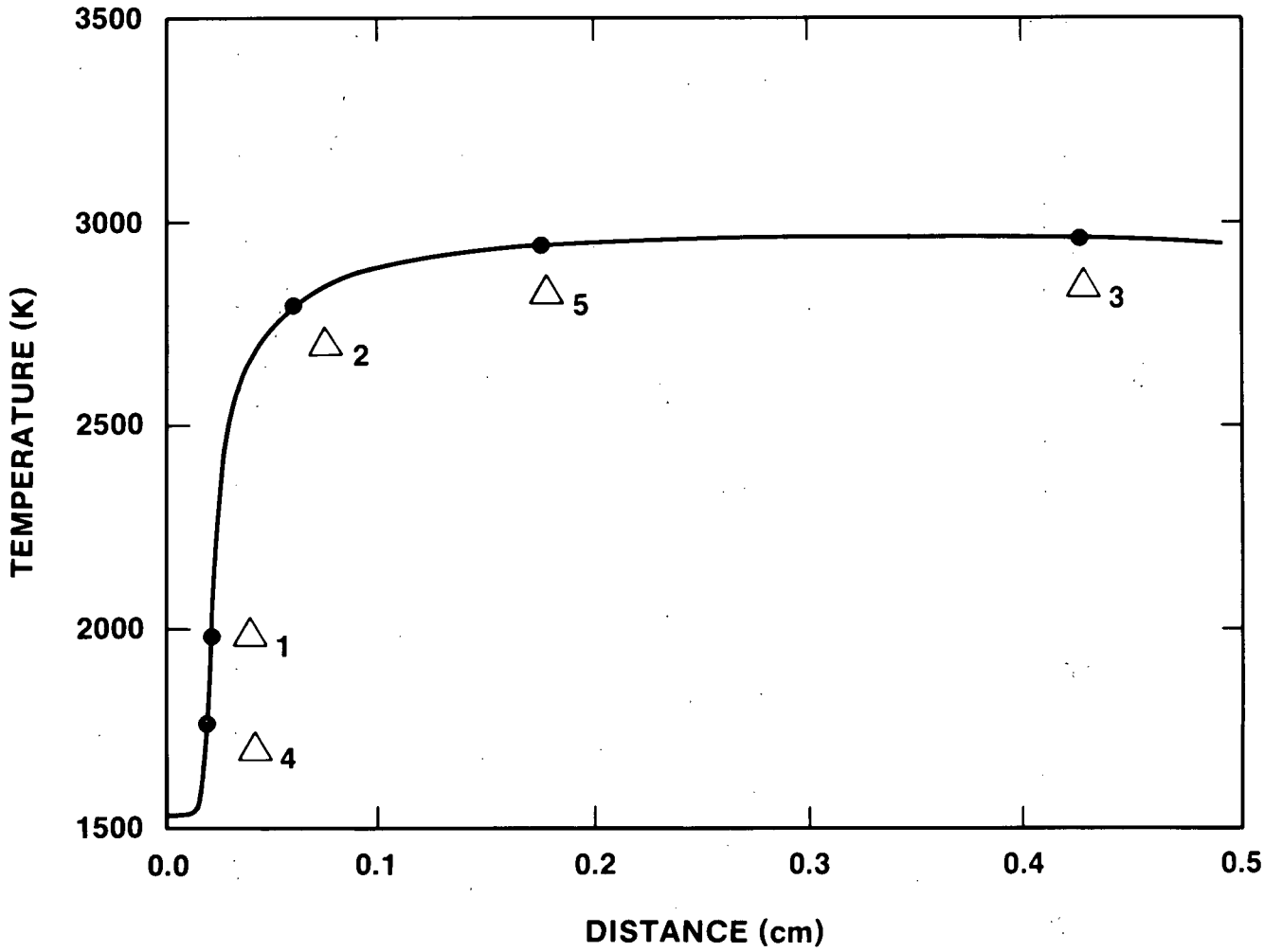

Figure 3.2 ZND reaction zone temperature profile for a stoichiometric hydrogen-air detonation at standard initial conditions, T_o = 298 K and P_o = 1 atm (from Reference 3.1). The reaction zone lengths, Δ_1-Δ_5, are described in Table 3.2.

Symbol	Definition	Values at ER = 1 Δ, cm	λ/Δ
	ZND Model		
Δ_1	$\left.\frac{dT}{dx}\right\|_{max}$	0.023	65.
Δ_2	M = 0.75	0.067	22.
Δ_3	M = 0.90	0.43	3.5.
	Constant-volume model		
Δ_4	$\left.\frac{dT}{dx}\right\|_{max}$	0.021	71.4.
Δ_5	$= - T_{vn} \left.\frac{\partial \Delta_4}{\partial T_{vn}}\right\|_{\rho}$	0.173	8.6.

M = Mach number. Δ = reaction zone length.
λ(ER = 1) = 1.5 cm for H_2-air mixtures initially at STP.

Table 3.2 Reaction zone lengths (from Reference 3.1)

The model has proven successful in correlating the detonation cell width for a wide range of hydrogen-air-diluent mixtures [3.3]. This range includes carbon dioxide- and steam-diluted mixtures at 298 K and 373 K with large variations in hydrogen concentration. While the model can be used to interpolate within the data base, caution should be exercised for extrapolations. For safety analysis, we recommend that the model be used only for conditions where experimental data are available.

3.2 References for Chapter 3

3.1 Shepherd, J. E., "Chemical Kinetics of Hydrogen-Air-Diluent Detonations," Dynamics of Explosions: Progress in Astronautics and Aeronautics, (edited by Bowen, Leyer, and Soloukhin) AIAA, New York, V106, pp. 263-293, 1986.

3.2 Miller, J. A., Mitchell, R. E., Smooke, M. D., and Kee, R. J., "Toward a Comprehensive Chemical Kinetic Mechanism for the Oxidation of Acetylene: Comparison of Model Predictions with Results from Flame and Shock Tube Experiments," Nineteenth Symposium (International) on Combustion, The Combustion Institute, pp. 181-196, 1982.

3.3 Tieszen, S. R., Sherman, M. P., Benedick, W. B., Shepherd, J. E., Knystautas, R., and Lee, J. H. S., "Detonation Cell Size Measurements in Hydrogen-Air-Steam Mixtures," Dynamics of Explosions: Progress in Astronautics and Aeronautics, (edited by Bowen, Leyer, and Soloukhin) AIAA, New York, V106, pp. 205-219, 1986.

4. RESULTS

4.1 Local and Global Detonations

A wide range of initial conditions can exist for hydrogen detonations in severe accidents. Large variations in hydrogen and diluent concentrations, pressure, and temperature can occur depending on the time after an accident begins and the nature of the accident. It is beyond the scope of this report to provide results for all the possible conditions that may exist. Therefore, we will present the results in two general categories: conditions that are typical, but not necessarily bounding, of accidents at early and late times.

Early in an accident, there can be large gradients throughout the containment. In the source compartment, large concentrations of hydrogen, steam, and/or carbon dioxide may exist at elevated temperatures. Depending on the quantity of gases released, the pressure can be at or above atmospheric pressure. Large concentration and temperature gradients can exist between compartments in the containment. If a detonation were initiated in one of the compartments, the transmission of the detonation to other compartments may be limited by fuel and diluent concentrations. If the detonation is restricted to a local region, we refer to this as a "local detonation."

Late in an accident, well-mixed conditions exist in the containment due to forced and natural convection. Hydrogen concentrations are below stoichiometric values. Typically, steam concentrations will correspond to saturated conditions at the containment temperature due to heat transfer to the structures or engineering safety features, such as the operation of sprays. If a detonation occurred under these globally well-mixed conditions, it is possible that the detonation could propagate throughout the entire containment and we refer to this as a "global detonation."

The results in this report are presented in the following manner. Experimental data and predictions for the detonation cell width are given for conditions typical of accidents first at early times and then for conditions at late times. These results are followed by the detonability limits of fuel-lean and fuel-rich hydrogen-air mixtures and stoichiometric hydrogen-air-steam mixtures obtained in the HDT.

4.2 Detonation Cell Widths for Early-Time Accident Conditions

Early in an accident, mixtures may be diluted with steam and/or carbon dioxide, with pressures at or above atmospheric pressure, and at elevated temperatures, depending on the accident scenario. Steam will be present when hydrogen is released from the primary system and carbon dioxide and steam can be generated during core-concrete interactions. Typically, all quantities, including fuel and diluent concentrations, pressure, and temperature, will vary spatially and temporally throughout the containment as the accident progresses. These quantities were varied individually in our study, however, to determine separate effects.

4.2.1 Dilution Effect

The effect of hydrogen concentration on the detonation cell width is shown by the bottom curve in Figure 4.1 for mixtures at 20°C and 1 atm. Stoichiometric mixtures (mixtures with equivalence ratios equal to one) have the smallest cell width and are the easiest to detonate. As the hydrogen concentration decreases or increases, λ increases rapidly and mixtures become increasingly difficult to detonate.

Also in Figure 4.1, the addition of carbon dioxide to mixtures at 20°C amd 1 atm increases the cell width for all mixtures. The same is true for mixtures at 100°C and 1 atm as shown in Figure 4.2. Stoichiometric mixtures with carbon dioxide concentrations of 10 and 20 percent for the conditions in Figure 4.2 increase the experimental cell width by factors of approximately 4.6 and 34.3, respectively, compared to stoichiometric mixtures without dilution. Because the critical initiation energy is proportional to the cube of λ for point charges, this means the addition of carbon dioxide decreases the likelihood of a detonation by factors of approximately 97 and 40,400, respectively.

The effect of steam addition is similar to that of carbon dioxide as shown in Figure 4.3 for mixtures at 100°C and 1 atm. Stoichoimetric mixtures with steam concentrations of 10, 20, and 30 percent increase the experimental cell width by factors of approximately 4, 23.6, and 92.8, respectively, compared to stoichiometric mixtures without steam. This corresponds to decreasing the likelihood of a detonation for these mixtures by factors of 64, 13,100, and 800,000.

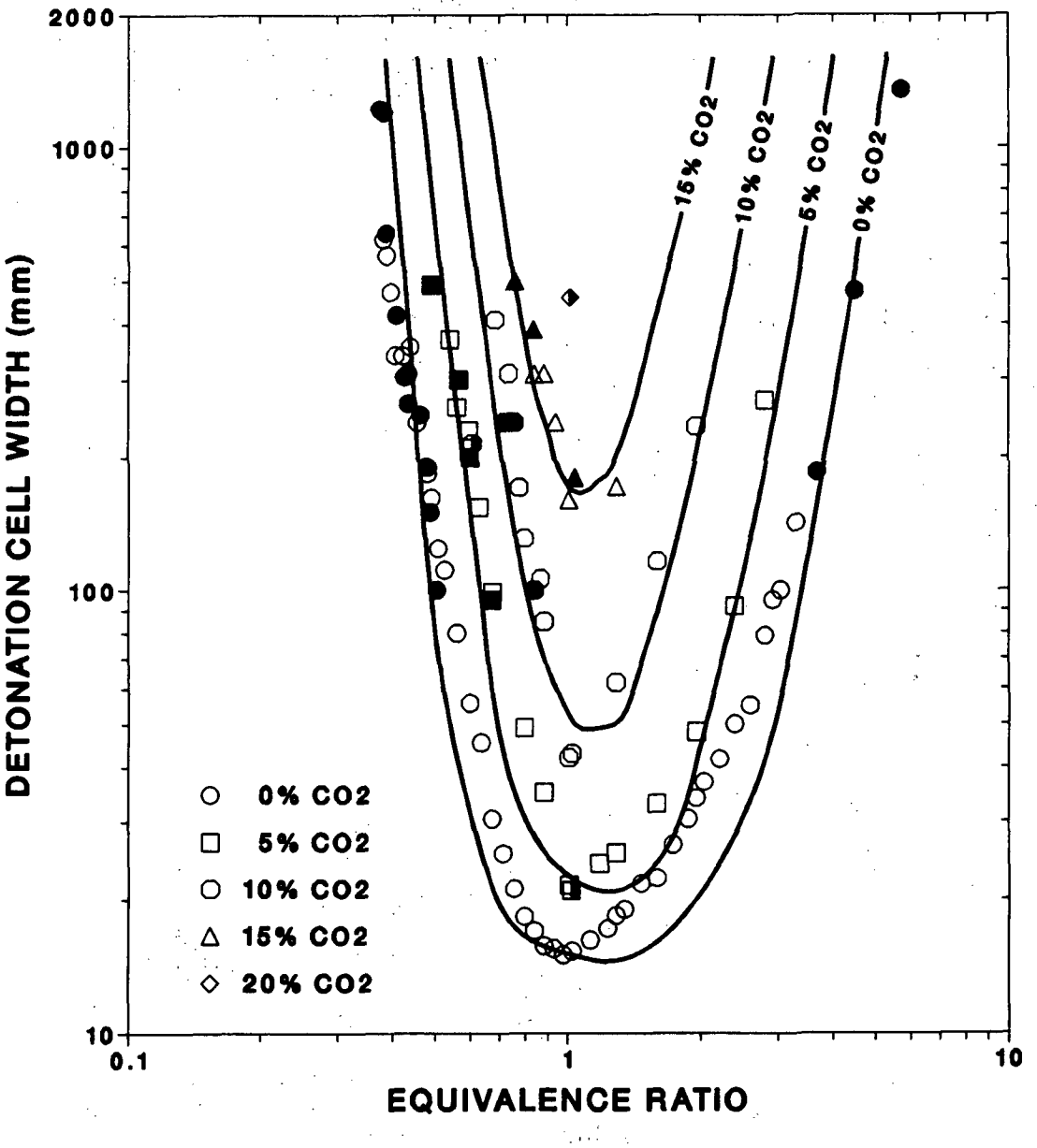

Figure 4.1 The effect of carbon dioxide dilution on the detonation cell width as a function of the equivalence ratio for hydrogen-air-carbon dioxide mixtures at 20°C initial temperature and 1 atm initial pressure (adapted from Reference 4.1) Closed and open symbols are HDT data [4.1] and McGill data [4.2], respectively. Half-closed symbols are HDT data from the present study.

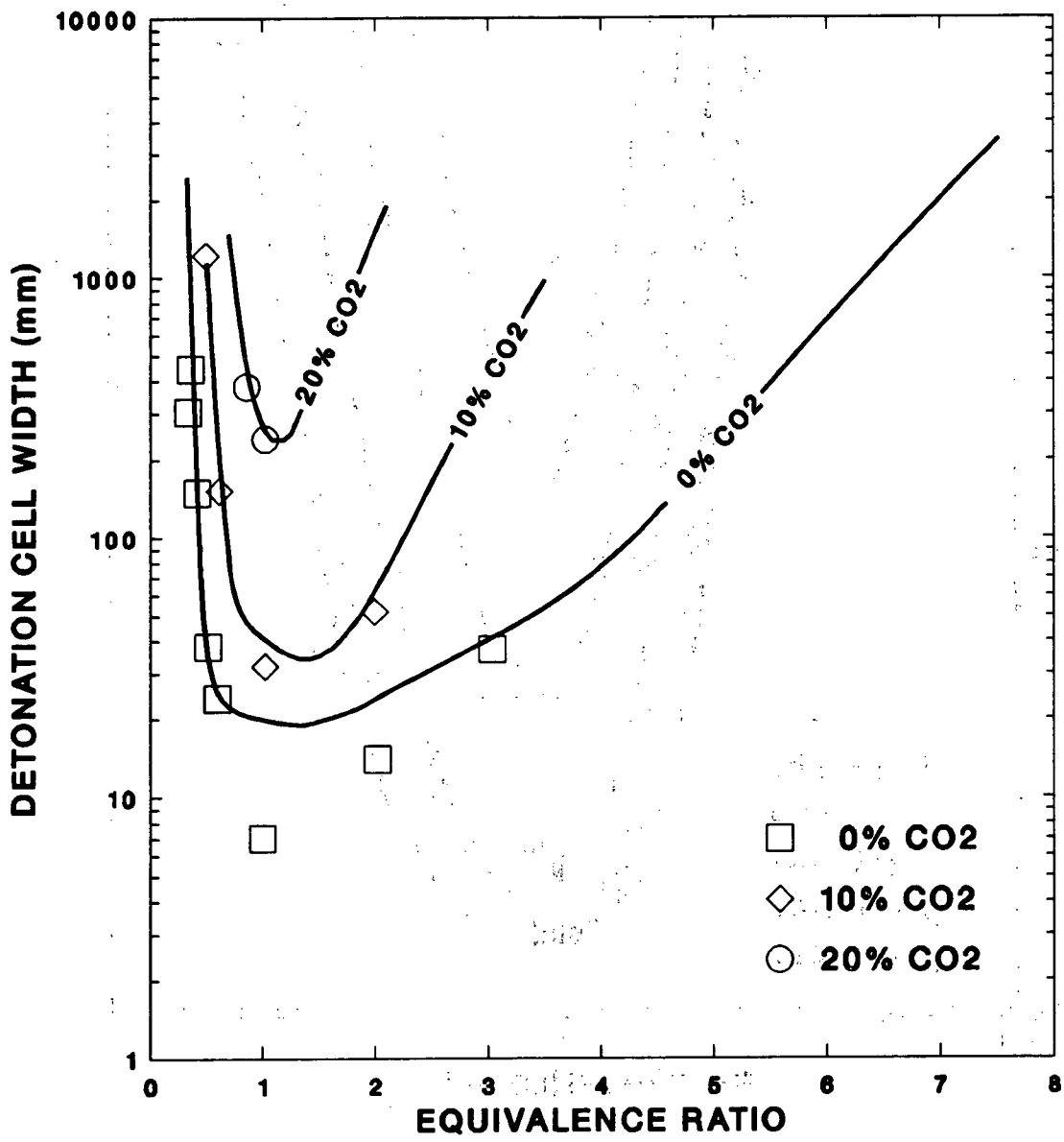

Figure 4.2 The effect of carbon dioxide dilution on the detonation cell width as a function of the equivalence ratio for hydrogen-air-carbon dioxide mixtures at 100°C initial temperature and 1 atm initial pressure.

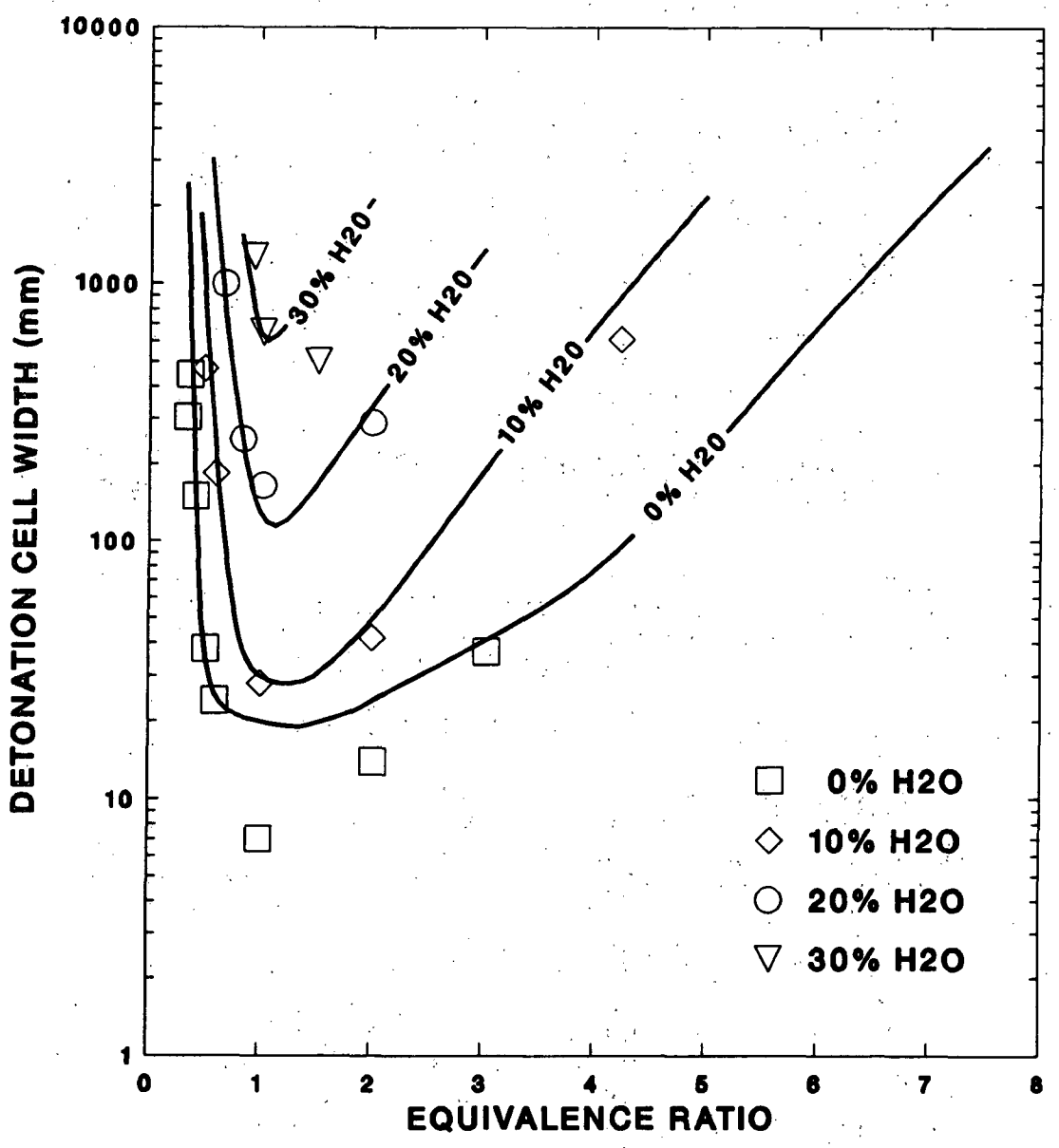

Figure 4.3 The effect of steam dilution on the detonation cell width as a function of the equivalence ratio for hydrogen-air-steam mixtures at 100°C initial temperature and 1 atm initial pressure.

Although Figure 4.3 shows the effect of large steam dilution, even small amounts of diluents can have some impact on λ. Saturated air at ambient temperatures contains around 3 percent water vapor. This condition could occur if sprays were used to condense steam, for example. One test, HT172, was conducted for a stoichiometric mixture with saturated air at 298 K and 3 percent water vapor. The cell width of 13 mm is measurably larger than the cell widths of 11 mm and 9 mm for the same mixture with dry air in tests HT97II and HT97III, respectively.

From a comparison of Figures 4.2 and 4.3, it can be seen that carbon dioxide is not only a better inhibitor than steam, but it becomes more effective relative to steam with increasing concentration. The increases in the cell width by factors of 4.6 and 34.3 for stoichiometric mixtures diluted with 10 and 20 percent carbon dioxide are progressively larger than the factors of 4 and 23.6 for 10 and 20 percent steam dilution. The data for stoichiometric mixtures and model predictions are summarized in Figure 4.4.

The experimental results in Figures 4.1-4.3 have been used to assess the ZND model for the wide range of hydrogen and diluent concentrations that may exist in an accident scenario.

4.2.2 Temperature Effect

The predicted cell width decreases, that is, detonability increases, for increases in the initial temperature up to a temperature corresponding to a minimum in λ. With further increases in temperature, λ increases slightly and the likelihood of a mixture to detonate decreases. As shown in Figure 4.5, a large decrease in λ of lean hydrogen-air mixtures at 1 atm is predicted as the temperature increases from about 300 to 500 K. For example, λ is predicted to decrease by a factor of 18.6 with a 200 K increase in temperature from 300 to 500 K for a lean mixture of 15 percent hydrogen in air (equivalence ratio equal to 0.425). The same trends exist for fuel-rich mixtures. Above 500 K to 600 K, the cell widths are comparable for all mixtures. This means that the distinction made between the difficulty in detonating fuel-lean or fuel-rich mixtures relative to stoichiometric mixtures at ambient temperatures may not be valid at elevated temperatures. All mixtures have a similar likelihood to detonate according to the predictions. The trends predicted by the model have been verified experimentally only up to 440 K.

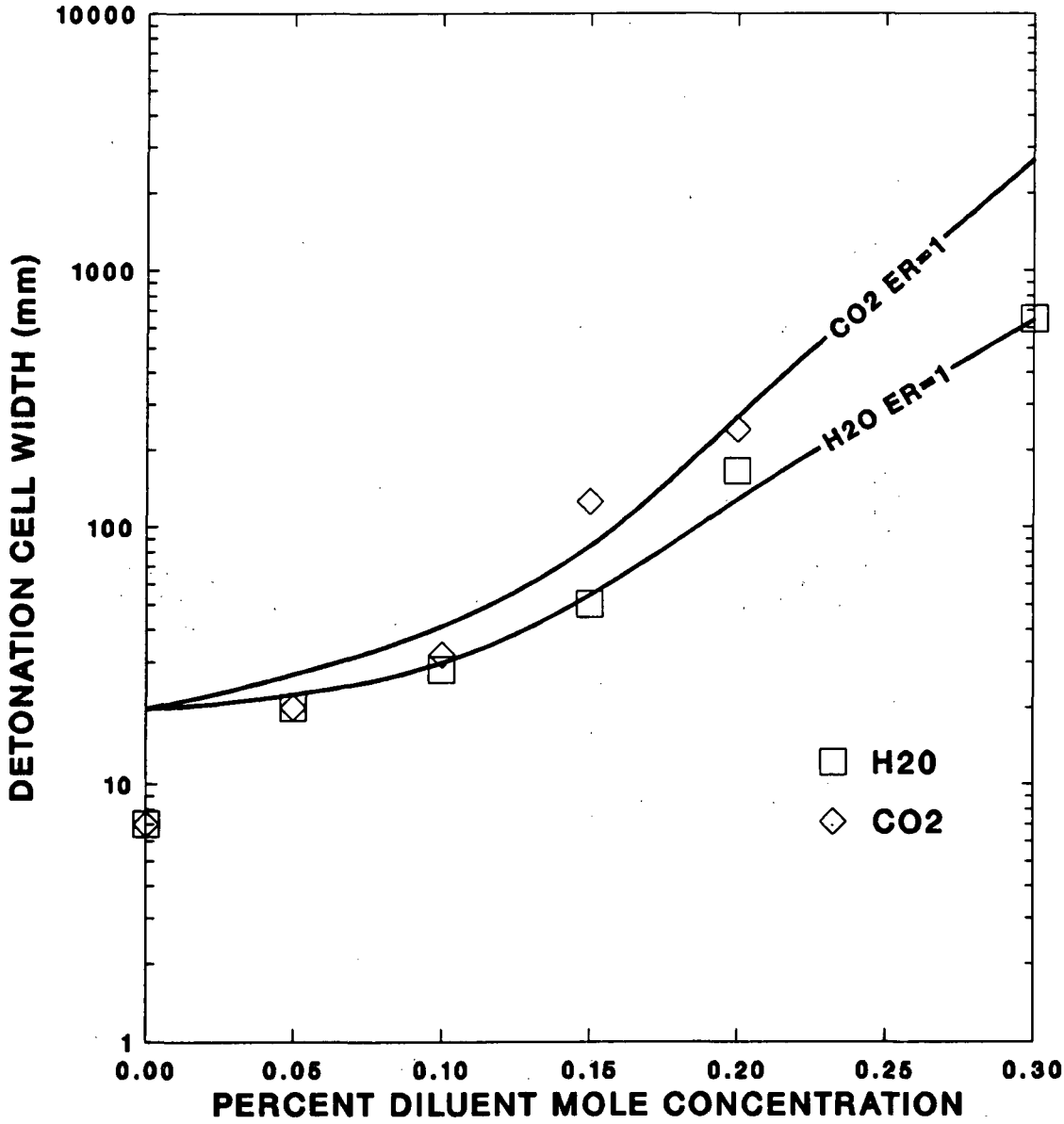

Figure 4.4 A comparison of the effect of carbon dioxide and steam dilution on the detonation cell width of stoichiometric hydrogen-air-diluent mixtures at 100°C initial temperature and 1 atm initial pressure.

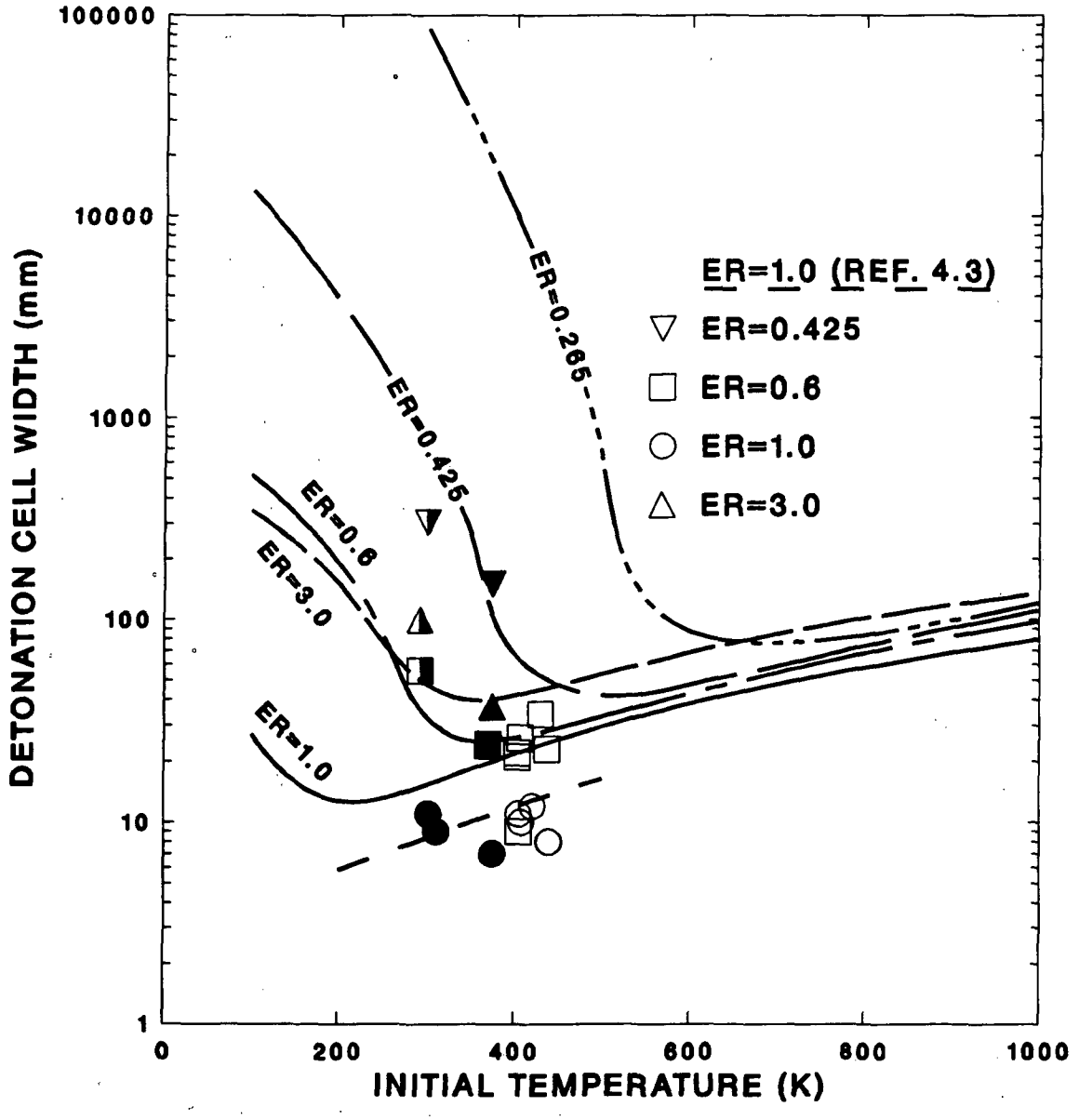

Figure 4.5 The effect of initial temperature on the detonation cell width as a function of the equivalence ratio (ER) for hydrogen-air mixtures at 1 atm initial pressure. Closed, half-closed, and open symbols represent HDT data, data from Reference [4.1], and data from F. Benz, NASA, White Sands Test Facility, respectively.

The cell width decreases with increasing temperature for mixtures at 1 atm initial pressure diluted with carbon dioxide or steam up to a temperature corresponding to a cell minimum as shown in Figures 4.6 and 4.7. With further increases in temperature, λ increases. For example, the cell width for stoichiometric mixtures diluted with 30 percent steam in Figure 4.7 decreases about an order-of-magnitude for a 300 K temperature rise. The effect of temperature on steam-diluted lean and rich mixtures is even larger. The cell width decreases almost three orders-of-magnitude for mixtures with equivalence ratios equal to 0.5 and 4.0 for a temperature rise of 400 to 500 K. That translates into a reduction of the required critical energy of a point charge by a factor of a billion. Figures 4.8 and 4.9 show the effect of temperature on lean hydrogen-air mixtures diluted with large amounts of steam. These figures are included because hydrogen released from the primary may be at elevated temperatures and highly diluted with steam at the release point.

Hydrogen-air mixtures diluted with carbon dioxide or steam have larger detonation cell widths than the same mixture without dilution. Carbon dioxide and steam mitigate the possibility of a detonation at temperatures close to ambient (293 K to 373 K) as discussed in the previous section. However, predictions imply that the mitigative effect of these diluents diminishes with increasing temperatures as shown in Figures 4.10 and 4.11 for stoichiometric mixtures at 1 atm. For example, the addition of 40 percent steam increases λ by about a factor of 200 at 380 K compared to no steam, but is predicted to increase λ by only a factor of 2 at 800 K. Carbon dioxide retains its ability to mitigate detonations better than steam at elevated temperatures.

The model has been assessed for diluted mixtures only up to 373 K. If the model is confirmed experimentally at higher temperatures, the model predictions indicate that detonations may be significantly more probable where the temperature is high.

4.3 Detonation Cell Widths for Late-Time Accident Conditions

During the course of an accident, hydrogen and steam may be added to air in the containment which is nominally at 20°C and 1 atm. The air density at these conditions is 41.6 moles/m^3. As the gases are added, the containment pressure increases due to mass addition and increased temperature. At

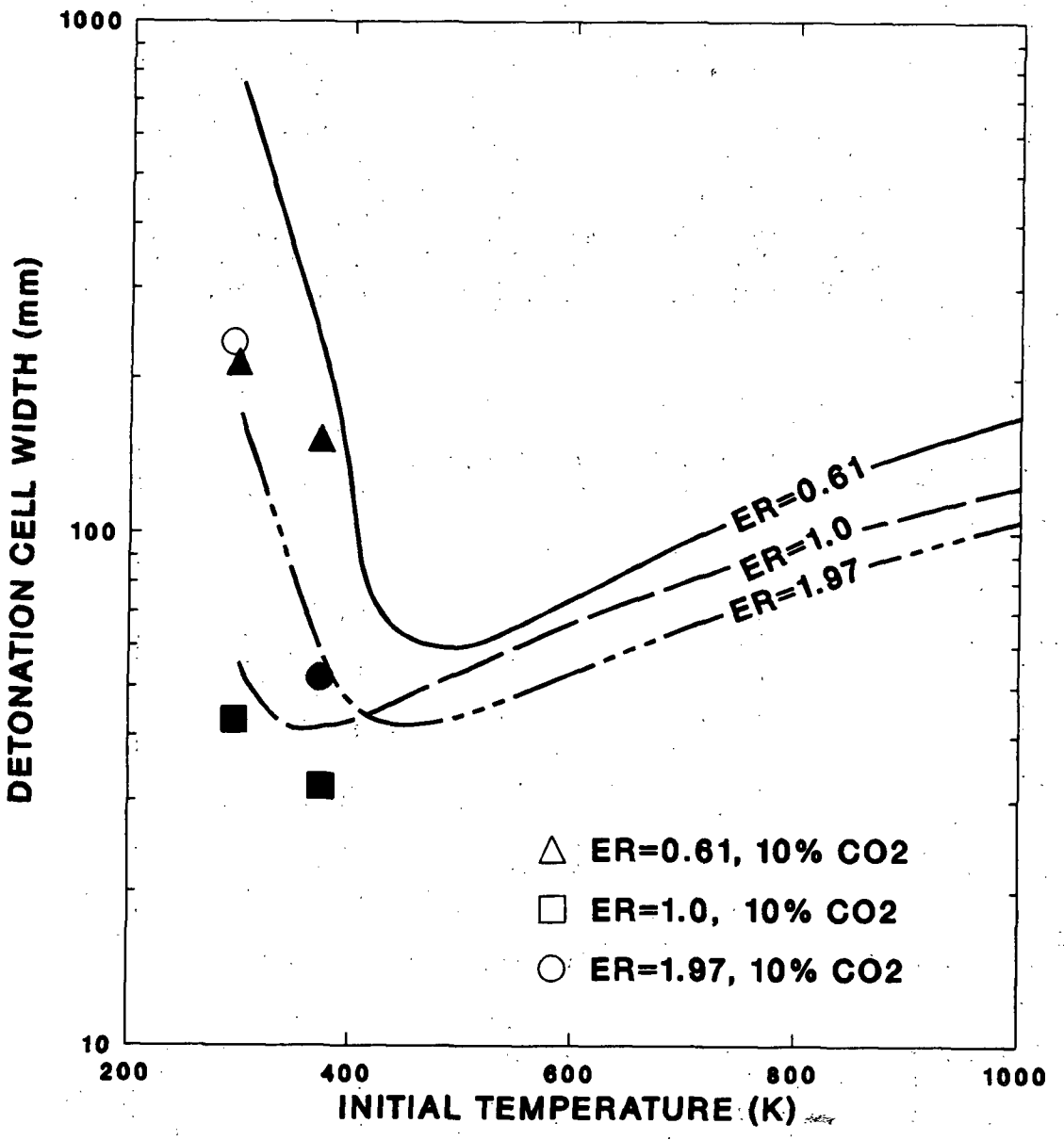

Figure 4.6 The effect of initial temperature on the detonation cell width as a function of the equivalence ratio (ER) for hydrogen-air-carbon dioxide mixtures at 1 atm initial pressure and 10% carbon dioxide dilution. Closed and open symbols represent HDT data and data from Reference 4.1, respectively.

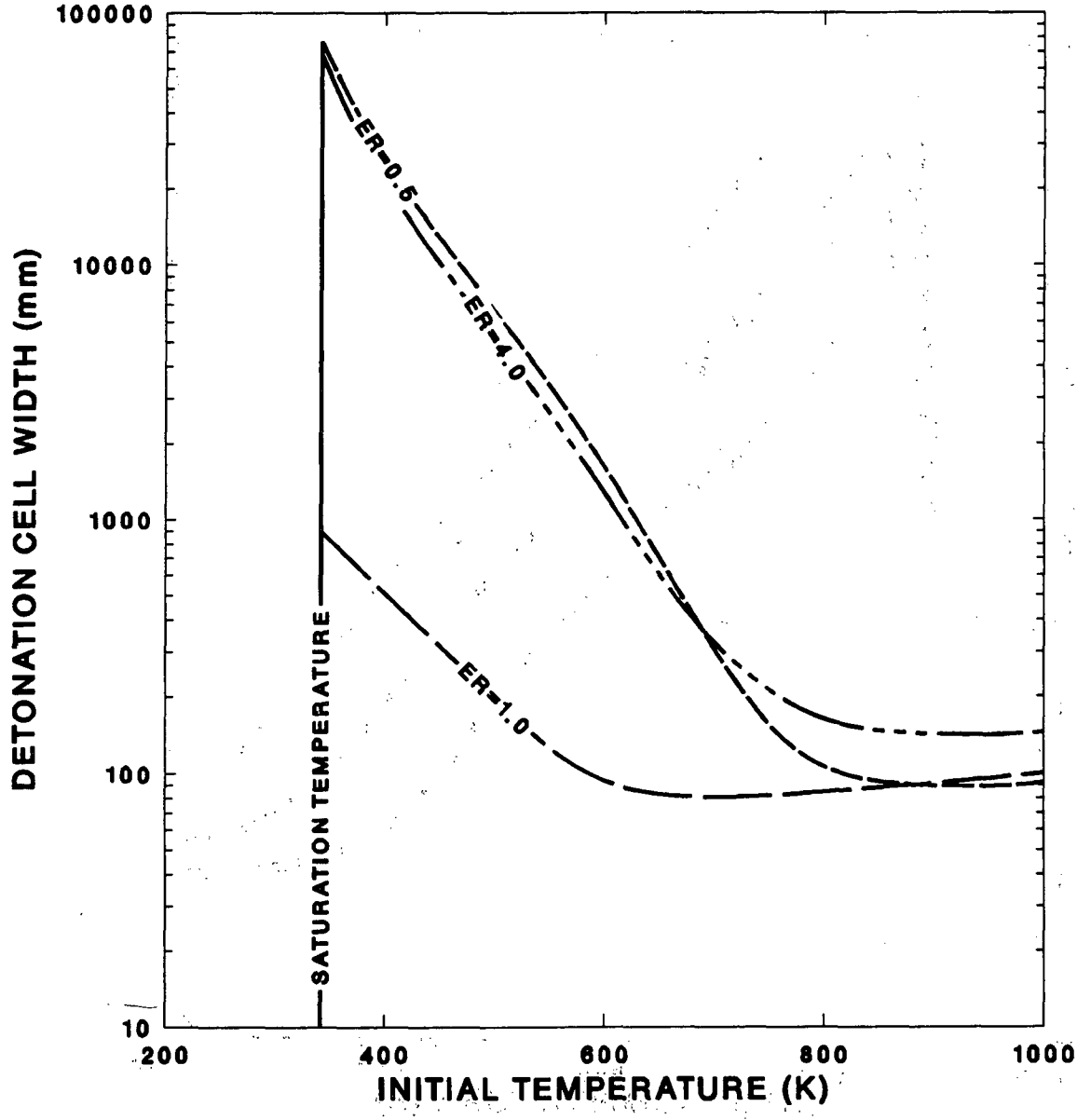

Figure 4.7 The effect of initial temperature on the detonation cell width as a function of the equivalence ratio (ER) for hydrogen-air-steam mixtures at 1 atm initial pressure and 30% steam dilution.

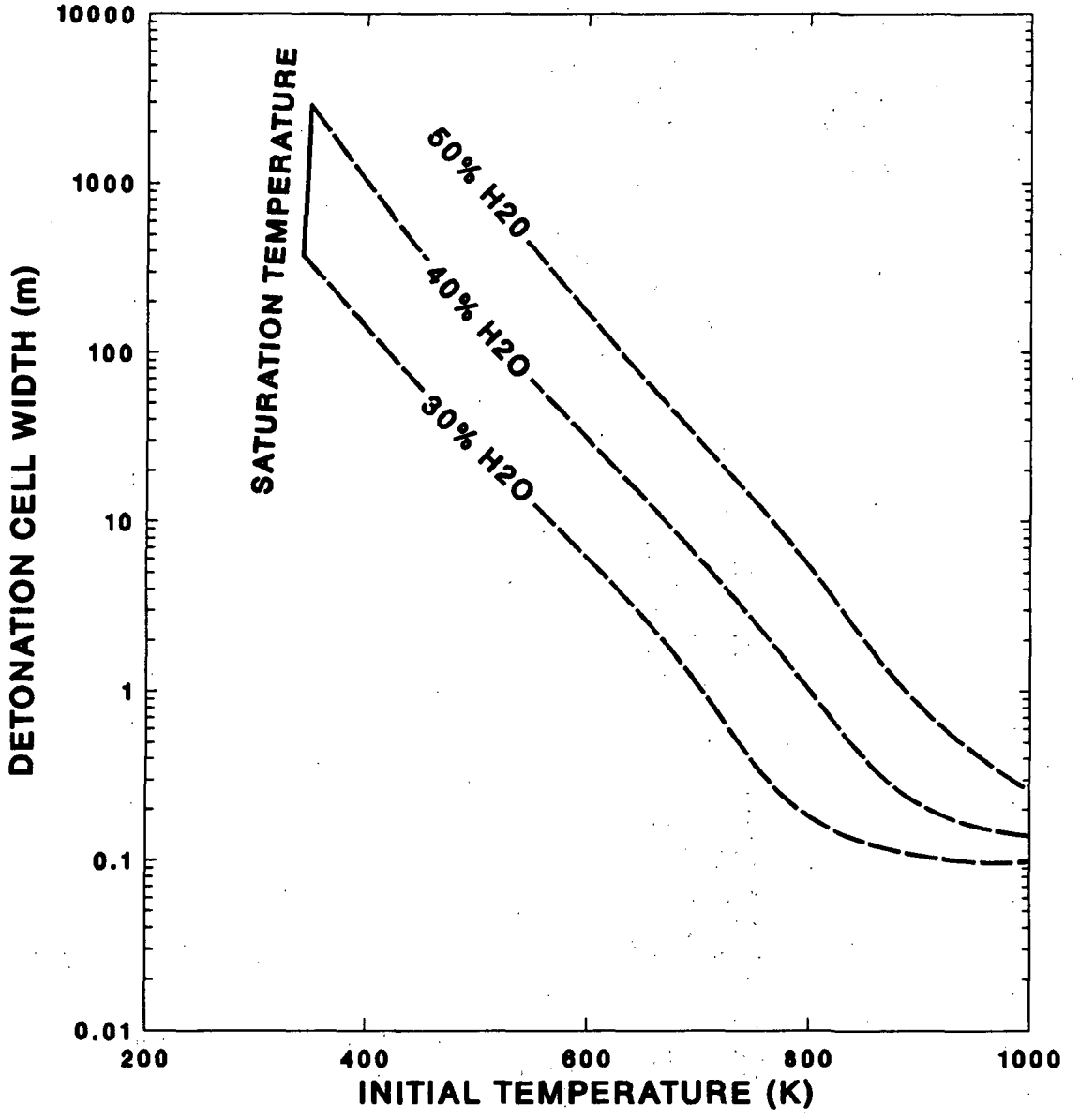

Figure 4.8 The effect of initial temperature on the detonation cell width of lean hydrogen-air-steam mixtures at 1 atm initial pressure (equivalence ratio 0.4) as a function of steam dilution.

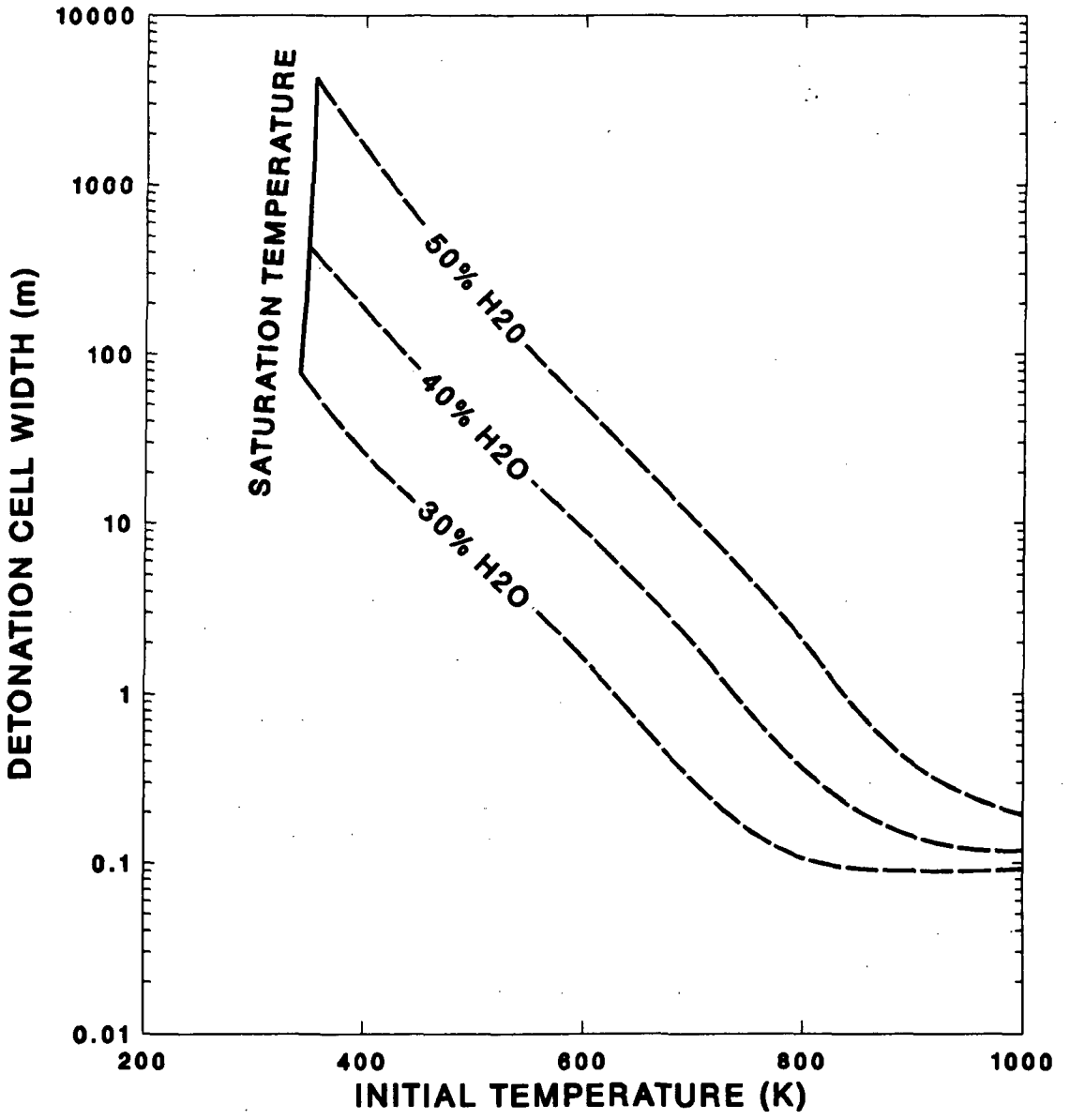

Figure 4.9 The effect of initial temperature on the detonation cell width of lean hydrogen-air-steam mixtures at 1 atm initial pressure (equivalence ratio 0.5) as a function of steam dilution.

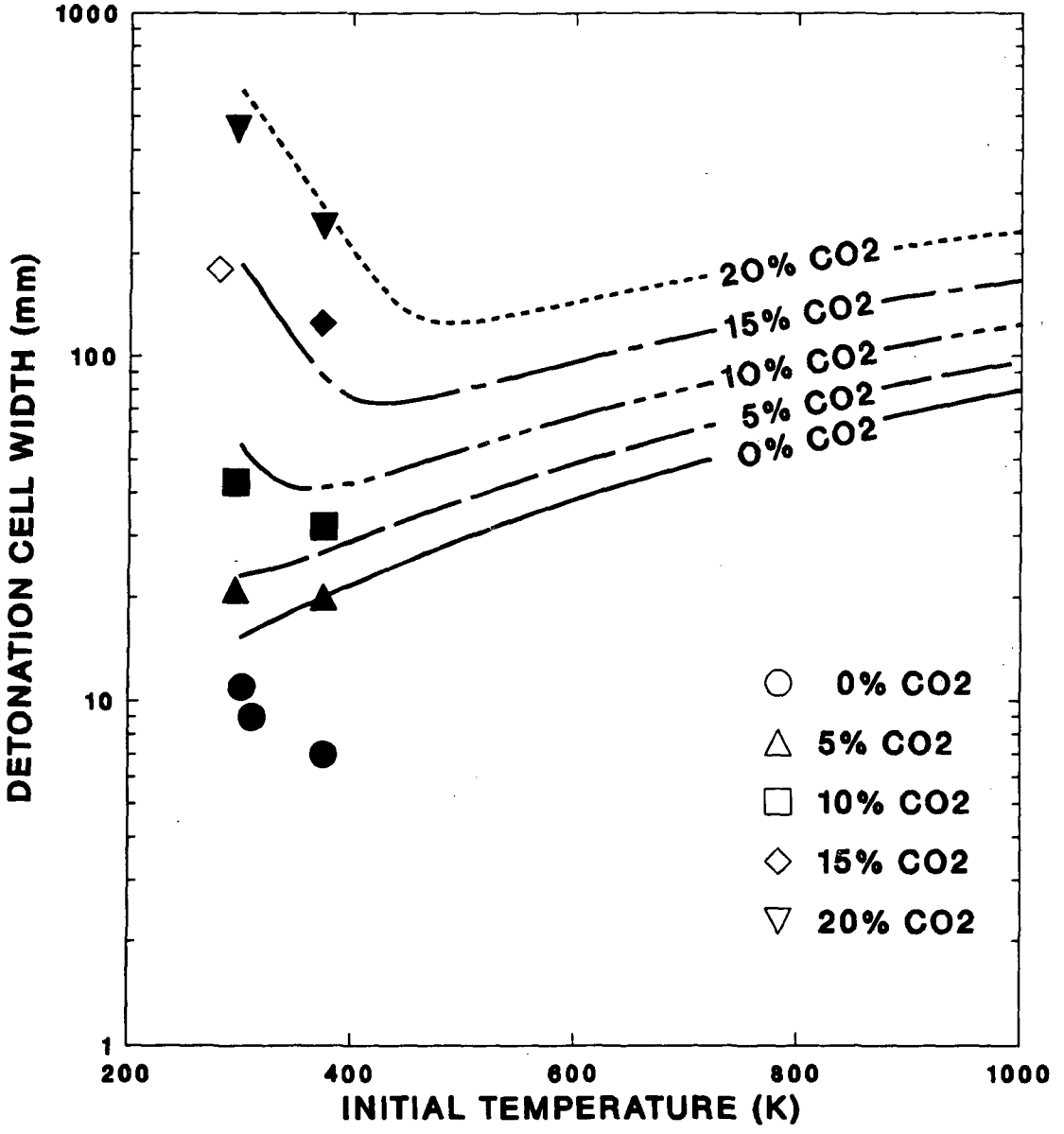

Figure 4.10 The effect of initial temperature on the detonation cell width as a function of carbon dioxide dilution for stoichiometric hydrogen-air-carbon dioxide mixtures at 1 atm initial pressure. Closed and open symbols represent HDT data and data from Reference 4.1, respectively.

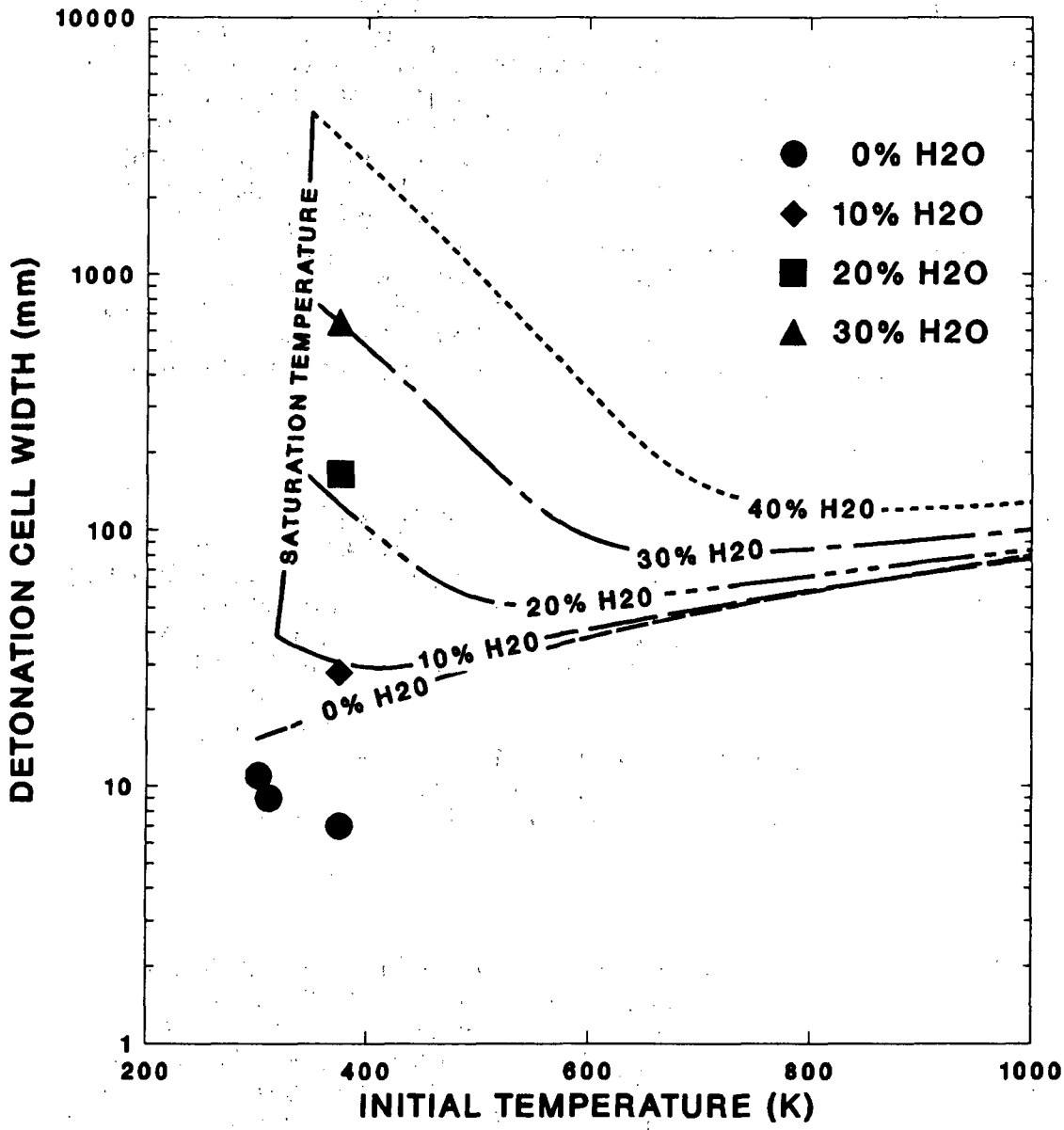

Figure 4.11 The effect of initial temperature on the detonation cell width as a function of steam dilution for stoichiometric hydrogen-air-steam mixtures at 1 atm initial pressure.

late times in the accident, the pressure may decrease from a maximum because heat transfer to the structures decreases the gas temperature and condensation removes some steam. However, noncondensable gases, like hydrogen, and saturated steam maintain pressures above atmospheric. Tests have been conducted in the HDT to simulate the conditions that may occur for a global detonation when hydrogen and steam are added to air initially at 20°C and 1 atm in the containment. The initial pressure of the mixture prior to the initiation of the detonation depends on the amount of hydrogen and steam added and the initial temperature of the mixture. For example, a stoichiometric hydrogen-air-steam mixture with 40 percent steam and an initial temperature of 110°C will have an initial total mixture pressure of approximately 3 atm. The effects of steam dilution, pressure, and temperature are discussed separately below.

4.3.1 Dilution Effect

Steam provides a mitigative effect when added to hydrogen-air mixtures having constant air density. The effect is similar to the addition of steam to mixtures having a total initial pressure of 1 atm. The data and model predictions show the influence of steam on λ in Figure 4.12 for hydrogen-air-steam mixtures nominally at 100°C and a constant initial air density of 41.6 moles/m^3. The cell width increases by factors of 6, 20, and 60 when 10, 20, and 30 percent steam is added to stoichiometric mixtures. This is comparable to the factors of approximately 4, 24, and 93 for corresponding amounts of steam added to mixtures with 1 atm total pressure.

4.3.2 Pressure Effect

An increase in initial pressure generally increases the likelihood of a mixture to detonate. The effect is small, however, for the range of pressures associated with most severe accident scenarios. Figure 4.13 shows the influence of pressure on hydrogen-air mixtures at ambient temperature (293 K). A large decrease in λ is predicted with an increase in pressure at low initial pressures. With further increases in pressure, λ passes through a local maximum and then decreases again slightly. For normal containment pressures (2/3 atm for subatmospheric and 1 atm for other types), however, increases in pressure have a small effect on λ. The cell width may increase or decrease depending on the mixture

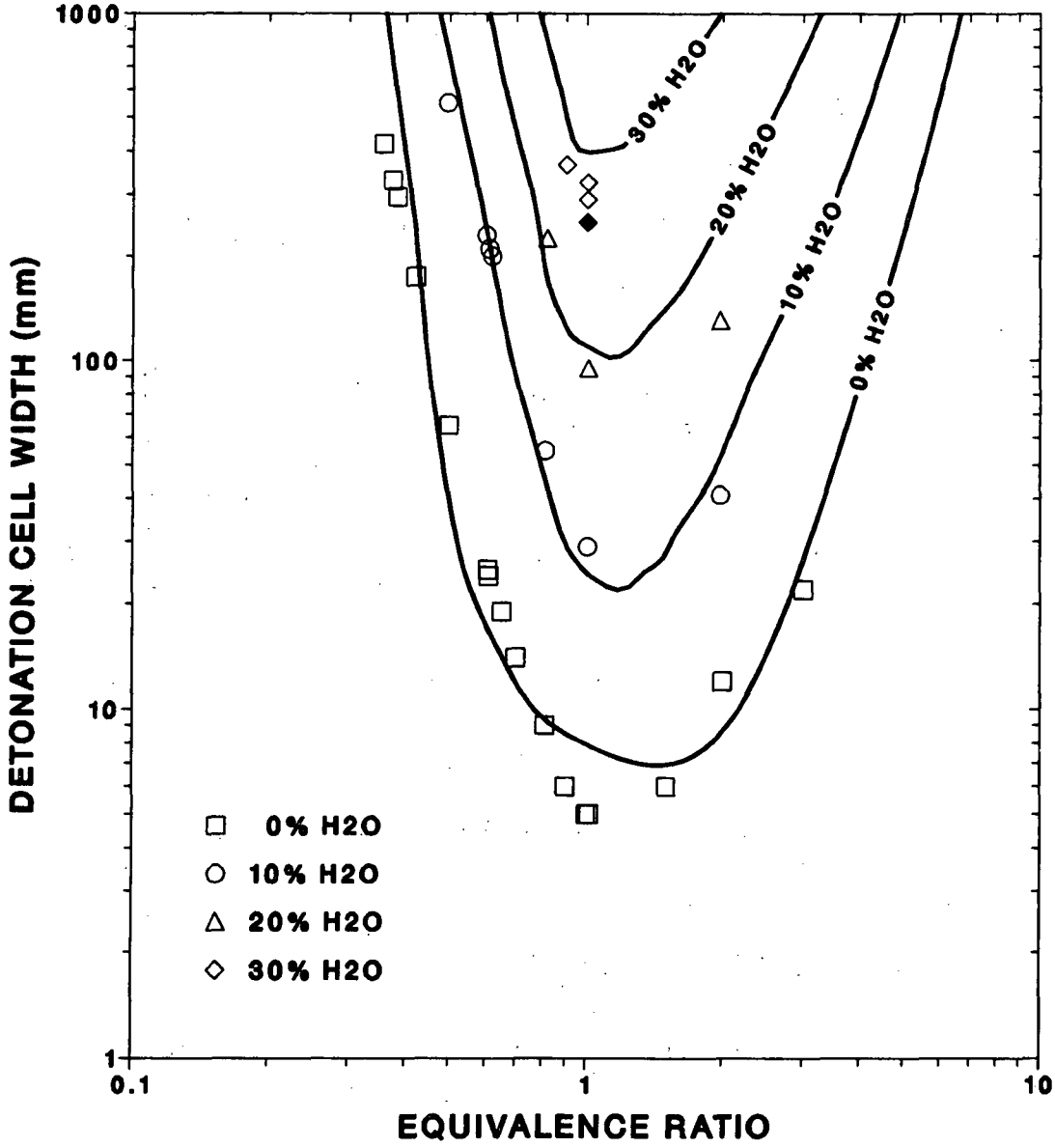

Figure 4.12 The effect of steam dilution on the detonation cell width as a function of the equivalence ratio for hydrogen-air-steam mixtures at 100°C initial temperature and an air density of 41.6 moles/m^3 (adapted from 4.1). Open and closed symbols are HDT data from Reference 4.1 and the present study, respectively.

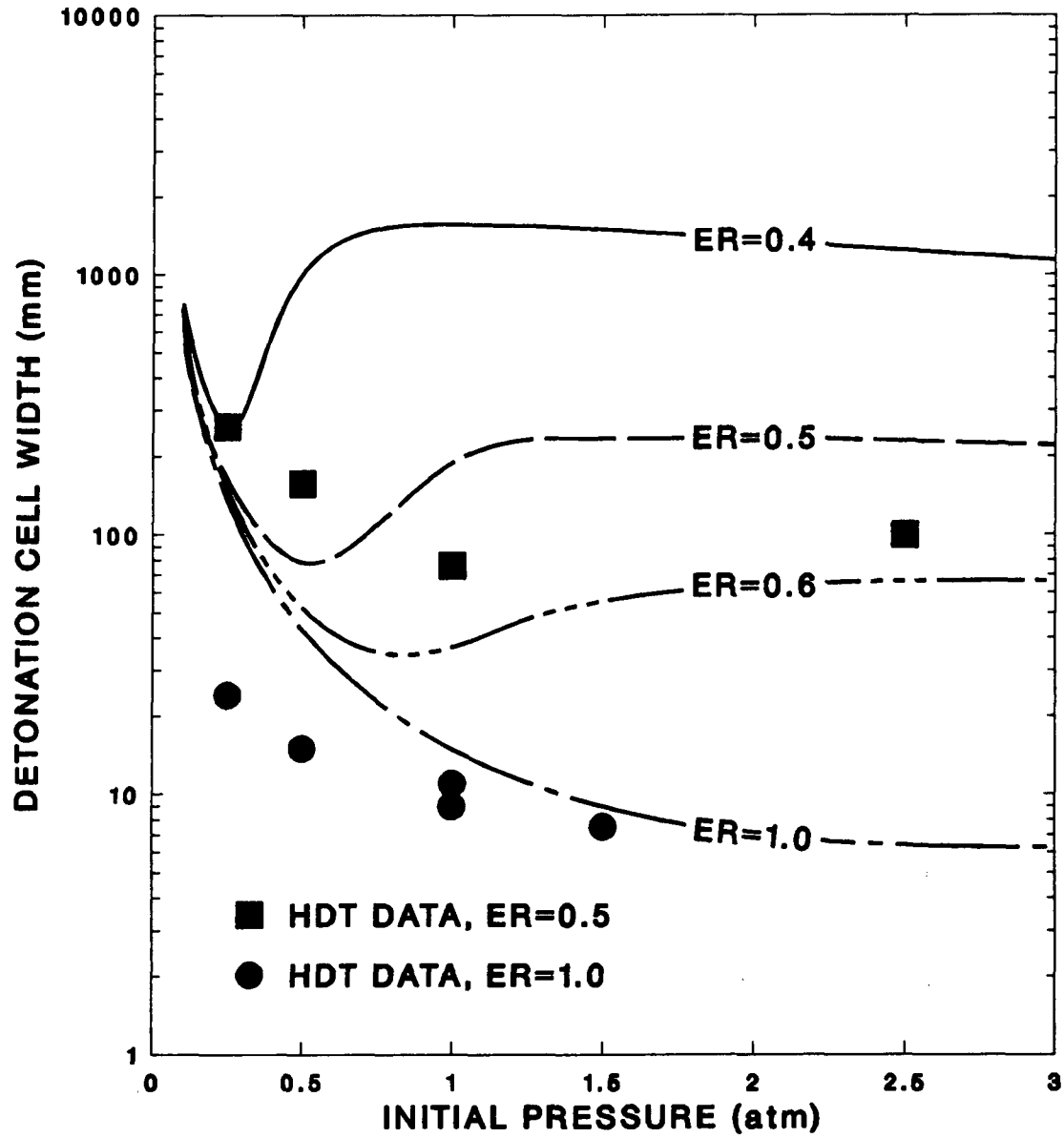

Figure 4.13 The effect of initial pressure on the detonation cell width as a function of the equivalence ratio (ER) for hydrogen-air mixtures at 293 K initial temperature.

stoichiometry. The same trend shown in Figure 4.13 for fuel-lean mixtures is also predicted to occur for fuel-rich mixtures.

Steam-diluted mixtures are also more likely to detonate as the mixture pressure increases. Figure 4.14 shows the influence of initial pressure on stoichiometric mixtures nominally at 373 K. Approximately a factor of 2 decrease in λ is possible for an increase in pressure from 1 to 3 atm. This corresponds to a factor of 8 increase in the likelihood of these mixtures to detonate.

4.3.3 Temperature Effect

Mixtures with constant air density are more likely to detonate as the initial temperature increases. Typically, the temperatures are much lower late in an accident than possible at early times. While local temperatures may be very high near the release early in the accident, the gas temperature decreases as heat is transferred to the containment at later times. Figure 4.15 shows the influence of temperature in the bottom two sets of data points for hydrogen-air mixtures at constant air density. For a stoichiometric mixture the cell width decreases by approximately a factor of two for an 80 K increase in temperature. The top two sets of data points in Figure 4.15 show an effective increase in pressure of hydrogen-air mixtures at constant temperature. For example, the stoichiometric mixture at 293 K and air density of 41.6 moles/m^3 has a total mixture pressure of about 1.4 atm. The cell width for this mixture decreases as the pressure increases from 1 to 1.4 atm.

The results presented in this section show that steam increases the detonation cell width and can mitigate detonations at temperatures near ambient. The effectiveness of steam, however, is decreased by increasing temperature and pressure. It is predicted that this effect is most pronounced early in an accident when temperature excursions may be larger than those likely at late times.

4.4 Detonation Limits

In our study, a detonation was considered to be self-sustaining if the velocity was constant in the latter section of the HDT and cellular structure was recorded on the sooted

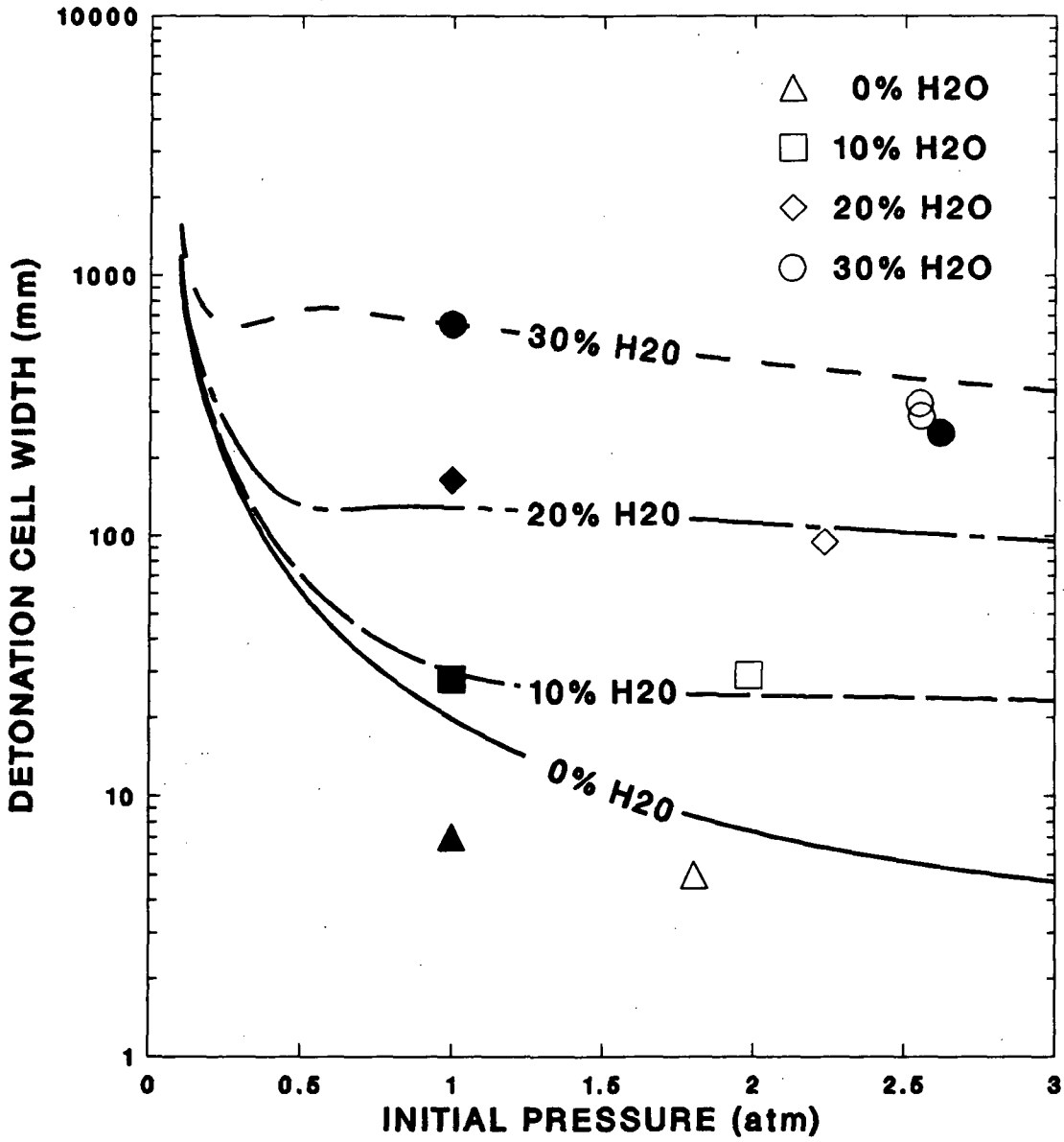

Figure 4.14 The effect of initial pressure on the detonation cell width as a function of steam dilution for stoichiometric hydrogen-air-steam mixtures at 373 K initial temperature. Open and closed symbols represent HDT data from Reference 4.1 and the present study, respectively.

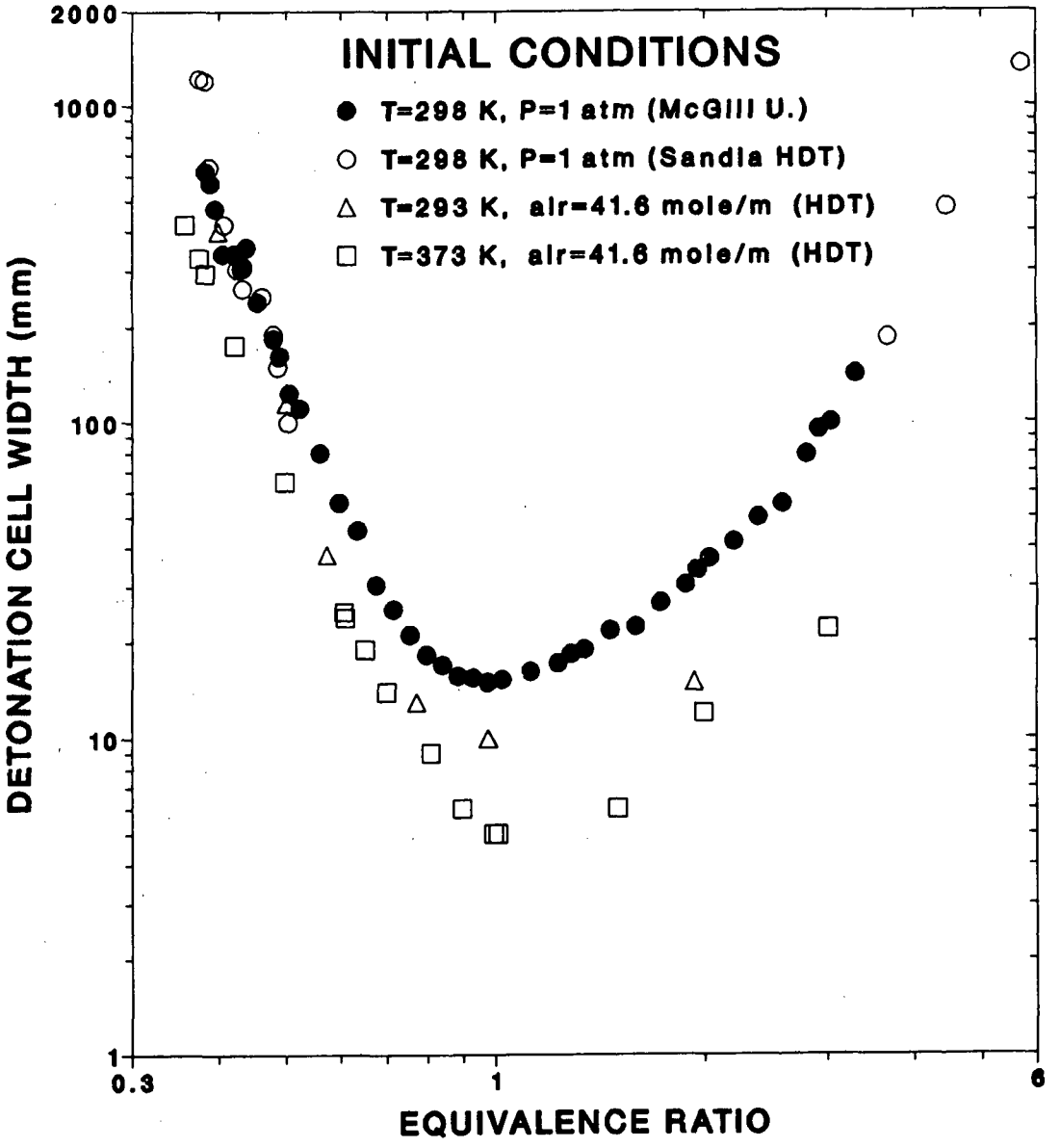

Figure 4.15 The effect of initial conditions on the detonation cell width of hydrogen-air mixtures (adapted from Reference 4.1). Open and closed symbols are HDT data and McGill data from Reference 4.1.

foils. Otherwise, if the velocity continuously decreased along the length of the HDT and no structure was recorded, the detonation was assumed to have failed. No cellular structure was ever observed when the velocity continuously decreased along the length of the HDT. Detonation limits may be determined by one of two criteria: propagation or initiation. With one exception, all limits obtained were due to the inability of a mixture to propagate a detonation. The ratio of the HDT length to diameter is approximately 30. The detonation limit obtained for hydrogen-air-steam mixtures with an air density of 41.6 moles/m^3 was different than the other limits obtained in the HDT. This limit was obtained due to insufficient charge strength. This was inferred since the cell size of the mixture prior to failure was well below the single-head spin regime that is associated with the propagation criterion.

The detonable range of hydrogen in a hydrogen-air mixture at 1 atm pressure and 20°C (293 K) in the HDT for a planar initiating charge of approximately 100 g of high explosive is between 11.6 and 74.9 percent by volume. This range is much wider than the range of 18 to 59 percent reported earlier by Shapiro and Moffette [4.4]. No detonation was observed at 11.4 percent and 75.9 percent hydrogen for lean and rich mixtures, respectively. At 100°C (373 K) initial temperature and 1 atm pressure, the range of detonable concentrations expands to between 9.4 and 76.9 percent. No detonation was observed at 8.8 percent and 77.9 percent hydrogen for lean and rich mixtures, respectively. The widening of the limits between 20°C and 100°C by approximately 2 percent hydrogen on a volume basis on both the lean and rich limits illustrates the important effect of increasing temperature.

The concentration of steam that prevents a detonation in the HDT was determined for stoichiometric hydrogen-air-steam mixtures with either 1 atm total pressure or with an air density of 41.6 moles/m^3. This concentration is between 38.8 and 40.5 percent steam for mixtures with 1 atm total pressure. For mixtures with an air density of 41.6 moles/m^3, this concentration is between 29.6 and 31.9 percent steam. This concentration depends on many physical factors and does not necessarily represent the limit in the HDT.

The concentration of steam that prevents a detonation depends strongly on the initiating charge geometry and

strength, in addition to tube scale and geometry. Three different charge geometries, which included a toroidal, helical, and planar geometry, with different initial strengths were used to determine this concentration for mixtures with an air density of 41.6 moles/m^3. For an initiation charge using primacord shaped in the form of a torus having a charge strength of 110 g of high explosive, a detonation propagated in the HDT with 29.6 percent steam and λ equal to 250 mm. This is in reasonable agreement with the values of 285 mm and 300 mm measured by Tieszen et al. [4.1] for the same mixture. No detonation was observed, however, for steam concentrations of approximately 32 to 37 percent for the toroidal charge geometry and charge strengths up to 125 g of high explosive. For an initiation charge using primacord shaped in the form of a helix, no detonation was observed for any steam concentration between approximately 30 and 37 percent for charge strengths of 100 g of high explosive. Likewise, no detonation was observed for a planar charge using detasheet for steam concentrations between 37 and 40 percent for charge strengths up to 94 g of high explosive. The important effect of charge geometry is illustrated by the failure of a helical charge to initiate a detonation in a stoichiometric hydrogen-air-steam mixture diluted with approximately 30 percent steam while a toroidal charge with approximately the same strength was successful.

We propose that the inability to obtain a detonation in the HDT for steam concentrations greater than 29.6 percent is due to an inadequate charge strength for initiation. The critical initiation energy is proportional to λ and the initial mixture pressure for planar initiation charges [4.5]. The effect of pressure on the critical initiation energy explains why the detonation limit in the HDT is so different for a stoichiometric hydrogen-air-steam mixture with the initial mixture pressure equal to 1 atm and an equivalent mixture with the air density equal to 41.6 moles/m^3. The maximum concentration of steam that will allow a detonation to propagate is 38.8 percent for a mixture with total pressure of 1 atm. For an equivalent mixture with 38.8 percent steam and an air density of 41.6 moles/m^3, however, the total pressure is slightly over 3 atm after the hydrogen and steam are added. A larger amount of energy would be necessary to initiate a detonation in this mixture because of the large increase in initial pressure. Because of facility restrictions, however, similar initiation strengths equal to the facility maximum are used. Therefore, the lower

detonation limit of only 29.6 percent steam for the stoichiometric hydrogen-air-steam mixture with an air density of 41.6 moles/m^3 is obtained compared to the limit of 38.8 percent steam for a stoichiometric mixture at 1 atm initial pressure. Since it is probable that the detonation limit obtained for a stoichiometric mixture with an air density of 41.6 moles/m^3 was limited by HDT restrictions, we caution against the use of this value for reactor safety applications.

The results from the two detonation limits for stoichiometric hydrogen-air-steam mixtures indicate that global detonations in reactor containments may be more difficult to initiate directly than local detonations. This is because initial pressures of globally well-mixed gases will be higher for accidents in which large quantities of steam and hydrogen are added to air initially at 20°C and 1 atm in the containment than pressures of approximately 1 atm for a potentially detonable mixtures near the source. The results, however, do not address the problem of detonation initiation through the flame acceleration and deflagration-to-detonation transition mechanism. The influence of pressure on this mechanism is currently not well known.

Detonations at the limits have characteristics different from the multiheaded detonations that exist between the limits. The mode of the detonation at the limits is characterized by either a single-rotating pressure wave (single-head spin) or counterrotating pressure waves. The detonation velocity at the limits is within approximately ±6 percent of the theoretically calculated CJ value. Both modes exist as a result of an acoustic coupling with the HDT cylindrical geometry. Either mode appears equally likely as the limits are approached.

The propagation criteria shown in Figure 1.1 in the Introduction section separates the regions of multiheaded detonations and the onset of single-head spin. Single-head spin may exist, however, for a range of concentrations before the detonation fails as shown in Table B.2. Therefore, it is nonconservative to use the propagation criteria to estimate detonability limits.

The cellular data recorded on the sooted foils exhibit a cellular substructure that indicates a possible secondary instability. This cellular substructure has been noted

previously [4.6] and it has been shown to exist when the ratio of the activation energy and postshock gas temperature exceeds a critical value. Additionally, a submillimeter cellular structure exists in the loci of triple-point intersections similar to that observed by Manzhalei and Mitrofanov [4.7]. Normally the triple point path is very narrow and appears as a line on the sooted foils for multiheaded detonations. For detonations near the limits of the HDT, however, the triple-point path may be up to 230 mm wide. Understanding subcellular structure may ultimately help reduce the uncertainty in cell size measurement.

4.5 References for Chapter 4

4.1 Tieszen, S. R., Sherman, M. P., Benedick, W. B., Shepherd, J. E., Knystautas, R., and Lee, J. H. S., "Detonation Cell Size Measurements in Hydrogen-Air-Steam Mixtures," Dynamics of Explosions: Progress in Aeronautics and Astronautics, (edited by Bowen, Leyer, and Soloukhin) AIAA, New York, V106, pp. 205-219, 1986.

4.2 Lee, J. H., Knystautas, R., Guirao, C., Benedick, W. B., Shepherd, J. E., "Hydrogen-Air Detonations," Proceedings of the Second International Conference on the Impact of Hydrogen on Water Reactor Safety, NUREG/CP-0038, EPRI RP 1932-35, SAND82-2456, pp. 961-1005, October 1982.

4.3 Westbrook, C. K., and Urtiew, P. A., "Chemical Kinetic Prediction of Critical Parameters in Gaseous Detonations," Nineteenth Symposium (International) on Combustion, The Combustion Institute, Pittsburgh, pp. 615-623, 1982.

4.4 Shapiro, Z. M., and Moffette, T. R., "Hydrogen Flammability Data and Application to PWR Loss-of-Coolant Accident," WAPD-SC-545, Bettis Plant, September 1957.

4.5 Benedick, W. B., Guirao, C. M., Knystautas, R., and Lee, J. H., "Critical Charge for the Direct Initiation of Detonation in Gaseous Fuel-Air Mixtures," Dynamics of Explosions: Progress in Astronautics and Aeronautics, (edited by Bowen, Leyer, and Soloukhin) AIAA, New York, V106, pp. 181-202, 1986.

4.6 Manzhalei, V. I., "Fine Structure of the Leading Front of a Gas Detonation," Fizika Goreniya i Vzryva, V13, No. 3, pp. 470-472, 1977.

4.7 Manzhalei, V. I., and Mitrofanov, V. V., "The Stability of Detonation Shock Waves with a Spinning Configuration," Fizika Goreniya i Vzryva, V9, No. 5, pp. 703-710, 1973.

5. DISCUSSION

5.1 High-Temperature Hydrogen Combustion

There are at least three accident scenarios that involve the combustion of hydrogen at elevated temperatures: (1) the in-cavity oxidation of combustible gases produced by core-concrete interactions, (2) the direct containment heating (DCH) hydrogen scenario, and (3) hot hydrogen-steam releases from the reactor coolant system (RCS).

In all scenarios, hot jets are injected into cooler downstream mixtures. The jets may be composed of a combination of hydrogen, carbon monoxide, steam, carbon dioxide, or nitrogen depending on the accident scenario. The downstream jet temperature may be above or below the autoignition temperature. In some cases, the jet temperature is initially below the autoignition temperature and gradually increases above it as the accident progresses. The downstream mixture may be nonflammable or combustible. A description of the conditions in the accident scenarios is given in [5.1] along with the potential consequences of high temperature hydrogen combustion.

Different modes of combustion may result in any of these scenarios depending on the competition between chemical and physical rates that govern the combustion process. If fuel is consumed at the same rate as it is injected into a compartment, then no hydrogen accumulates and the resulting combustion mode is a standing diffusion flame (Figure 5.1a). If the fuel is injected faster than it is consumed, then hydrogen accumulates and the subsequent combustion mode may be a diffusion flame, deflagration, or a detonation (Figure 5.1b). The probability that a particular mode will exist depends on the competition between the convective mixing rate, the mass diffusion rate, and the chemical reaction rate (Figure 5.2). If both the mass diffusion rate of molecular species (hydrogen and oxygen towards the reaction zone and water away from the zone) and the chemical reaction rate exceed the convective mixing rate, a diffusion flame will exist. On the other hand, if either the chemical reaction rate or mass diffusion rate is slower than the convective mixing rate, the hydrogen and oxygen will mix and a deflagration or a detonation can occur. A premixed situation may also exist if the ignition delay time is large relative to the mixing time.

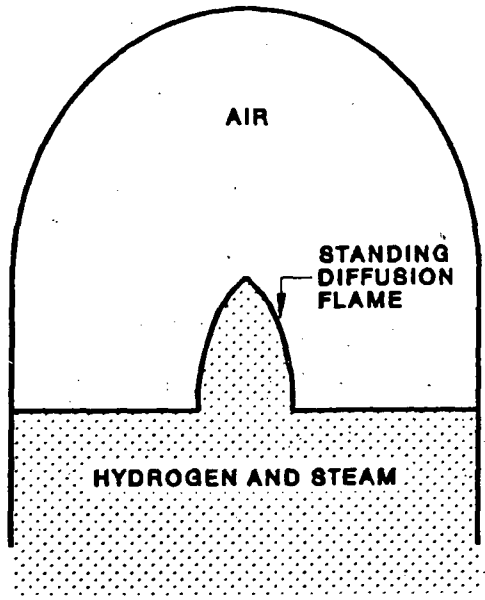

(a)

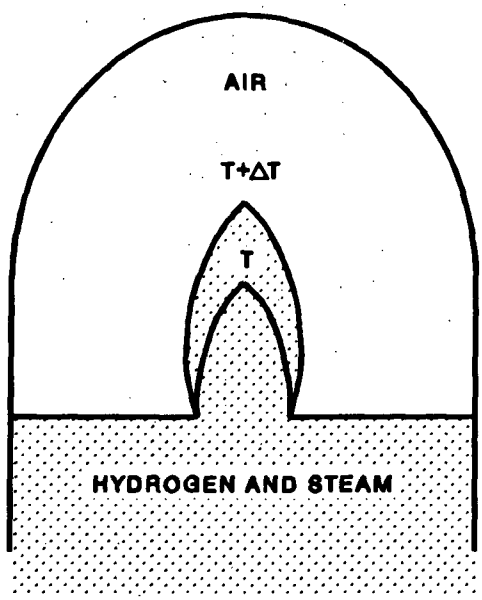

(b)

Figure 5.1 Various combustion modes that may exist (a) no hydrogen accumulation and combustion mode is a diffusion flame (b) hydrogen accumulates and the subsequent combustion mode may be a diffusion flame, deflagration, or a detonation.

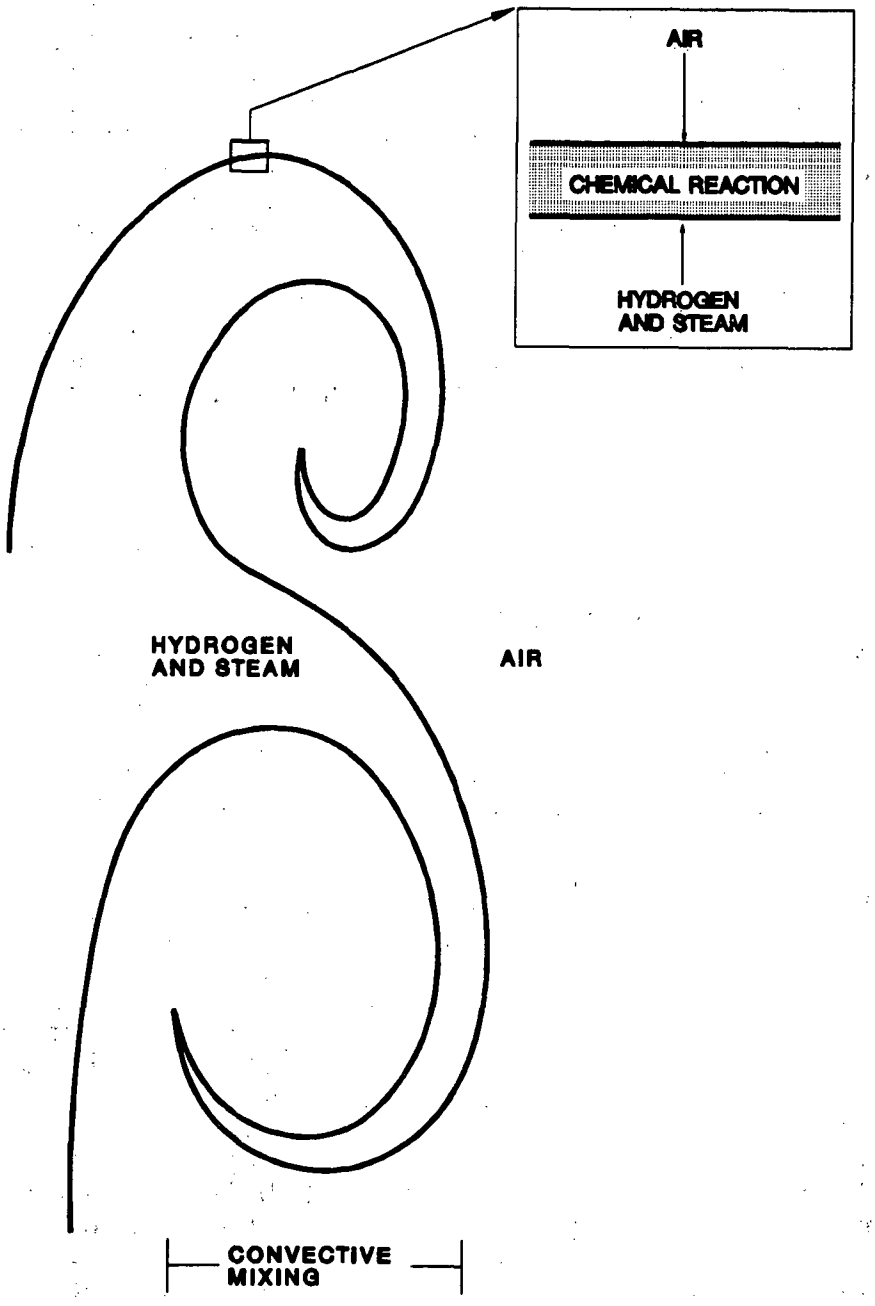

Figure 5.2 The mode of combustion depends on the relative rates of mass diffusion, chemical reaction, and convective mixing.

Based on the predicted results presented in Section 4.2.2, the possibility of a local detonation in any of the accident scenarios listed above may be more likely than previously considered. For all the scenarios, the hydrogen can be diluted with large amounts of steam or carbon dioxide near the release. At the same time, however, gas temperatures are usually very high, reducing the effectiveness of the diluent. For temperatures that are high but below the mixture autoignition temperature, all mixtures are predicted to have a similar likelihood to detonate. The energy necessary to initiate a detonation directly in a diluted off-stoichiometric mixture at elevated temperatures is substantially less than the same mixture at lower temperatures.

5.2 Combustion Limits

A comparison of the flammability, flame acceleration, and detonability limits is shown in Table 5.1. The detonability limits are not intrinsic but depend on scale, geometry, and initiation charge strength. The flame acceleration limit is defined as the location where the flow is choked (flame speed equal to the speed of sound of the combustion products). The flame acceleration limits are also not intrinsic. These limits depend not only on scale, geometry, and initiation strength as with the detonability limits, but also on other parameters such as obstacle type, spacing, and blockage ratio. Flammability limits are scale independent for sufficiently large vessels (diameters greater than 5 cm and lengths greater than 1.2 m) but depend on direction for lean hydrogen mixtures.

Several important points can be made from the comparison of the various combustion limits. First, a comparison of the detonability limits for hydrogen-air mixtures shows the important effect of increasing initial temperature. The widening of the limits from 20°C to 100°C by approximately 2 percent hydrogen on a volume basis on both the lean and rich limits illustrates the important sensitizing effect of increasing initial temperature. Second, a comparison of the flame acceleration and detonability limits indicates the limits are similar for most mixtures tested. And finally, a comparison of the flammmability and detonability limits for the mixtures in Table 5.1 shows that the limits are similar for some mixtures and, while there is a discrepancy between the limits for the other mixtures, the limits are much closer than previously thought. For those mixtures in which the limits are similar, if the mixture can deflagrate it can also

COMPOSITION	THERMODYNAMIC STATE	FLAMMABILITY LIMITS	FLAME ACCELERATION LIMITS +	DETONATION LIMITS
Lean H_2-Air	T=20°C, P=1 atm	4.3-9.4% H_2[5.2]-[5.3] (UP-DP)*	10% H_2§	11.6% H_2
Lean H_2-Air	T=100°C, P=1 atm	4.0-8.7% H_2[5.2]-[5.3] (UP-DP)δ		9.4% H_2
Rich H_2-Air	T=20°C, P=1 atm	75% H_2[5.2]#	72.5% H_2§	74.9% H_2
Rich H_2-Air	T=100°C, P=1 atm	77.4% H_2[5.2]&		76.9% H_2
Steam-Diluted Stoichiometric H_2-Air	T=100°C 0.2 atm<P<0.5 atm	63.3% H_2O[5.4]α	45% H_2O@	38.8% H_2

+ Acceleration of flame to the isobaric sound speed

* The range of reported values for upward propagation (UP) is 4.2% H_2[5.5]-5% H_2[5.6] and the range for downward propagation (DP) is 8.3% H_2[5.6] - 10% H_2[5.6]

δ The range of reported values for upward propagation is 4.0% H_2[5.2]-4.5% H_2[5.6] and the range for downward propagation is 8.6% H_2[5.4]-8.7% H_2[5.3]

\# The range of reported values for upper flammability limits is 71.3% H_2[5.3]-75.2% H_2[5.7]

& The range of reported values for upper flammability limits is 73.6% H_2[5.3]-77.4% H_2[5.2]

α The reported steam-inerting limit varies from 49% H_2O[5.8] - 63.3% H_2O[5.4]

@ The range of values for flame acceleration limits is 35% H_2O[5.9]-45% H_2O reported by Slezak, S. E., "Flame Acceleration in H_2-Air-Steam Mixtures," Sandia National Laboratories, Albuquerque, NM, SAND89-1046, to be published.

§ Reported by Lee, J. H. and Knystautas, R., Flame Acceleration Due to Obstacles and Transition to Detonation in Tubes, Final Report on Joint McGill-SNL Studies of Hydrogen Explosion and Threat to Nuclear Reactors, to be published.

Table 5.1 A comparison of the limits of various combustion modes.

Plant Name	Fuel Design ID	75% Wt. of Zr (lb)	Vol. of H_2 STP (ft^3)*	Containment Vol. (ft^3)	H_2 Conc. in Dry Air (%)
Arkansas-1	B&W B-2,3,4	31382	268432	1.78×10^6	13.10
Bellefonte 1,2	B&W Mark C	35793	306159	3.00×10^6	9.26
Millstone-2	CE 14x14	31111	266109	1.90×10^6	12.29
Palisades	CE 15x15	35415	302928	1.64×10^6	15.59
Arkansas-2	CE 16x16	30958	264807	1.78×10^6	12.95
Point Beach 1,2	W 14x14	16686	142728	1.00×10^6	12.49
Turkey Pt. 3,4	W 15x15	24674	211057	1.55×10^6	11.98
Zion 1,2	W 15x15	30332	259452	2.60×10^6	9.07
Trojan	W 17x17	32124	274775	2.00×10^6	12.08
Fort Calhoun	Exxon CE-14	22460	192116	1.10×10^6	14.87
Palisades	Exxon CE-14	34450	294674	1.64×10^6	15.23
Maine Yankee	Exxon CE-14	36645	313452	1.80×10^6	14.83
Fort Calhoun	Exxon CE-15	22713	194283	1.10×10^6	15.01
Palisades	Exxon CE-15	34839	297998	1.64×10^6	15.38
Maine Yankee	Exxon CE-15	37059	316988	1.80×10^6	14.97
Ginna	Exxon W-15	23259	198948	0.997×10^6	16.64
Robinson-2	Exxon W-15	30179	258139	2.10×10^6	10.95
Ginna	Exxon W-17	21327	182424	0.997×10^6	15.47
Robinson-2	Exxon W-17	27672	236699	2.10×10^6	10.13

*1 lbm of Zr will generate 0.044 lbm of H_2 and density of H_2 at STP = 5.144×10^{-3} lbm/ft^3

Table 5.2 H_2 production due to 75% Zr-water reaction (from Reference 5.10)

detonate. The ability to determine which mode of combustion is most likely to occur depends on the likelihood of flame acceleration and DDT.

The concentration of hydrogen at the detonability limits is below the well-mixed hydrogen concentration for many large-dry and subatmospheric PWR containments shown in Table 5.2. Several important points should be noted. Hydrogen concentration is given as a volume percentage in dry air. Typically steam will be present and the addition of steam reduces the volume percentage of hydrogen. However the amount of steam available is uncertain due to condensation or the use of engineering safety features such as sprays. An arbitrary amount, 75 percent, of zirconium-water reaction was assumed. Finally, hydrogen and steam are assumed to be well mixed within the containment. Prior to sufficient mixing in the containment, locally higher concentrations of hydrogen may exist near the source.

Even though the concentration of hydrogen at the detonability limits is below the well-mixed hydrogen concentration for many containments, the possibility of a direct initiation of a detonation in mixtures near the limits may be unlikely in a severe accident due to the large energy requirements. A more likely mode of initiation of a detonation would be through flame acceleration and DDT. Direct initiation of a detonation may be more likely at higher temperatures, however, based on the predictions discussed in Section 4.2.2. A qualitative methodology has been developed to estimate the likelihood of a DDT in a reactor containment during a degraded-core accident [5.11].

5.3 References for Chapter 5

5.1 Stamps, D. W., Worthington, P. R., and Wong, C. C., "Uncertainties in Hydrogen Combustion for Nuclear Reactor Safety," presented at the Third International Seminar on Containment of Nuclear Reactors, Los Angeles, CA, August 1989.

5.2 Desoete, G. G., "The Flammability of Hydrogen-Oxygen-Nitrogen Mixtures at High Temperatures," La Rivista dei Combustibili, V29, pp. 166-172, 1975.

5.3 White, A. G., "Limits for the Propagation of Flame in Inflammable Gas-Air Mixtures, Part III. The Effect of Temperature on the Limits," Journal of the Chemical Society, V127, pp. 672-684, 1925.

5.4 Kumar, R. K., "Flammability Limits of Hydrogen-Oxygen-Diluent Mixtures," Journal of Fire Sciences, V3, pp. 245-262, 1985.

5.5 Karim, G. A., Wierzba, I., and Boon, S., "Some Considerations of the Lean Flammability Limits of Mixtures Involving Hydrogen," International Journal of Hydrogen Energy, V10, No. 1, pp. 117-123, 1985.

5.6 Hustad, J. E. and Sonju, O. K., "Experimental Studies of Lower Flammability Limits of Gases and Mixtures of Gases at Elevated Temperature," Combustion and Flame, V71, pp. 283-294, 1988.

5.7 Wierzba, I., Karim, G. A., Cheng, H., and Hanna, M., "The Flammability of Rich Mixtures of Hydrogen and Ethylene in Air," Journal of the Institute of Energy, V60, pp. 3-7, 1987.

5.8 Zabetakis, M. G., "Research on the Combustion and Explosion Hazards of Hydrogen-Water Vapor-Air Mixtures," Bureau of the Mines, Division of Explosives Technology, Pittsburgh, PA, NTIS, USAEC Report AECU-3327 (September 1956).

5.9 Brehm, N., "Ein Beitrag zum Phänomen des Uberganges Deflagration-Detonation," PhD Thesis, Lehrstuhl A für Thermodynamik, Technische Universität München, 1987.

5.10 Wong, C. C., "Hydrogen Production and Combustion-Induced Loadings of the Large-Dry and Subatmospheric PWR Containment," Sandia National Laboratories, letter report to Dr. Patricia Worthington, USNRC, June 1986.

5.11 Sherman, M. P. and Berman, M., "The Possibility of Local Detonations During Degraded-Core Accidents in the Bellefonte Nuclear Power Plant," Nuclear Technology, V81, pp. 63-77, 1988.

6. SUMMARY

6.1 Conclusions

The present study investigates the detonability of hydrogen-air-diluent mixtures. The detonation cell widths are obtained experimentally using the Heated Detonation Tube for hydrogen-air-diluent mixtures with variations in hydrogen and diluent concentration, initial temperature, and initial pressure. The data are correlated using a semi-empirical ZND chemical kinetics model for the same effects. The model's predictions are extrapolated beyond the present data base for the effects of temperature and pressure. The detonation limits are obtained experimentally for lean and rich hydrogen-air mixtures and stoichiometric hydrogen-air-steam mixtures.

The addition of a diluent increases the detonation cell width for all mixtures. The addition of 10 percent and 20 percent carbon dioxide to stoichiometric hydrogen-air mixtures at 100°C and 1 atm increases the experimental cell width by factors of approximately 4.6 and 34.3, respectively, compared to a stoichiometric mixture without dilution. For the same conditions, the addition of 10 percent, 20 percent, and 30 percent steam increases the experimental cell width by factors of approximately 4, 23.6, and 92.8, respectively. Based on a comparison between 10 percent and 20 percent dilution, carbon dioxide not only produces a larger increase in the cell width than steam, but it becomes more effective relative to steam with increasing concentration. The addition of 10 percent, 20 percent, and 30 percent steam to stoichiometric hydrogen-air mixtures nominally at 100°C and a constant initial air density of 41.6 moles/m^3 increases the cell width by factors of 6, 20, and 60, respectively. These are comparable to those for the same amounts of steam added to stoichiometric mixtures at 100°C and 1 atm.

An increase in the initial pressure generally decreases the detonation cell width. Although the effect is most pronounced at low initial pressures, the cell width does not vary more than a factor of two over the pressure range from 1 atm to 3 atm for the cases considered.

Temperature is predicted to have a large influence on the detonation cell width. Three important conclusions can be summarized from the ZND model predictions. First, the detonation cell width is predicted to decrease with increasing

initial temperature up to a critical temperature for all mixtures. Second, at elevated temperatures, all mixtures are predicted to have similar cell widths. Unlike mixtures at ambient temperatures, this means that all mixtures, regardless of variations in stoichiometry or diluent concentration, have a comparable likelihood to detonate. Third, the mitigative effect of a diluent, such as steam or carbon dioxide, decreases with increasing temperature. The model has been assessed only up to 440 K. If the model is confirmed experimentally at higher temperatures, the model predictions indicate that detonations may be significantly more probable in at least three accident scenarios.

The ZND model was assessed against data including the effects of diluent concentration, pressure, and temperature. Qualitatively, the model predicts the correct trends for steam or carbon dioxide dilution on the cell width as well as for variations in initial pressure. The temperature range over which experimental data is available is too narrow to determine if the model predicts the correct trend for temperature variations. The model is useful for safety analysis when predictions are made to interpolate within the existing data base. Because of the nonlinear nature of the chemical and physical processes governing detonations, uncertainty in the model's predictions cannot be estimated for conditions beyond the existing data base. Model predictions should be used with caution for these conditions.

The detonable range of hydrogen obtained in the HDT for hydrogen-air mixtures at 20°C and 1 atm is between 11.6 percent and 74.9 percent by volume. Increasing the initial temperature to 100°C, expands the range to 9.4 percent and 76.9 percent by volume and illustrates the important effect of increasing temperature. The detonation limit is between 38.8 percent and 40.5 percent steam for stoichiometric hydrogen-air-steam mixtures at 100°C and 1 atm initial pressure. A lower concentration is observed for stoichiometric hydrogen-air-steam mixtures at 100°C and an air density of 41.6 moles/m^3. The value between 29.6 percent and 31.9 percent may not represent an intrinsic limit for the HDT and is probably due to insufficient charge strength to initiate the detonation. All detonation limits are scale and geometry dependent. This means that a wider range of detonable concentrations may be obtained in reactor scales.

A comparison between the various combustion limits yields two important conclusions. First, the detonability limits are similar to the flammability limits for some mixtures. While there is a discrepancy between the limits for the other mixtures, the limits are much closer than previously thought. Second, the detonability limits and flame acceleration limits are similar for most mixtures tested.

6.2 Recommendations

The model's predictions for the effect of temperature on the detonability of hydrogen-air-diluent mixtures indicate that detonations may be significantly more likely at elevated temperatures. At least three accident scenarios involve the combustion of hydrogen at elevated temperatures and several plant types are affected. The model has not been assessed at sufficiently high temperatures to support the predicted trends. We recommend that the experimental detonation cell width be obtained for hydrogen-air-diluent mixtures at elevated temperatures and high diluent concentrations to assess the model.

Both the detonability and flammability limits widen with increasing temperature. The difference between the two limits, however, decreases with increasing temperature. We recommend that the detonability and flammability limits for hydrogen-air-steam mixtures be obtained to determine if the two limits are similar at elevated temperatures. The flame acceleration limits are similar to the detonability limits for most mixtures tested. We recommend that flame acceleration limits for hydrogen-air-steam mixtures be obtained and compared to the detonability limits to determine if this is true at elevated temperatures.

For many compositions, if a mixture can deflagrate it can also detonate. For some mixtures, the flammability and detonability limits are similar. The probability of a detonation in a reactor accident will likely depend on the ability of a flame to accelerate and transition to a detonation. We recommend that research be conducted on flame acceleration and DDT for hydrogen-air-steam mixtures under prototypical conditions including the effects of temperature, scale, obstacle type and spacing.

APPENDIX A ESTIMATE OF UNCERTAINTY BOUNDS

A.1 Detonation Cell Width

The detonation cell width was determined using the method of selecting high-contrast long-running parallel lines termed the dominant-mode method [A.1]. Hydrogen-air detonations may produce irregularly spaced lines or cells that make the dominant-mode method difficult to use. Low-contrast foils and small sample size due to large cells also make the selection of the dominant mode more difficult. Since analytical techniques to measure the dominant cell, such as digital image processing [A.2], are still in the early stages of development, the cell width must be measured through a subjective human judgment process.

Assuming the sensitivity of a hydrogen-air-diluent mixture can be represented by a single dominant cell, the uncertainty in the cell width measurement is estimated by two independent measurements of each test. With sufficient number of tests, a statistical average and standard deviation for the variation between observers for the entire test series can be obtained. Independent measurements are taken by the authors for about half of the data. The uncertainty for this set of data is assumed to be representative of the entire set of data.

The ratio of the cell width measured by Stamps to that measured by Tieszen is used for the statistical analysis. The average of the ratio for the data available was 1.16. In other words, the measurements by Stamps are slightly larger than those of Tieszen on the average. Presumably, the measurements between the two observers will be the same (ratio equal to one) for a sufficiently large population. The most probable value for the cell width listed in Appendix B is our best estimate, and, with 95 percent confidence, the true value is believed to lie within the range $0.372\ \lambda_{MP} < \lambda_{MP} < 1.628\ \lambda_{MP}$. Because of human bias, however, we recommend the most probable cell width measurements be divided by 2 for safety analyses.

A.2 Thermodynamic State

The uncertainty in the thermodynamic variables is estimated using the technique termed single-sample uncertainty analysis [A.3]. In this technique, the uncertainty of the independent (measured) variables, such as temperature, T, and pressure, P,

is based on an estimate of the fixed and variable errors in the measurements. A fixed error is any error that will not change during the course of the experiment such as the tolerance on a pressure gauge. The variable error is estimated from the standard deviation of any fluctuations that occur during the recording of the variable such as fluctuations in the digital temperature readout. The uncertainty of the dependent (inferred) variables, such as equivalence ratio, ϕ, air density, ρ_A, or diluent mole fraction, X_D, can be calculated from the functional relationship between the dependent and independent variables.

If a dependent variable, R, is a function of several independent variables, X_i

$$R = R(X_1, X_2, X_3 \ldots X_N) \qquad \text{Eq. A.1}$$

then the uncertainty in R, δR, is

$$\delta R = \left\{ \sum_{i=1}^{N} \left(\frac{\partial R}{\partial X_i} \delta X_i \right)^2 \right\}^{1/2} \qquad \text{Eq. A.2}$$

In the present analysis, X_i = T or P, and R = ϕ, ρ_A, or X_D. The uncertainty in the independent variable, δX_i, is estimated from the fixed and variable errors according to

$$\delta X_i = \left\{ (\delta X_{i,\ \text{fixed}})^2 + (\delta X_{i,\ \text{variable}})^2 \right\}^{1/2} . \qquad \text{Eq. A.3}$$

The value of the dependent variable listed in Appendix B, R_i (measured), is the best estimate and, with a 95 percent confidence, the true value is believed to lie within the range

$$R_i = R_i \text{ (measured)} \pm \delta R_i \qquad \text{Eq. A.4}$$

Temperature and pressure are measured at each thermodynamic state and up to four states are measured. Each state is designated by a number as shown below. For tests without diluent gases, conditions at State 3 equal those at State 2.

Measurement	Condition
(P_1, T_1)	Pressure and temperature after adding air
(P_2, T_2)	Pressure and temperature after adding hydrogen to air
(P_3, T_3)	Pressure and temperature after adding steam or carbon dioxide to hydrogen-air mixture
(P_4, T_4)	Pressure and temperature before test is conducted

The uncertainty in the equivalence ratio, $\delta\phi$, can be computed from Eq. A.2, the definition of the equivalence ratio, and the equation of state for an ideal gas. The equivalence ratio is defined as

$$\phi = \left[\frac{n_{H2}}{n_{AIR}} \right] \Big/ \left[\frac{n_{H2}}{n_{AIR}} \right]_{STOICHIOMETRIC} = \beta \left[\frac{n_{H2}}{n_{AIR}} \right] . \qquad \text{Eq. A.5}$$

where $\beta = (n_{air}/n_{fuel})$ at perfect stoichiometry and $\beta = 2.38691$ for hydrogen-air mixtures. Using the ideal gas equation of state, $n_i = P_iV/RT_i$, the uncertainty in the equivalence ratio is

$$\delta\phi = \beta \frac{T_1P_2}{P_1T_2} \left\{ \left[\frac{\delta T_1}{T_1} \right]^2 + \left[\frac{\delta P_1}{P_1} \right]^2 + \left[\frac{\delta T_2}{T_2} \right]^2 + \left[\frac{\delta P_2}{P_2} \right]^2 \right\}^{1/2} \qquad \text{Eq. A.6}$$

The air density, ρ_A is $\rho_A = P_1/RT_1$ and, using Eq. A.2, the uncertainty in the air density is

$$\delta\rho_A = \frac{P_1}{RT_1} \left\{ \left[\frac{\delta P_1}{P_1} \right]^2 + \left[\frac{\delta T_1}{T_1} \right]^2 \right\}^{1/2} \qquad \text{Eq. A.7}$$

The diluent mole fraction, X_D, is defined as $X_D = n_D/n_{TOTAL}$ where n is the number of moles of gas at each state. Using the equation of state and Eq. A.2, the uncertainty in the diluent mole fraction is

$$\delta X_D = \frac{P_2 T_3}{T_2 P_3} \left\{ \left(\frac{\delta T_2}{T_2} \right)^2 + \left(\frac{\delta P_2}{P_2} \right)^2 + \left(\frac{\delta T_3}{T_3} \right)^2 + \left(\frac{\delta P_3}{P_3} \right)^2 \right\}^{1/2} \qquad \text{Eq. A.8}$$

The uncertainty in the measured pressure depends on the type of gauge used.

Gauge Type	Uncertainty (δP)
50 psig	0.039 psig (2.03 mm Hg)
800 mm Hg	0.48 mm Hg
100 mm Hg	0.46 mm Hg

The estimates are valid for all states i = 1, 2, 3 and 4. The only exception is for steam-diluted tests in which condensation occurred. In this case, the final pressure corrected for temperature changes will be less than P_3. The uncertainty in the final pressure, δP_4, is then equal to $P_3 - P_4 * T_3/T_4$ or the value listed above, whichever is larger.

Temperature
$T_i = 1°C$ for i = 1, 2, 3, and 4

A.3 Detonation Velocity

The detonation velocity was determined from time-of-arrival measurements. The arrival of the detonation was recorded by up to 12 axially spaced piezoelectric pressure transducers with a resonance frequency of approximately 500 kHz. Initially, the detonation was overdriven due to the effects of the high explosive. However, it was determined in a previous study [A.4] that the detonation achieves a steady velocity within the first 2.5 m of the HDT for approximately the same size charge used in this study.

A standard statistical package was used to determine the velocity and uncertainty bounds. The velocity was determined from the slope of a linear regression fit of the time-of-arrival data. The uncertainty bounds were determined from the standard error estimate in the slope. The detonation velocities and uncertainty bounds are listed in Appendix B.

A.4 References

A.1 Moen, I. O., Murry, S. B., Bjerketvedt, O., Rinnan, A., Knystautas, R., and Lee, J. H. S., "Diffraction of Detonation From Tubes Into A Large Fuel-Air Explosive Cloud," Nineteenth Symposium (International) on Combustion, The Combustion Institute, Pittsburgh, PA, pp. 635-645, 1982.

A.2 Shepherd, J. E. and Tieszen, S. R., "Detonation Cellular Structure and Image Processing," Sandia National Laboratories, Albuquerque, NM, SAND86-0033, June 1986.

A.3 Moffat, R.J., "Describing the Uncertainties in Experimental Results," Experimental Thermal and Fluid Science, V1, pp. 3-17, 1988.

A.4 Tieszen, S. R., Sherman, M. P., Benedick, W. B., and Berman, M., "Detonability of H_2-Air-Diluent Mixtures," Sandia National Laboratories, Albuquerque, NM, NUREG/CR-4905, SAND85-1263, June 1987.

APPENDIX B TABULATED DATA

B.1 Summary

The data are tabulated according to test series. Table B.1 lists the conditions in each test series. The detonation cell widths, detonation velocities, and thermodynamic conditions are listed in Tables B.2, B.3, and B.4, respectively. In all tables, the data are listed for mixtures with increasing equivalence ratio and increasing diluent mole fraction.

The detonation cell width and uncertainty bounds are listed in Table B.2. The most probable (MP) cell width was measured and the lower bound (LB) and upper bound (UB) values are based on the 95 percent confidence level discussed in Appendix A, Section A.1. The predicted reaction zone length where the Mach number reaches 0.75 is listed in column headed by Z.75. The numbers under the column DCW/Z.75 are the most probable cell width divided by the reaction zone length. The last column is the predicted cell width. It is obtained by multiplying the predicted reaction zone by a proportionality factor equal to 22. This value was used successfully in a previous study [B.1] and was determined by a single point fit to a stoichiometric hydrogen-air mixture at ambient temperature and pressure.

The experimental and theoretical velocities are listed in Table B.3. The number of time-of-arrival values (or pressure transducer locations) are listed in the column with the #OBS heading. These values are used to compute the most probable (MP) detonation velocity. The lower bound (LB) and upper bound (UB) velocities are calculated as described in Appendix A Section A.3. The Chapman-Jouguet velocities are computed from a standard equilibrium code.

Table B.4 lists the thermodynamic state of all mixtures. The uncertainty bounds are calculated according to the equations in Appendix A Section A.2.

B.2 Reference

B.1 Tieszen, S. R., Sherman, M. P., Benedick, W. B., and Berman, M., "Detonability of H_2-Air-Diluent Mixtures," Sandia National Laboratories, Albuquerque, NM, NUREG/CR-4905, SAND85-1263, June 1987.

Table B.1 Initial Conditions for the HDT Test Series

Test Series		
Series #	Description	# of Tests in Series
2II	H_2-Air-CO_2 @ P = 1 atm, T = 20°C	7
4II	H_2-Air-H_2O @ ρ_{AIR} = 41.6 moles/m^3, T = 100°C	10
8	H_2-Air-H_2O @ P = 1 atm, T = 100°C	40
9	H_2-Air-CO_2 @ P = 1 atm, T = 100°C	9
10	H_2-Air @ P = 1 atm, T = 20°C	14
11	H_2-Air @ T = 20°C	13

TEST SERIES 2II

The 2 sigma limits for T,P for the entire series are:

295.9 < T(K) < 300.3
101.4 < P(kPa) < 101.7

TEST	EQUIVALENCE RATIO			CO2 MOLE FRACTION			DETONATION CELL WIDTH (MM)			Z.75 (MM)	MODEL DCW/Z.75	22*Z.75 (MM)
	LB	MP	UB	LB	MP	UB	LB	MP	UB			
HT119	0.9911	1.0144	1.0376	0.0445	0.0503	0.0562	7.8	21.	34.	1.04	20.2	22.9
HT158	0.5925	0.6073	0.6220	0.0937	0.0981	0.1025	80.	215.	350.	34.8	6.18	766.
HT120	0.9977	1.0214	1.0452	0.0777	0.0834	0.0891	16.	43.	70.	1.72	25.0	37.8
HT121	1.0037	1.0294	1.0551	0.1943	0.1994	0.2045	170.	457.	744.	26.1	17.5	574.
HT121II	0.9909	1.0164	1.0420	0.1981	0.2032	0.2083	134.	360.	586.	29.3	12.3	645.
HT121III	0.9926	1.0096	1.0266	0.1930	0.1969	0.2009	171.	460.	749.	25.7	17.9	565.
HT168	0.9774	0.9943	1.0111	0.2447	0.2483	0.2520	SM	SM	SM	83.7	SM	1840.

SM - SPIN MODE

TEST SERIES 4II

The 2 sigma limits for T, air density for the entire series are:

372.0 < T(K) < 389.0
41.3 < Air Density (Moles/M**3) < 42.3

TEST	EQUIVALENCE RATIO			STEAM MOLE FRACTION			DETONATION CELL WIDTH (MM)			Z.75 (MM)	MODEL DCW/Z.75	22*Z.75 (MM)
	LB	MP	UB	LB	MP	UB	LB	MP	UB			
HT170	0.9779	0.9933	1.0087	0.2958	0.2990	0.3021	ND	ND	ND	18.0	ND	396.
HT170II	0.9846	1.0001	1.0156	0.2924	0.2956	0.2987	93.	250.	407.	16.8	14.8	369.
HT171	0.9861	1.0017	1.0172	0.3155	0.3192	0.3228	ND	ND	ND	23.5	ND	517.
HT169	0.9746	0.9897	1.0049	0.3359	0.3399	0.3438	ND	ND	ND	29.6	ND	651.
HT169II	0.9838	0.9989	1.0140	0.3330	0.3398	0.3466	ND	ND	ND	28.4	ND	625.
HT167	0.9859	1.0007	1.0155	0.3642	0.3668	0.3694	ND	ND	ND	38.3	ND	843.
HT167II	1.0555	1.0707	1.0860	0.3664	0.3689	0.3715	ND	ND	ND	38.8	ND	854.
HT167III	0.9809	0.9958	1.0106	0.3639	0.3684	0.3728	ND	ND	ND	39.5	ND	869.
HT147	0.9803	0.9954	1.0105	0.3560	0.3588	0.3615	ND	ND	ND	37.6	ND	827.
HT132	0.9833	0.9984	1.0135	0.3950	0.3977	0.4005	ND	ND	ND	63.0	ND	1390.

ND - NO DETONATION

Table B.2 Detonation cell width data

TEST SERIES 8A

The 2 sigma limits for T,P for the entire series are:

369.6 < T(K) < 376.0
101.5 < P(kPa) < 102.2

TEST	EQUIVALENCE RATIO			DETONATION CELL WIDTH (MM)			Z.75 (MM)	MODEL DCW/Z.75	22*Z.75 (MM)
	LB	MP	UB	LB	MP	UB			
HT153	0.1835	0.1936	0.2037	ND	ND	ND	19200.	ND	4.22E05
HT155	0.2030	0.2131	0.2232	ND	ND	ND	7100.	ND	1.56E05
HT156	0.2209	0.2311	0.2413	ND	ND	ND	3160.	ND	69500.
HT152	0.2375	0.2478	0.2581	SM	SM	SM	1590.	SM	35000.
HT146	0.2661	0.2765	0.2869	SM	SM	SM	532.	SM	11700.
HT144	0.2928	0.3033	0.3138	SM	SM	SM	212.	SM	4660.
HT134	0.3289	0.3396	0.3502	113.	305.	496.	68.8	4.43	1510.
HT102	0.3448	0.3601	0.3753	165.	444.	724.	40.4	11.0	889.
HT101	0.4005	0.4163	0.4321	55.8	150.	244.	8.90	16.8	196.
HT162	0.5066	0.5180	0.5293	14.1	38.	61.9	1.51	25.2	33.2
HT100	0.5794	0.5966	0.6137	8.9	24.	39.1	1.15	20.9	25.3
HT99	0.9878	1.0081	1.0285	7.6	20.	33.4	0.896	22.9	19.7
HT99II	0.9892	1.0025	1.0159	2.6	7.	11.4	0.913	7.67	20.1
HT103	1.9904	2.0202	2.0499	5.2	14.	22.8	1.10	12.7	24.2
HT104	3.0004	3.0417	3.0830	13.8	37.	60.2	1.88	19.7	41.4
HT161	7.4996	7.5458	7.5921	SM	SM	SM	156.	SM	3430.
HT165	7.9125	7.9614	8.0103	SM	SM	SM	232.	SM	5100.
HT164	8.3598	8.4115	8.4633	ND	ND	ND	353.	ND	7770.
HT157	9.3622	9.4209	9.4795	ND	ND	ND	862.	ND	19000.

ND - NO DETONATION
SM - SPIN MODE

Table B.2 (Continued) Detonation cell width data

TEST SERIES 8B

The 2 sigma limits for T,P for the entire series are:

373.5 < T(K) < 375.6
100.5 < P(kPa) < 102.8

TEST	EQUIVALENCE RATIO			STEAM MOLE FRACTION			DETONATION CELL WIDTH (MM)			Z.75 (MM)	MODEL DCW/Z.75	22*Z.75 (MM)
	LB	MP	UB	LB	MP	UB	LB	MP	UB			
HT122	0.9888	1.0098	1.0307	0.0453	0.0504	0.0556	7.4	20.	32.6	1.02	19.6	22.4
HT107	0.4779	0.4951	0.5124	0.0940	0.0990	0.1039	175.	470.	765.	39.4	11.9	867.
HT106	0.5858	0.6039	0.6221	0.0861	0.0911	0.0961	68.4	184.	300.	7.77	23.7	171.
HT105	0.9862	1.0079	1.0296	0.1101	0.1150	0.1198	10.4	28.	45.6	1.55	18.1	34.1
HT108	1.9768	2.0086	2.0405	0.1005	0.1054	0.1103	15.6	42.	68.4	2.42	17.4	53.2
HT109	4.1671	4.2298	4.2926	0.0934	0.0983	0.1033	227.	610.	993.	38.0	16.0	836.
HT123	1.0288	1.0517	1.0746	0.1440	0.1487	0.1535	16.7	45.	73.3	2.33	19.3	51.3
HT123II	1.0257	1.0486	1.0715	0.1449	0.1496	0.1544	18.6	50.	81.4	2.40	20.8	52.8
HT124	0.6474	0.6675	0.6876	0.1985	0.2030	0.2076	372.	1000.	1628.	42.2	23.7	928.
HT125	0.8173	0.8391	0.8608	0.1963	0.2010	0.2056	93.0	250.	407.	11.3	22.1	249.
HT126	1.0046	1.0282	1.0518	0.1966	0.2011	0.2057	61.4	165.	269.	5.53	29.8	122.
HT127	1.9676	2.0024	2.0371	0.1937	0.1983	0.2028	108.	290.	472.	14.4	20.1	317.
HT128	0.9054	0.9304	0.9553	0.2945	0.2990	0.3035	472.	1270.	2068.	37.2	34.1	818.
HT129	0.9957	1.0217	1.0476	0.2954	0.2996	0.3038	242.	650.	1058.	27.5	23.6	605.
HT130	1.4858	1.5179	1.5499	0.2946	0.2988	0.3030	186.	500.	814.	45.6	11.0	1000.
HT131	0.9775	1.0049	1.0324	0.3504	0.3544	0.3584	SM	SM	SM	69.8	SM	1540.
HT163II	0.9853	0.9994	1.0136	0.3672	0.3699	0.3726	SM	SM	SM	91.9	SM	2021.
HT163	5.8886	5.9322	5.9759	0.3679	0.3705	0.3732	ND	ND	ND	59000.	ND	1.30E06
HT173	0.9928	1.0071	1.0213	0.3852	0.3877	0.3902	SM	SM	SM	122.	SM	2684.
HT175	1.0025	1.0168	1.0311	0.4027	0.4052	0.4077	ND	ND	ND	164.	ND	3608.
HT174	0.9870	1.0013	1.0156	0.4175	0.4198	0.4222	ND	ND	ND	217.	ND	4774.

ND - NO DETONATION
SM - SPIN MODE

Table B.2 (Continued) Detonation cell width data

TEST SERIES 9

The 2 sigma limits for T,P for the entire series are:

373.6 < T(K) < 375.5
101.0 < P(kPa) < 101.4

TEST	EQUIVALENCE RATIO			CO2 MOLE FRACTION			DETONATION CELL WIDTH (MM)			Z.75 (MM)	MODEL DCW/Z.75	22*Z.75 (MM)
	LB	MP	UB	LB	MP	UB	LB	MP	UB			
HT110	0.9957	1.0167	1.0377	0.0439	0.0491	0.0542	7.4	20.	32.6	1.21	16.5	26.6
HT111	0.4771	0.4944	0.5116	0.0939	0.0988	0.1037	453.	1219.	1984.	52.6	23.2	1160.
HT112	0.5962	0.6144	0.6326	0.0962	0.1011	0.1060	56.7	152.	248.	9.72	15.7	214.
HT113	1.0025	1.0242	1.0460	0.0953	0.1002	0.1052	11.9	32.	52.1	1.85	17.3	40.7
HT114	1.9652	1.9969	2.0287	0.0953	0.1002	0.1052	19.3	52.	84.6	2.82	18.4	62.0
HT115	1.0251	1.0480	1.0709	0.1455	0.1502	0.1550	46.5	125.	203.	3.74	33.4	82.3
HT116	0.8178	0.8395	0.8613	0.1950	0.1996	0.2041	142.	381.	620.	22.4	17.0	493.
HT117	1.0025	1.0261	1.0498	0.1952	0.1998	0.2043	89.3	240.	391.	11.6	20.7	255.
HT118	1.9630	1.9977	2.0324	0.1952	0.1998	0.2043	SM	SM	SM	65.5	SM	1440.

SM - SPIN MODE

TEST SERIES 10

The 2 sigma limits for T,P for the entire series are:

281.6 < T(K) < 311.3
101.4 < P(kPa) < 101.8

TEST	EQUIVALENCE RATIO			STEAM MOLE FRACTION			DETONATION CELL WIDTH (MM)			Z.75 (MM)	MODEL DCW/Z.75	22*Z.75 (MM)
	LB	MP	UB	LB	MP	UB	LB	MP	UB			
HT145	0.2889	0.3057	0.3226	0.0000	0.0000	0.0000	ND	ND	ND	946.	ND	20800.
HT150	0.3007	0.3139	0.3272	0.0000	0.0000	0.0000	SM	SM	SM	723.	SM	15900.
HT148	0.3112	0.3245	0.3378	0.0000	0.0000	0.0000	SM	SM	SM	511.	SM	11200.
HT133	0.3216	0.3349	0.3482	0.0000	0.0000	0.0000	SM	SM	SM	369.	SM	8120.
HT97II	0.9778	0.9942	1.0105	0.0000	0.0000	0.0000	4.1	11.	17.9	0.704	15.6	15.5
HT97III	0.9814	0.9973	1.0132	0.0000	0.0000	0.0000	3.3	9.	14.6	0.729	12.4	16.0
HT172	1.0270	1.0462	1.0654	0.0293	0.0309	0.0329	4.8	13.	21.2	0.782	16.6	17.2
HT98	0.9573	0.9803	1.0033	0.0000	0.0000	0.0000	5.6	15.	24.6	0.659	22.9	14.5
HT166	5.6154	5.6571	5.6988	0.0000	0.0000	0.0000	MD	MD	MD	67.4	MD	1480.
HT166II	5.6344	5.6765	5.7187	0.0000	0.0000	0.0000	SM	SM	SM	73.1	SM	1610.
HT149	6.4151	6.4623	6.5095	0.0000	0.0000	0.0000	SM	SM	SM	196.	SM	4310.
HT151	7.0893	7.1409	7.1926	0.0000	0.0000	0.0000	SM	SM	SM	413.	SM	9090.
HT160	7.4497	7.5043	7.5589	0.0000	0.0000	0.0000	ND	ND	ND	654.	ND	14400.
HT154	7.9097	7.9673	8.0250	0.0000	0.0000	0.0000	ND	ND	ND	1050.	ND	23100.

MD - MISSING DATA
ND - NO DETONATION
SM - SPIN MODE

Table B.2 (Continued) Detonation cell width data

TEST SERIES 11

The 2 sigma limits for T for the entire series are:

296.0 < T(K) < 302.9

TEST	EQUIVALENCE RATIO			DETONATION CELL WIDTH (MM)			Z.75 (MM)	MODEL DCW/Z.75	22*Z.75 (MM)
	LB	MP	UB	LB	MP	UB			
HT135	0.4689	0.4996	0.5302	20.8	56.	91.2	35.4	1.58	779.
HT135II	0.4596	0.4901	0.5207	78.1	210.	342.	34.9	6.02	768.
HT135III	0.4671	0.4977	0.5282	93.0	250.	407.	35.9	6.96	790.
HT159	0.4656	0.4890	0.5124	80.0	215.	350.	17.1	12.6	376.
HT136	0.4601	0.4779	0.4957	167.	450.	733.	7.37	61.0	162.
HT136II	0.4847	0.5026	0.5205	96.7	260.	423.	7.53	34.5	166.
HT137	0.4731	0.4880	0.5029	58.4	157.	256.	3.84	40.9	84.5
HT138	0.4817	0.4958	0.5099	28.3	76.	124.	8.58	8.86	189.
HT139	0.4774	0.4919	0.5064	37.2	100.	163.	10.7	9.34	235.
HT140	0.9523	0.9912	1.0301	14.5	39.	63.5	30.6	1.27	673.
HT141	0.9798	1.0018	1.0239	8.9	24.	39.1	6.27	3.83	138.
HT142	0.9634	0.9812	0.9990	5.6	15.	24.4	1.94	7.73	42.7
HT143	0.9625	0.9817	1.0009	2.8	7.5	12.2	0.416	18.0	9.15

Table B.2 (Continued) Detonation cell width data

TEST SERIES 2II

The 2 sigma limits for T,P for the entire series are:

295.9 < T(K) < 300.3
101.4 < P(kPa) < 101.7

TEST	EQUIVALENCE RATIO			CO2 MOLE FRACTION			#	DETONATION VELOCITY (KM/S)			C-J VELOCITY (KM/S)
	LB	MP	UB	LB	MP	UB	OBS.	LB	MP	UB	
HT119	0.9911	1.0144	1.0376	0.0445	0.0503	0.0562	9	1.8763	1.8799	1.8835	1.8648
HT158	0.5925	0.6073	0.6220	0.0937	0.0981	0.1025	9	1.5636	1.5755	1.5876	1.5461
HT120	0.9977	1.0214	1.0452	0.0777	0.0834	0.0891	9	1.8018	1.8051	1.8083	1.8027
HT121	1.0037	1.0294	1.0551	0.1943	0.1994	0.2045	9	1.4619	1.5198	1.5825	1.6040
HT121II	0.9909	1.0164	1.0420	0.1981	0.2032	0.2083	9	MD	MD	MD	1.5948
HT121III	0.9926	1.0096	1.0266	0.1930	0.1969	0.2009	9	1.5856	1.5940	1.6026	1.6033
HT168	0.9774	0.9943	1.0111	0.2447	0.2483	0.2520	8	1.4403	1.4582	1.4766	1.5178

MD - MISSING DATA

TEST SERIES 4II

The 2 sigma limits for T, air density for the entire series are:

372.0 < T(K) < 389.0
41.3 < Air Density (Moles/M**3) < 42.3

TEST	EQUIVALENCE RATIO			STEAM MOLE FRACTION			#	DETONATION VELOCITY (KM/S)			C-J VELOCITY (KM/S)
	LB	MP	UB	LB	MP	UB	OBS.	LB	MP	UB	
HT170	0.9779	0.9933	1.0087	0.2958	0.2990	0.3021	6	0.7700	0.7967	0.8252	1.7802
HT170II	0.9846	1.0001	1.0156	0.2924	0.2956	0.2987	8	1.5548	1.6719	1.8081	1.7854
HT171	0.9861	1.0017	1.0172	0.3155	0.3192	0.3228	9	0.8454	0.9107	0.9869	1.7671
HT169	0.9746	0.9897	1.0049	0.3359	0.3399	0.3438	6	0.7535	0.7811	0.8109	1.7457
HT169II	0.9838	0.9989	1.0140	0.3330	0.3398	0.3466	7	0.9082	0.9402	0.9745	1.7493
HT167	0.9859	1.0007	1.0155	0.3642	0.3668	0.3694	4	0.6206	0.6401	0.6610	1.7270
HT167II	1.0555	1.0707	1.0860	0.3664	0.3689	0.3715	6	0.7772	0.7981	0.8201	1.7341
HT167III	0.9809	0.9958	1.0106	0.3639	0.3684	0.3728	7	0.8460	0.8750	0.9061	1.7239
HT147	0.9803	0.9954	1.0105	0.3560	0.3588	0.3615	8	0.8006	0.8482	0.9017	1.7318
HT132	0.9833	0.9984	1.0135	0.3950	0.3977	0.4005	8	0.7694	0.8105	0.8562	1.6982

Table B.3 Detonation velocity data

TEST SERIES 8A

The 2 sigma limits for T,P for the entire series are:

369.6 < T(K) < 376.0
101.5 < P(kPa) < 102.2

TEST	EQUIVALENCE RATIO			#	DETONATION VELOCITY (KM/S)			C-J VELOCITY (KM/S)
	LB	MP	UB	OBS.	LB	MP	UB	
HT153	0.1835	0.1936	0.2037	8	0.8500	0.9201	1.0028	1.1631
HT155	0.2030	0.2131	0.2232	9	0.8916	0.9637	1.0485	1.2025
HT156	0.2209	0.2311	0.2413	9	0.9455	1.0019	1.0655	1.2368
HT152	0.2375	0.2478	0.2581	9	1.2314	1.2765	1.3250	1.2671
HT146	0.2681	0.2765	0.2869	8	1.3653	1.3833	1.4018	1.3166
HT144	0.2928	0.3033	0.3138	8	1.3639	1.3754	1.3870	1.3597
HT134	0.3289	0.3396	0.3502	8	1.4021	1.4325	1.4642	1.4141
HT102	0.3448	0.3601	0.3753	9	1.4530	1.4688	1.4849	1.4426
HT101	0.4005	0.4163	0.4321	9	1.5200	1.5277	1.5355	1.5157
HT162	0.5066	0.5180	0.5293	9	1.6567	1.6698	1.6831	1.6300
HT100	0.5794	0.5966	0.6137	8	1.7298	1.7335	1.7372	1.7046
HT99	0.9878	1.0081	1.0285	9	1.9723	1.9793	1.9863	1.9615
HT99II	0.9892	1.0025	1.0159	9	1.9429	1.9655	1.9886	1.9588
HT103	1.9904	2.0202	2.0499	8	2.1487	2.1586	2.1685	2.1430
HT104	3.0004	3.0417	3.0830	9	2.2357	2.2415	2.2474	2.2249
HT161	7.4996	7.5458	7.5921	8	2.3192	2.3495	2.3806	2.3560
HT165	7.9125	7.9614	8.0103	9	2.2765	2.3374	2.4017	2.3608
HT164	8.3596	8.4115	8.4633	9	1.7125	1.8148	1.9301	2.3651
HT157	9.3622	9.4209	9.4795	9	1.6528	1.7287	1.8119	2.3725

Table B.3 (Continued) Detonation velocity data

TEST SERIES 8B

The 2 sigma limits for T,P for the entire series are:

373.5 < T(K) < 375.6
100.5 < P(kPa) < 102.8

TEST	EQUIVALENCE RATIO			STEAM MOLE FRACTION			#	DETONATION VELOCITY (KM/S)			C-J VELOCITY (KM/S)
	LB	MP	UB	LB	MP	UB	OBS.	LB	MP	UB	
HT122	0.9888	1.0098	1.0307	0.0453	0.0504	0.0556	8	1.8099	1.8957	1.9901	1.9349
HT107	0.4779	0.4951	0.5124	0.0940	0.0990	0.1039	9	1.5273	1.5405	1.5538	1.5520
HT106	0.5858	0.6039	0.6221	0.0861	0.0911	0.0961	9	1.6553	1.6621	1.6690	1.6599
HT105	0.9862	1.0079	1.0296	0.1101	0.1150	0.1198	9	1.9028	1.9093	1.9160	1.8990
HT108	1.9768	2.0086	2.0405	0.1005	0.1054	0.1103	9	2.0174	2.0229	2.0284	2.0324
HT109	4.1671	4.2298	4.2926	0.0934	0.0983	0.1033	9	2.0587	2.0768	2.0952	2.1099
HT123	1.0288	1.0517	1.0746	0.1440	0.1487	0.1535	9	1.8891	1.8965	1.9039	1.8935
HT123II	1.0257	1.0486	1.0715	0.1449	0.1496	0.1544	9	1.8783	1.8885	1.8987	1.8921
HT124	0.6474	0.6675	0.6876	0.1985	0.2030	0.2076	9	1.5961	1.6097	1.6235	1.6432
HT125	0.8173	0.8391	0.8608	0.1963	0.2010	0.2056	9	1.7220	1.7315	1.7410	1.7637
HT126	1.0046	1.0282	1.0518	0.1966	0.2011	0.2057	9	1.8156	1.8254	1.8353	1.8537
HT127	1.9676	2.0024	2.0371	0.1937	0.1983	0.2028	9	1.8993	1.9107	1.9223	1.9290
HT128	0.9054	0.9304	0.9553	0.2945	0.2990	0.3035	9	1.6043	1.6558	1.7108	1.7453
HT129	0.9957	1.0217	1.0476	0.2954	0.2996	0.3038	9	1.7369	1.7476	1.7584	1.7829
HT130	1.4858	1.5179	1.5499	0.2946	0.2988	0.3030	9	1.7763	1.7874	1.7987	1.8092
HT131	0.9775	1.0049	1.0324	0.3504	0.3544	0.3584	9	1.6680	1.6823	1.6968	1.7344
HT163II	0.9853	0.9994	1.0136	0.3672	0.3699	0.3726	10	1.6097	1.6387	1.6687	1.7195
HT163	5.8886	5.9322	5.9759	0.3679	0.3705	0.3732	9	1.1156	1.1790	1.2499	1.6345
HT173	0.9928	1.0071	1.0213	0.3852	0.3877	0.3902	10	1.6261	1.6411	1.6565	1.7064
HT175	1.0025	1.0168	1.0311	0.4027	0.4052	0.4077	10	1.0577	1.1137	1.1758	1.6929
HT174	0.9870	1.0013	1.0156	0.4175	0.4198	0.4222	9	1.0274	1.0853	1.1501	1.6756

Table B.3 (Continued) Detonation velocity data

TEST SERIES 9

The 2 sigma limits for T,P for the entire series are:

373.6 < T(K) < 375.5
101.0 < P(kPa) < 101.4

TEST	EQUIVALENCE RATIO			CO2 MOLE FRACTION			#	DETONATION VELOCITY (KM/S)			C-J VELOCITY (KM/S)
	LB	MP	UB	LB	MP	UB	OBS.	LB	MP	UB	
HT110	0.9957	1.0167	1.0377	0.0439	0.0491	0.0542	9	1.8541	1.8612	1.8684	1.8595
HT111	0.4771	0.4944	0.5116	0.0939	0.0988	0.1037	9	1.4138	1.4301	1.4467	1.4484
HT112	0.5962	0.6144	0.6326	0.0962	0.1011	0.1060	9	1.5432	1.5490	1.5548	1.5492
HT113	1.0025	1.0242	1.0460	0.0953	0.1002	0.1052	9	1.7649	1.7695	1.7742	1.7645
HT114	1.9652	1.9969	2.0287	0.0953	0.1002	0.1052	9	1.8556	1.8633	1.8711	1.8432
HT115	1.0251	1.0480	1.0709	0.1455	0.1502	0.1550	4	1.5211	1.5463	1.5724	1.6840
HT116	0.8178	0.8395	0.8613	0.1950	0.1996	0.2041	4	1.5211	1.5463	1.5724	1.5318
HT117	1.0025	1.0261	1.0498	0.1952	0.1998	0.2043	9	1.5652	1.6305	1.7014	1.5980
HT118	1.9630	1.9977	2.0324	0.1952	0.1998	0.2043	9	1.5434	1.5775	1.6132	1.5906

TEST SERIES 10

The 2 sigma limits for T,P for the entire series are:

281.6 < T(K) < 311.3
101.4 < P(kPa) < 101.8

TEST	EQUIVALENCE RATIO			STEAM MOLE FRACTION			#	DETONATION VELOCITY (KM/S)			C-J VELOCITY (KM/S)
	LB	MP	UB	LB	MP	UB	OBS.	LB	MP	UB	
HT145	0.2889	0.3057	0.3226	0.0000	0.0000	0.0000	9	1.0044	1.0578	1.1172	1.3541
HT150	0.3007	0.3139	0.3272	0.0000	0.0000	0.0000	9	1.3624	1.3747	1.3872	1.3669
HT148	0.3112	0.3245	0.3378	0.0000	0.0000	0.0000	10	1.2959	1.3404	1.3880	1.3832
HT133	0.3216	0.3349	0.3482	0.0000	0.0000	0.0000	9	1.3841	1.3987	1.4135	1.3989
HT97II	0.9778	0.9942	1.0105	0.0000	0.0000	0.0000	9	1.9856	1.9929	2.0003	1.9645
HT97III	0.9814	0.9973	1.0132	0.0000	0.0000	0.0000	9	1.9706	1.9786	1.9867	1.9648
HT172	1.0270	1.0462	1.0654	0.0293	0.0309	0.0329	8	1.9776	1.9870	1.9965	1.9677
HT98	0.9573	0.9803	1.0033	0.0000	0.0000	0.0000	9	1.9714	1.9774	1.9835	1.9614
HT166	5.6154	5.6571	5.6988	0.0000	0.0000	0.0000	9	2.3091	2.3328	2.3571	2.3100
HT166II	5.6344	5.6765	5.7187	0.0000	0.0000	0.0000	9	2.3000	2.3204	2.3411	2.3097
HT149	6.4151	6.4623	6.5095	0.0000	0.0000	0.0000	9	2.2760	2.3155	2.3564	2.3213
HT151	7.0893	7.1409	7.1926	0.0000	0.0000	0.0000	8	2.2748	2.3159	2.3586	2.3303
HT160	7.4497	7.5043	7.5589	0.0000	0.0000	0.0000	8	1.4529	1.5299	1.6156	2.3329
HT154	7.9097	7.9673	8.0250	0.0000	0.0000	0.0000	9	1.4451	1.5211	1.6054	2.3367

Table B.3 (Continued) Detonation velocity data

TEST SERIES 11

The 2 sigma limits for T for the entire series are:

296.0 < T(K) < 302.9

TEST	EQUIVALENCE RATIO			#	DETONATION VELOCITY (KM/S)			C-J VELOCITY (KM/S)
	LB	MP	UB	OBS.	LB	MP	UB	
HT135	0.4689	0.4996	0.5302	5	1.8150	1.8836	1.9576	1.5930
HT135II	0.4596	0.4901	0.5207	9	1.6481	1.6732	1.6991	1.5913
HT135III	0.4671	0.4977	0.5282	9	1.5884	1.6032	1.6183	1.5990
HT159	0.4656	0.4890	0.5124	9	1.6318	1.6539	1.6767	1.5913
HT136	0.4601	0.4779	0.4957	9	1.4888	1.5065	1.5246	1.5808
HT136II	0.4847	0.5026	0.5205	8	1.5788	1.5894	1.6001	1.6069
HT137	0.4731	0.4880	0.5029	9	1.5932	1.6041	1.6152	1.5933
HT138	0.4817	0.4958	0.5099	9	1.6054	1.6136	1.6219	1.6032
HT139	0.4774	0.4919	0.5064	9	1.6167	1.6250	1.6333	1.6007
HT140	0.9523	0.9912	1.0301	8	2.0977	2.1535	2.2123	1.9103
HT141	0.9798	1.0018	1.0239	9	1.9484	1.9600	1.9716	1.9372
HT142	0.9634	0.9812	0.9990	9	1.9437	1.9537	1.9637	1.9452
HT143	0.9625	0.9817	1.0009	9	1.9980	2.0084	2.0189	1.9681

Table B.3 (Continued) Detonation velocity data

TEST SERIES 2II

TEST	TEMPERATURE (K)			PRESSURE (kPa)			AIR DENSITY (MOLES/M**3)			CO2 MOLE FRACTION		
	LB	MP	UB	LB	MP	UB	LB	MP	UB	LB	MP	UB
HT119	295.3	296.4	297.4	101.08	101.35	101.62	27.279	27.423	27.566	0.0445	0.0503	0.0562
HT158	296.6	297.6	298.7	101.46	101.52	101.59	29.404	29.507	29.611	0.0937	0.0981	0.1025
HT120	294.9	295.9	297.0	101.08	101.35	101.62	26.299	26.441	26.582	0.0777	0.0834	0.0891
HT121	295.2	296.3	297.3	101.12	101.39	101.66	22.921	23.056	23.191	0.1943	0.1994	0.2045
HT121II	295.2	296.3	297.3	101.12	101.39	101.66	22.898	23.033	23.167	0.1981	0.2032	0.2083
HT121III	295.2	296.3	297.3	101.42	101.48	101.55	23.156	23.240	23.323	0.1930	0.1969	0.2009
HT168	299.2	300.3	301.3	101.59	101.66	101.73	21.547	21.624	21.701	0.2447	0.2483	0.2520

TEST SERIES 4II

TEST	TEMPERATURE (K)			PRESSURE (kPa)			AIR DENSITY (MOLES/M**3)			STEAM MOLE FRACTION		
	LB	MP	UB	LB	MP	UB	LB	MP	UB	LB	MP	UB
HT170	373.7	374.8	375.8	260.41	260.90	261.38	41.582	41.723	41.865	0.2958	0.2990	0.3021
HT170II	374.0	375.0	376.1	261.38	261.86	262.35	41.660	41.802	41.944	0.2924	0.2956	0.2987
HT171	371.0	372.0	373.1	265.06	266.00	266.94	41.471	41.613	41.754	0.3155	0.3192	0.3228
HT169	379.4	380.5	381.5	282.41	283.65	284.88	41.776	41.916	42.056	0.3359	0.3399	0.3438
HT169II	381.3	382.4	383.4	281.20	283.86	286.51	41.277	41.414	41.552	0.3330	0.3398	0.3466
HT167	387.9	389.0	390.0	302.50	302.89	303.27	41.992	42.129	42.266	0.3642	0.3668	0.3694
HT167II	387.8	388.9	389.9	303.58	303.85	304.12	41.130	41.265	41.401	0.3664	0.3689	0.3715
HT167III	387.6	388.6	389.7	304.72	306.47	308.22	42.187	42.325	42.464	0.3639	0.3684	0.3728
HT147	379.7	380.8	381.8	289.10	289.51	289.92	41.590	41.728	41.866	0.3560	0.3588	0.3615
HT132	381.5	382.5	383.6	310.30	310.95	311.60	41.829	41.968	42.107	0.3950	0.3977	0.4005

Table B.4 Initial thermodynamic state

TEST SERIES 8A

TEST	TEMPERATURE (K)			PRESSURE (kPa)			AIR DENSITY (MOLES/M**3)		
	LB	MP	UB	LB	MP	UB	LB	MP	UB
HT153	374.4	375.5	376.5	101.34	101.40	101.47	29.965	30.048	30.131
HT155	375.0	376.0	377.1	101.34	101.40	101.47	29.692	29.775	29.857
HT156	374.5	375.5	376.6	101.39	101.46	101.52	29.543	29.625	29.707
HT152	373.8	374.9	375.9	101.33	101.39	101.46	29.391	29.473	29.555
HT146	374.2	375.3	376.3	101.34	101.40	101.47	29.047	29.128	29.209
HT144	374.7	375.8	376.8	101.33	101.39	101.46	28.716	28.796	28.876
HT134	374.4	375.5	376.5	101.33	101.39	101.46	28.356	28.435	28.514
HT102	371.5	372.5	373.5	101.08	101.35	101.62	28.320	28.436	28.551
HT101	368.6	369.6	370.7	101.08	101.35	101.62	27.964	28.080	28.196
HT162	374.2	375.3	376.3	102.17	102.23	102.30	26.849	26.924	26.999
HT100	368.9	370.0	371.0	100.84	101.11	101.38	26.186	26.299	26.412
HT99	370.2	371.3	372.3	101.08	101.35	101.62	22.978	23.085	23.192
HT99II	374.3	375.4	376.4	101.33	101.39	101.46	22.815	22.880	22.945
HT103	373.0	374.0	375.1	101.15	101.42	101.69	17.564	17.663	17.762
HT104	373.3	374.4	375.4	101.08	101.35	101.62	14.223	14.318	14.412
HT161	373.1	374.1	375.2	101.33	101.39	101.46	7.803	7.832	7.862
HT165	373.7	374.8	375.8	101.33	101.39	101.46	7.477	7.506	7.535
HT164	373.8	374.9	375.9	101.26	101.32	101.39	7.158	7.186	7.215
HT157	373.8	374.9	375.9	101.33	101.39	101.46	6.549	6.576	6.604

Table B.4 (Continued) Initial thermodynamic state

TEST SERIES 8B

TEST	TEMPERATURE (K)			PRESSURE (kPa)			AIR DENSITY (MOLES/M**3)			STEAM MOLE FRACTION		
	LB	MP	UB	LB	MP	UB	LB	MP	UB	LB	MP	UB
HT122	373.8	374.9	375.9	101.08	101.35	101.62	21.592	21.696	21.800	0.0453	0.0504	0.0556
HT107	374.5	375.5	376.6	101.08	101.35	101.62	24.119	24.227	24.335	0.0940	0.0990	0.1039
HT106	373.9	375.0	376.0	100.19	100.46	100.73	23.270	23.377	23.483	0.0861	0.0911	0.0961
HT105	373.6	374.6	375.7	102.53	102.80	103.07	20.459	20.562	20.665	0.1101	0.1150	0.1198
HT108	373.7	374.8	375.8	101.29	101.56	101.83	15.751	15.847	15.943	0.1005	0.1054	0.1103
HT109	374.0	375.0	376.1	101.22	101.49	101.76	10.478	10.569	10.660	0.0934	0.0983	0.1033
HT123	373.9	375.0	376.0	101.01	101.28	101.55	19.105	19.206	19.306	0.1440	0.1487	0.1535
HT123II	372.6	373.6	374.7	101.01	101.28	101.55	19.122	19.223	19.323	0.1449	0.1496	0.1544
HT124	373.6	374.6	375.7	101.15	101.42	101.69	20.228	20.330	20.433	0.1985	0.2030	0.2076
HT125	374.1	375.1	376.2	101.68	101.97	102.27	19.188	19.289	19.390	0.1963	0.2010	0.2056
HT126	374.6	375.6	376.7	101.29	101.56	101.83	18.084	18.183	18.282	0.1966	0.2011	0.2057
HT127	374.4	375.5	376.5	100.95	101.21	101.48	14.049	14.144	14.238	0.1937	0.1983	0.2028
HT128	373.9	375.0	376.0	101.13	101.49	101.85	16.296	16.393	16.490	0.2945	0.2990	0.3035
HT129	374.0	375.0	376.1	101.15	101.42	101.69	15.857	15.954	16.050	0.2954	0.2996	0.3038
HT130	374.1	375.1	376.2	101.01	101.28	101.55	13.817	13.911	14.006	0.2946	0.2988	0.3030
HT131	373.4	374.5	375.5	101.01	101.28	101.55	14.722	14.817	14.913	0.3504	0.3544	0.3584
HT163II	373.3	374.4	375.4	101.14	101.30	101.46	14.427	14.471	14.515	0.3672	0.3699	0.3726
HT163	372.5	373.5	374.6	100.73	100.89	101.04	5.863	5.889	5.915	0.3679	0.3705	0.3732
HT173	373.8	374.9	375.9	100.78	100.90	101.02	13.954	13.997	14.040	0.3852	0.3877	0.3902
HT175	373.6	374.6	375.7	100.93	101.07	101.22	13.516	13.557	13.599	0.4027	0.4052	0.4077
HT174	373.7	374.8	375.8	102.78	102.84	102.91	13.493	13.535	13.577	0.4175	0.4198	0.4222

TEST SERIES 9

TEST	TEMPERATURE (K)			PRESSURE (kPa)			AIR DENSITY (MOLES/M**3)			CO2 MOLE FRACTION		
	LB	MP	UB	LB	MP	UB	LB	MP	UB	LB	MP	UB
HT110	374.0	375.0	376.1	101.08	101.35	101.62	21.583	21.687	21.791	0.0439	0.0491	0.0542
HT111	374.4	375.5	376.5	101.08	101.35	101.62	24.138	24.246	24.354	0.0939	0.0988	0.1037
HT112	372.6	373.6	374.7	100.88	101.15	101.41	23.188	23.295	23.401	0.0962	0.1011	0.1060
HT113	374.3	375.4	376.4	101.08	101.35	101.62	20.351	20.453	20.555	0.0953	0.1002	0.1052
HT114	373.1	374.1	375.2	100.91	101.18	101.45	15.835	15.932	16.028	0.0953	0.1002	0.1052
HT115	372.6	373.6	374.7	100.74	101.01	101.28	19.115	19.216	19.317	0.1455	0.1502	0.1550
HT116	373.8	374.9	375.9	101.01	101.28	101.55	19.141	19.241	19.342	0.1950	0.1996	0.2041
HT117	373.2	374.3	375.3	101.12	101.39	101.66	18.144	18.243	18.343	0.1952	0.1998	0.2043
HT118	373.7	374.8	375.8	101.08	101.35	101.62	14.076	14.170	14.265	0.1952	0.1998	0.2043

Table B.4 (Continued) Initial thermodynamic state

TEST SERIES 10

TEST	TEMPERATURE (K)			PRESSURE (kPa)			AIR DENSITY (MOLES/M**3)			STEAM MOLE FRACTION		
	LB	MP	UB	LB	MP	UB	LB	MP	UB	LB	MP	UB
HT145	294.8	295.9	296.9	101.22	101.49	101.76	36.359	36.525	36.691	0.0000	0.0000	0.0000
HT150	294.9	295.9	297.0	101.39	101.52	101.66	36.290	36.416	36.542	0.0000	0.0000	0.0000
HT148	295.5	296.5	297.6	101.55	101.62	101.68	36.177	36.304	36.430	0.0000	0.0000	0.0000
HT133	296.1	297.1	298.2	101.46	101.52	101.59	35.925	36.050	36.175	0.0000	0.0000	0.0000
HT97II	301.4	302.4	303.5	101.55	101.62	101.69	28.409	28.508	28.606	0.0000	0.0000	0.0000
HT97III	310.2	311.3	312.2	101.39	101.46	101.52	27.543	27.635	27.728	0.0000	0.0000	0.0000
HT172	296.9	298.0	299.0	101.46	101.52	101.59	27.476	27.606	27.737	0.0293	0.0309	0.0329
HT98	280.6	281.6	282.7	99.84	101.77	103.69	31.231	31.393	31.556	0.0000	0.0000	0.0000
HT166	303.7	304.8	305.8	101.47	101.54	101.60	11.847	11.893	11.940	0.0000	0.0000	0.0000
HT166II	300.2	301.3	302.3	101.56	101.62	101.69	11.965	12.012	12.060	0.0000	0.0000	0.0000
HT149	297.9	298.9	300.0	101.33	101.39	101.46	10.958	11.003	11.048	0.0000	0.0000	0.0000
HT151	298.4	299.4	300.5	101.42	101.52	101.63	10.183	10.226	10.269	0.0000	0.0000	0.0000
HT160	294.6	295.6	296.7	101.32	101.40	101.49	9.920	9.963	10.006	0.0000	0.0000	0.0000
HT154	295.5	296.5	297.6	101.43	101.55	101.68	9.441	9.483	9.524	0.0000	0.0000	0.0000

TEST SERIES 11

TEST	TEMPERATURE (K)			PRESSURE (kPa)			AIR DENSITY (MOLES/M**3)		
	LB	MP	UB	LB	MP	UB	LB	MP	UB
HT135	299.3	300.4	301.4	10.16	10.22	10.29	3.351	3.378	3.406
HT135II	296.9	297.9	299.0	10.12	10.18	10.25	3.371	3.399	3.426
HT135III	301.9	302.9	304.0	9.90	10.02	10.15	3.308	3.335	3.362
HT159	295.4	296.4	297.5	15.29	15.36	15.43	5.116	5.147	5.179
HT136	295.1	296.1	297.2	25.43	26.40	27.36	8.567	8.606	8.645
HT136II	297.8	298.9	299.9	25.44	25.78	26.13	8.419	8.458	8.496
HT137	296.0	297.0	298.1	50.67	50.73	50.79	16.984	17.048	17.111
HT138	295.8	296.9	297.9	101.38	101.47	101.56	33.954	34.072	34.191
HT139	299.8	300.9	301.9	254.96	264.07	273.18	84.190	84.495	84.799
HT140	297.1	298.1	299.2	9.90	10.02	10.15	2.867	2.894	2.920
HT141	295.0	296.0	297.1	25.37	25.43	25.50	7.232	7.268	7.304
HT142	295.2	296.3	297.3	51.02	51.25	51.47	14.624	14.680	14.737
HT143	295.8	296.9	297.9	148.95	150.58	152.21	43.515	43.700	43.884

Table B.4 (Continued) Initial thermodynamic state

DISTRIBUTION:

E. S. Beckjord, NRC/RES
F. Eltawila, NRC/RES
W. S. Farmer, NRC/RES
G. W. Knighton, NRC/NRR
T. Lee, NRC/RES
R. Meyer, NRC/RES
J. Mitchell, NRC/RES
J. Murphy, NRC/RES
C. W. Nilsen, NRC/RES
A. NotaFrancesco, NRC/RES
R. Palla, NRC/NRR
K. I. Parczewski, NRC/NRR
D. F. Ross, NRC/RES
B. W. Sheron, NRC/RES
T. P. Speis, NRC/RES
C. G. Tinkler, NRC/RES
P. Worthington, NRC/RES (20)
R. W. Wright, NRS/RES
D. D. Yue, NRC/NRR

U.S. Department of Energy
R. W. Barber
Office of Nuclear Safety Coordination
Washington, DC 20545

U. S. Department of Energy (2)
Albuquerque Operations Office
Attn: J. R. Roeder, Director
Transportation Safeguards
J. A. Morley, Director
Energy Research Technology
For: R. N. Holton
C. B. Quinn
P.O. Box 5400
Albuquerque, NM 87185

Acurex Corporation
485 Clyde Avenue
Mountain View, CA 94042

Argonne National Laboratory (5)
Attn: R. Anderson
D. Armstrong
L. Baker, Jr.
Dae Cho
B. Spencer
9700 South Cass Avenue
Argonne, IL 60439

Prof. S. G. Bankoff
Northwestern University
Chemical Engineering Department
Evanston, IL 60201

Battelle Columbus Laboratory (2)
Attn: P. Cybulskis
R. Denning
505 King Avenue
Columbus, OH 43201

Brookhaven National Laboratory (4)
Attn: R. A. Bari
T. Ginsberg
G. Greene
T. Pratt
Upton, NY 11973

Professor Karl T. Chuang
University of Alberta
Edmonton, Alberta
CANADA T6G2E1

Lyn Connor
Document Search NRC
P.O. Box 7
Cabin John, MD 20818

Prof. M. L. Corradini
University of Wisconsin
Nuclear Engineering Department
1500 Johnson Drive
Madison, WI 53706

A. Pete Dzmura
NE 43
U.S. DOE
Washington, DC 20545

Electric Power Research Institute (4)
Attn: J. Haugh
W. Loewenstein
B. R. Sehgal
G. Thomas
3412 Hillview Avenue
Palo Alto, CA 94303

Factory Mutual Research Corporation
Attn: R. Zalosh
P. O. Box 688
Norwood, MA 02062

Fauske & Associates (2)
Attn: R. Henry
M. Plys
16W070 West 83rd St.
Burr Ridge, IL 60521

GPU Nuclear
Attn: J. E. Flaherty
100 Interpace Parkway
Parsippany, NJ 07054

General Electric Corporation
Attn: K. W. Holtzclaw
175 Curtner Avenue
Mail Code N 1C157
San Jose, CA 95125

General Electric Corporation
Advanced Reactor Systems Dept.
Attn: M. I. Temme, Manager
Probabilistic Risk Assessment
P.O. Box 3508
Sunnyvale, CA 94088

General Public Utilities
Three Mile Island Nuclear Station
Attn: N. Brown
P.O. Box 480
Middletown, PA 17057

Institute of Nuclear Power Operation (3)
Attn: Henry Piper
S. Visner
E. Zebroski
1100 Circle 75 Parkway, Suite 1500
Atlanta, GA 30339

International Technical Services
Attn: Hideko Komoriya
420 Lexington Ave.
New York, NY 10170

Knolls Atomic Power Lab (2)
Attn: Jack Bast
R. L. Matthews
General Electric Company
Box 1072
Schnectady, NY 12301

Professor C. K. Law
Department of Mechanical Engineering
Davis, CA 95616

Los Alamos National Laboratory (4)
Attn: W. R. Bohl
F. J. Edeskuty
R. Gido
H. Sullivan
P. O. Box 1663
Los Alamos, NM 87545

University of Michigan
Department of Aerospace Engineering
Attn: Prof. M. Sichel
Ann Arbor, MI 47109

University of Michigan
Nuclear Engineering Department
Ann Arbor, MI 48104

Mississippi Power & Light
Attn: S. H. Hobbs
P. O. Box 1640
Jackson, MS 39205

Oak Ridge National Laboratory (2)
NRC Programs
Attn: A. P. Malinauskas
T. Kress
P.O. Box X, Bldg. 4500S
Oak Ridge, TN 37831

Dr. J. E. Shepherd
Rensselaer Polytechnic Institute
Troy, NY 12180-3590

Cheryl L. Mitchell (5)
Sandia National Laboratories
P.O. Box 5800
Albuquerque, NM 87185

Dr. L. T. Pong
Division 219
Science Applications Inter. Corp.
2109 Air Park Rd. SE
Albuquerque, NM 87106

Dr. Roger Strehlow
505 South Pine Street
Champaign, IL 61820

Texas A & M University
Nuclear Engineering Dept.
College Station, TX 77843

Prof. T. G. Theofanous
Chemical and Nuclear Engineering Dept.
University of California
Santa Barbara, CA 93106

TVA
400 Commerce
W9C157-CD
Knoxville, TN 37902

UCLA
Nuclear Energy Laboratory (2)
Attn: Prof. I. Catton
Prof. D. Okrent
405 Hilgard Avenue
Los Angeles, CA 90024

Westinghouse Electric Corporation (2)
Bettis Atomic Power Laboratory
Attn: Donald R. Connors
Richard F. Beyer
P.O. Box 79
West Mifflin, PA 15122

Westinghouse Hanford Company (3)
Attn: G. R. Bloom
L. Mulstein
R. D. Peak
P.O. Box 1970
Richland, WA 99352

Professor Lue Gillon
University of Louvain la Neuve
Batiment Cyclotron
B1348 Louvain La Neuve
BELGIUM

Director of Research, Science & Education
CEC
Attn: B. Tolley
Rue De La Loi 200
1049 Brussels
BELGIUM

Atomic Energy Ltd. (4)
Whiteshell Nuclear Research Establishment
Attn: D. Liu
C. Chan
K. Tennankore
D. Wren
Pinawa, Manitoba
CANADA

Atomic Energy Canada Ltd.
Attn: P. Fehrenbach
Bill Seddon
Chalk River, Ontario
CANADA KOJ 1JO

Defence Research Establishment Suffield
Attn: Dr. Ingar O. Moen
Ralston, Alberta TOJ 2NO
CANADA

McGill University
Attn: Prof. John H. S. Lee
315 Querbes
Outremont, Quebec H2V 3W1
CANADA

CEA
Attn: M. Georges Berthoud
B.P. No. 85X-Centre de
F-38041 Grenoble Cedex
FRANCE

Battelle Institut E. V. (5)
Attn: Dr. Werner Baukal
Werner Geiger
Dr. Guenter Langer
Dr. Manfred Schildknecht
Dr. Lothar Wolf
Am Roemerhof 35
6000 Frankfurt am Main 90
FEDERAL REPUBLIC OF GERMANY

Gesellschaft für Reaktorsicherheit (2)
Attn: Dr. E. F. Hicken
Dr. H. L. Jahn
8046 Garching
Forschungsgelande
FEDERAL REPUBLIC OF GERMANY

Universität Heidelberg
Attn: Juergen Warnatz
Heidelberg
FEDERAL REPUBLIC OF GERMANY

Institute für Kernenergetik und Energiesysteme (2)
University of Stuttgart
Attn: M. Buerger
G. Froehlich
H. Unger
Stuttgart
FEDERAL REPUBLIC OF GERMANY

Kernforschungszentrum Karlsruhe (3)
Attn: Dr. Wolfgang Breitung
Dr. Guenther Kessler
Dr. Helmut Jacobs
Postfach 3640
7500 Karlsruhe
FEDERAL REPUBLIC OF GERMANY

Kraftwerk Union (2)
Attn: Dr. M. Peehs
Dr. K. Hassman
Hammerbacherstrasse 12 & 14
Postfach 3220
D-8520 Erlangen 2
FEDERAL REPUBLIC OF GERMANY

Kraftwerk Union A. G. (2)
Attn: Dr. R. Heck
Dr. W. Siegler
D-ST224
6050 Offenbach
FEDERAL REPUBLIC OF GERMANY

Lehrgebiet für Mechanik der
RWTH Aachen
Attn: Prof. Dr. Ing. N. Peters
Templergraben 55
D5100 Aachen
FEDERAL REPUBLIC OF GERMANY

Technische Universität München
Attn: Dr. H. Karwat
Prof. Dr.-Ing. F. Mayinger
8046 Garching
FEDERAL REPUBLIC OF GERMANY

CNEN NUCLIT
Attn: A. Morici
Rome
ITALY

ENEA Nuclear Energ Alt Disp (2)
Attn: P. L. Ficara
G. Petrangeli
Via V. Brancati
00144 Roma
ITALY

ISPRA
Commission of the European Communities
Attn: Dr. Heinz Kottowski
C.P. No. 1, I-21020 Ispra (Varese)
ITALY

Universita Degli Studi Di Pisa
Attn: M. Carcassi
Dipartmento Di Costruzioni
Meccaniche E. Nucleari
Facolta Di Ingegneria
Via Diotisalvi 2
56100 Pisa
ITALY

Japan Atomic Energy Research Institute
Attn: Dr. K. Soda, Manager
Chemical Engineering Safety Laboratory
Dept. of Nuclear Fuel Safety
Tokai-mura, Naku-gun Ibaraki-ken
319-11
JAPAN

Japan Atomic Energy Research Institute
Attn: Dr. T. Fujishiro, Manager
Dept. of Fuel Safety Research
Tokai-mura, Naka-gun, Ibaraki-ken
319-11
JAPAN

Japan Atomic Energy Research Institute
Attn: Mr. Kazuo Sato, Director
Dept. of Reactor Safety Research
Tokai-mura, Naka-gun Ibaraki-ken
319-11
JAPAN

Power Reactor Nuclear Fuel
Development Corp. (PNC)
FBR Project
Attn: Dr. Watanabe
9-13, 1-Chome, Akasaka
Minato-Ku, Tokyo
JAPAN

Nuclear Power Engineering Test Center (2)
Attn: Dr. Akira Nonaka
Dr. Kenji Takumi
Shuwa Kamiyaeho Bldg.
3-13, 4-Chome, Toranomon
Minato-ku, Tokyo, 105
JAPAN

Netherlands Energy Research Foundation
Attn: K. J. Brinkmann
P.O. Box 1
1755ZG Petten NH
NETHERLANDS

Royal Institute of Technology
Dept. of Nuclear Reactor Engineering
Attn: Prof. Kurt M. Becker
Stockholm S-10044
SWEDEN

Statens Karnkraftinspektion
Attn: L. Hammar
P.O. Box 27106
S-10252 Stockholm
SWEDEN

Studsvik Energiteknik AB
Attn: K. Johansson
S-611 82 Nykoping
SWEDEN

Wiktor Frid
Swedish Nuclear Power Inspectorate
P. O. Box 27106
Stockholm S-10252
SWEDEN

Swedish State Power Board
Attn: Eric Ahlstroem
181-Och Vaermeteknik
SWEDEN

AERE Harwell
Attn: J. R. Matthews, TPD
Didcot
Oxfordshire OX11 ORA
UNITED KINGDOM

Central Electricity Generating Board (3)
Berkeley Nuclear Laboratory
Attn: J. E. Antill
S. J. Board
N. Buttery
Berkeley GL 139PB
Gloucestershire
UNITED KINGDOM

British Nuclear Fuels, Ltd.
Attn: W. G. Cunliffe
Building 396
Springfield Works
Salwick, Preston
Lancs
UNITED KINGDOM

Imperial College of Science and Technology
Dept. of Mechanical Engineering
Attn: Dr. A. D. Gosman
Exhibition Road
London SW7 2BX
UNITED KINGDOM

National Nuclear Corp. Ltd.
Attn: R. May
Cambridge Road
Whetestone, Leicester, LE8 3LH
UNITED KINGDOM

Simon Engineering Laboratory (2)
University of Manchester
Attn: Prof. W. B. Hall
S. Garnett
M139PL
UNITED KINGDOM

Anthony R. Taig
GDCD/CEGB
Barnwood, Gloucester
Gloucestershire
UNITED KINGDOM

UKAEA Safety & Reliability Directorate (4)
Attn: J. G. Collier
J. H. Gittus
S. F. Hall
M. R. Hayns
Wigshaw Lane, Culcheth
Warrington WA3 4NE
Cheshire
UNITED KINGDOM

UKAEA, Culham Laboratory (4)
Attn: F. Briscoe
Ian Cook
D. Fletcher
B. D. Turland
Abingdon
Oxfordshire OX14 3DB
UNITED KINGDOM

UKAEA AEE Winfrith (4)
Attn: M. Bird
T. Butland
R. Potter
A. Wickett
Dorchester
Dorset DT2 8DH
UNITED KINGDOM

University of Aston in Birmingham (2)
Dept. of Chemistry
Attn: A. T. Chamberlain
F. M. Page
Gosta Green, Birmingham B47ET
UNITED KINGDOM

Sandia Distribution:
1510 J. C. Cummings
3141 S. A. Landenberger (5)
3151 W. I. Klein
6400 D. J. McCloskey
6412 A. L. Camp
6420 W. B. Gauster
6422 D. A. Powers
6422 M. Pilch
6424 K. D. Bergeron
6424 D. C. Williams
6460 J. V. Walker
6463 M. Berman (8)
6463 D. F. Beck
6463 K. W. Boyack
6463 L. S. Nelson
6463 M. J. Rightley
6463 M. P. Sherman
6463 S. E. Slezak
6463 D. W. Stamps (10)
6463 S. R. Tieszen (10)
8524 J. A. Wackerly

NRC FORM 335 (2-84) NRCM 1102, 3201, 3202

U.S. NUCLEAR REGULATORY COMMISSION

BIBLIOGRAPHIC DATA SHEET

SEE INSTRUCTIONS ON THE REVERSE.

1. REPORT NUMBER (Assigned by TIDC, add Vol. No., if any)

NUREG/CR-5525
SAND89-2398

2. TITLE AND SUBTITLE

Hydrogen-Air-Diluent Detonation Study for Nuclear Reactor Safety Analyses

3. LEAVE BLANK

4. DATE REPORT COMPLETED

MONTH	YEAR
December	1990

5. AUTHOR(S)

Douglas W. Stamps, William B. Benedick, and Sheldon R. Tieszen

6. DATE REPORT ISSUED

MONTH	YEAR
January	1991

7. PERFORMING ORGANIZATION NAME AND MAILING ADDRESS (Include Zip Code)

Sandia National Laboratories
Albuquerque, NM 87185-5800

8. PROJECT/TASK/WORK UNIT NUMBER

9. FIN OR GRANT NUMBER

A1246

10. SPONSORING ORGANIZATION NAME AND MAILING ADDRESS (Include Zip Code)

Division of Systems Research
Office of Nuclear Regulatory Research
U.S. Nuclear Regulatory Commission
Washington, DC 20555

11a. TYPE OF REPORT

Technical

b. PERIOD COVERED (Inclusive dates)

12. SUPPLEMENTARY NOTES

13. ABSTRACT (200 words or less)

The detonability of hydrogen-air-diluent mixtures was investigated experimentally in the 0.43 m diameter, 13.1 m long Heated Detonation Tube (HDT) for the effects of variations in hydrogen and diluent concentration, initial pressure, and initial temperature. The data were correlated using a ZND chemical kinetics model. The detonation limits in the HDT were obtained experimentally for lean and rich hydrogen-air mixtures and stoichiometric hydrogen-air-steam mixtures.

The addition of a diluent, such as steam or carbon dioxide, increases the detonation cell width for all mixtures. In general, an increase in the initial pressure or temperature produces a decrease in the cell width. In the HDT, the detonable range of hydrogen in a hydrogen-air mixture initially at 1 atm pressure is between 11.6 percent and 74.9 percent for mixtures at 20°C, and 9.4 percent and 76.9 percent for mixtures at 100°C. The detonation limit is between 38.8 percent and 40.5 percent steam for a stoichiometric hydrogen-air-steam mixture initially at 100° C and 1 atm. The detonation limit is between 29.6 percent and 31.9 percent steam for a stoichiometric hydrogen-air-steam mixture with a final predetonation mixture temperature and pressure of approximately 100°C and 2.6 atm.

14. DOCUMENT ANALYSIS - a. KEYWORDS/DESCRIPTORS

Hydrogen combustion, detonation

b. IDENTIFIERS/OPEN-ENDED TERMS

15. AVAILABILITY STATEMENT

Unlimited

16. SECURITY CLASSIFICATION

(This page)
Unclassified
(This report)
Unclassified

17. NUMBER OF PAGES

18. PRICE

UNITED STATES
NUCLEAR REGULATORY COMMISSION
WASHINGTON, D.C. 20555

OFFICIAL BUSINESS
PENALTY FOR PRIVATE USE, $300

SPECIAL FOURTH-CLASS RATE
POSTAGE & FEES PAID
USNRC

PERMIT No. G-67